DISSERTATION

INTEGRATING GENOMICS AND TELOMERE DYNAMICS TO UNDERSTAND CLIMATE ADAPTATION IN A MIGRATORY SONGBIRD

Submitted by

Marina D. Rodriguez

Department of Biology

In partial fulfillment of the requirements

For the Degree of Doctor of Philosophy

Colorado State University

Fort Collins, Colorado

Spring 2025

Doctoral Committee:

Advisor: Kristen C. Ruegg

Susan F. Bailey
Rachael A. Bay
Kim L. Hoke

ABSTRACT

INTEGRATING GENOMICS AND TELOMERE DYNAMICS TO UNDERSTAND CLIMATE ADAPTATION IN A MIGRATORY SONGBIRD

Declines in avian species have become widespread due to numerous threats, including anthropogenic climate change. Migratory birds, which occupy multiple environments throughout their annual cycle, are particularly vulnerable. Understanding and predicting the response of migratory bird species to climate change is critical for targeted conservation efforts and the mitigation of further declines. A key factor in species resilience lies in their ability to genetically adapt to changing environments. Recent advances in conservation genomics have improved our ability to detect local adaptation and predict maladaptation to climate change in non-model species. In my dissertation, I test the overall hypothesis that integrating telomere dynamics and conservation genomics will allow for the identification and validation of fitness-related traits in studies of local adaptation. With this hypothesis, I aim to uncover potential mechanisms of local adaptation and assess the impacts of climate change on the yellow warbler (*Setophaga petechia*). In my first chapter, I link genetic, phenotypic, and environmental data with telomere length measurements to enhance our understanding of local adaptation and the effects of climate change in this species. In the second chapter, I combine models of genomic offsets with telomere data to validate the prediction that yellow warblers inhabiting regions with high genomic offset experience elevated physiological stress due to climate change. Finally, in my third chapter, I investigate local adaptation to the non-breeding grounds and test whether climate tracking

reflects local adaptation across the annual cycle in this migratory species. Taken together, my doctoral research highlights the importance of understanding local adaptation to inform population responses to the changing climate. Importantly, this work represents the first demonstration of how integrating methodologies from modern genomics and assessment of biological measures of stress like telomeres can advance our knowledge of wild species' responses to environmental change and enhance conservation efforts.

ACKNOWLEDGEMENTS

I am deeply thankful to my advisor, Dr. Kristen Ruegg, for being an exceptional mentor throughout my PhD journey. Her guidance has made me a better scientist, her enthusiasm for discovery has fueled my curiosity, and her belief in me has strengthened my confidence. I am especially grateful for her openness to diverse avenues of research, which allowed me to integrate my background in telomere biology with my growing expertise in conservation genomics. Beyond research, her support has helped me grow as a teacher, mentor, and leader—ultimately shaping me into a more well-rounded human being. I also deeply appreciate her continued encouragement of my commitment to diversity, equity, and inclusion, which has been integral to my personal and professional development.

I am grateful to my committee members, Drs. Susan Bailey, Rachael Bay, and Kim Hoke, for their invaluable guidance and support throughout my doctoral research. I especially want to thank Susan for her steadfast support, which began during my Master's degree. Susan welcomed me into the world of telomeres with open arms and enthusiastically embraced the addition of birds to her primarily human-focused research. Her mentorship and teaching over the past eight years have been instrumental in my growth as a telomere biologist. Rachael has provided a strong foundation for my research on the yellow warbler. Her earlier work on this remarkable species served as a critical starting point for my deeper exploration into local adaptation and vulnerability to climate change. I am incredibly grateful for Rachael's insights and guidance, which have been invaluable to my work. I also want to thank Kim for offering fresh perspectives from different fields, which challenged me to think about my research from new angles. This broader view has been crucial for my development as a scientist. Additionally, I

deeply appreciate Kim's kindness and support in my endeavors beyond research, for which she was always generous and helpful.

In the Colorado State University Biology Department, I have been fortunate to be part of an incredible community that has significantly contributed to my growth as a scientist and individual. I am especially grateful to my amazing colleagues in the Ruegg lab, who have been steadfast sources of support, friendship, and laughter. A heartfelt thank you to Christen Bossu, Sheela Turbek, Matt DeSaix, Christine Rayne, Taylor Bobowski, Erica Robertson, Holden Fox, Amanda Carpenter, Caitlin Miller, Marius Somveille, Joan Ferrier, Josie Paris, and Adrian Pullaro. I could not have asked for a better group to share this journey with. I am also deeply thankful to the many non-Ruegg lab members who have made a significant impact on my life both in and out of school. Special thanks to Amanda Cicchino, Mariana Rodriguez, Amir Alayoubi, Beth Whittman, Shanelle Wikramanayake, Juliana Mendez, Kat Stroh, Mackenzie Woods, Rebecca Cheek, Lily Durkee, Brenna Forester, Bennett Hardy, Coby McDonald, Dominic Montano, Jennifer Brady, and Andrew Patton. I would also like to extend my gratitude to Lisa Angeloni for her unwavering support, which has continued since my undergraduate years. Lisa is one of the most compassionate and genuinely caring people I know, and her encouragement has meant so much to me. I am also grateful to many other faculty members who have influenced and guided me during my time as a PhD student. Thank you to Eric Anderson, Chris Funk, Meena Balgopal, Shane Kannatous, and Debbie Garrity for their mentorship and inspiration.

I am fortunate to have worked with and learned from a wide range of collaborators outside of CSU. Thank you to Tim Kita for your invaluable help with sample collection in Pennsylvania; your love and dedication to the natural world are truly inspiring, and I am so

grateful to have worked with you. To Brenda and Rich Keith, thank you for your hard work collecting yellow warbler samples in Michigan while running a banding station—I deeply appreciate your efforts in monitoring birds year after year. I am also grateful to Sergio Gomez for his dedication to collecting yellow warbler samples across Mexico. Thank you for the countless hours you've spent in the field, working tirelessly to coax birds down from the tree canopies. A special thank you to Maddie Sutton, who became a close friend and colleague after spending a week with me in a windowless lab—a shared experience I will always remember fondly. I would also like to thank Clifford Berek, Andrea Patterson, John Loegering, Chuck Hathcock, Heidi Carlisle, Robert Thobaben, Lauren diBiccari, Meredith McBurney, Shannon Mendia, Simon Duval, Darshawn Narang, Ingrid Tello-Lopez, Rafa Rueda-Hernandez, Richard Feldman, and the many volunteers from the Institute for Bird Populations, MAPS, and Bird Conservancy of the Rockies for their contributions to the collection of yellow warbler samples. Additionally, I am deeply grateful to all the field technicians and researchers who have contributed to the collection of yellow warbler samples over the past 20 years—your efforts have been instrumental to this work.

My PhD work was made possible thanks to the generous funding from numerous sources. I am deeply grateful to Tom and Vicki Kirchner, whose generosity reflects their dedication to supporting science and CSU students. A heartfelt thank you to Barbara Bailey and the Estes Park P.E.O. sisterhood, not only for funding the final year of my PhD but also for the love, friendship, and kindness you have shown me over the past two years. I also extend my gratitude to the National Science Foundation, the Colorado Chapter of The Wildlife Society, the American Ornithological Society, the American Field Ornithologists, the Colorado Field Ornithologists, the CSU Office for the Vice President of Research, and the American Association of University

Women for their invaluable support. Additionally, I am grateful to the many generous donors to the CSU Biology Department whose contributions helped support my research.

Furthermore, I am indebted to numerous people who have inspired me, mentored me, and provided me with unyielding support throughout all my time at CSU. Thank you to Mary Swanson, Paul Doherty, Kate Huyvaert, Rick Knight, Rocky Coleman, Pat Rastall, Ken Wilson, Ann Randall, Larissa Bailey, Kevin Bestgen, Liba Pejar, Joyce Pratt, Bob Sturtevant, and John Hayes.

Finally, I want to thank my friends and family for your endless love and encouragement. To my best friend, Alyssa—my ride or die—you are such an integral part of my life. I am so lucky our paths crossed, and I treasure the countless unforgettable memories we've shared. Thank goodness for our shared sense of humor, which made every situation one to laugh about. To the other amazing and important people who mean the world to me: Ben Wasserstein, Cam Walford, Megan Riveros, Keith McCaskell, and Brianna Baker—thank you for your love and support. To my second set of parents, Diane and Rod—thank you for treating me as one of your own and supporting both me and Chase through all our endeavors. To my grandmothers—Chepie, Oma, and Sandy—thank you for being shining examples of tough, compassionate women whose love for their families knows no bounds. To my brothers: Dimitri, thank you for always being an inspiration with your kindness and strength; Marty, thank you for sharing a love of nature with me and catching birds together during two unforgettable summers; and Ian, for being the epitome of coolness and creativity. I am so grateful to my stepdad, Jorge, for your unwavering love and support, often shown through ensuring our cars and phones were always working and up to date. And to my mom, Candy—thank you for your countless sacrifices, love, time, and energy. Whether I wanted to be a veterinarian, politician, WNBA star, or biologist, you

were always my #1 fan and believed in whatever I was dreaming. You are the most caring, intelligent, and badass woman I know, and I can't believe how lucky I am to have you as my mother.

To my babies, Tippet and Bear-Bear—thank you for your unconditional love and support. Whether I'm watching TV, eating, or working, you are always right by my side (or in my face). You are the best co-workers a person could ask for. And finally, to Chase—thank you for loving me and supporting me through all the twists and turns. You make sure I laugh and smile every day, and that truly is the greatest gift anyone could receive. I love you with all my heart and am so excited to see where life takes us together.

DEDICATION

To Chase, for giving me a reason to smile everyday

TABLE OF CONTENTS

INTRODUCTION

Human-induced environmental change poses a significant threat to global biodiversity, with increasing periods of drought and thermal stress expected to profoundly impact species' local environments (Parmesan 2006, Somero 2015, Urban 2015). In response to climate change, species employ three primary strategies to avoid decline or extinction: (1) shifting their distributions to track ecological niches, (2) exhibiting phenotypic plasticity to endure environmental changes, and (3) undergoing genetic evolution to adapt to novel conditions. Among these strategies, genetic adaptation is considered the most critical for ensuring long-term fitness (Waldvogel et al. 2020). Understanding the ability of natural populations to genetically adapt to environmental changes is therefore essential for predicting their responses to climate change (Valladares et al. 2014, Chirgwin et al. 2015, Peterson et al. 2019, Waldvogel et al. 2020). This understanding requires insights into the genomic basis of current climate adaptation, the traits mediating local climate adaptation, and the physiological costs associated with future climate change. In this dissertation, I test the hypothesis that integrating telomere dynamics and conservation genomics would allow for the identification and validation of fitness-related traits in studies of local adaptation. To test this hypothesis, I focus on the integration of genomic approaches with assessment of telomere length to characterize patterns of local adaptation and assess fitness effects in response to climate change in a migratory songbird, the yellow warbler (*Setophaga petechia*).

Populations locally adapt when divergent selection causes individuals to exhibit higher average fitness in their local environment compared to individuals from foreign environments (Kawecki and Ebert 2004, Blanquart et al. 2013, Savolainen et al. 2013). Local adaptation arises

from the interplay of natural selection, gene flow, and genetic drift, with selection playing a dominant role (Kawecki and Ebert 2004, Savolainen et al. 2013). Heterogeneous environments dictate which traits are favored by selection, driving changes in allele frequencies at loci underlying these traits. Over time, this process results in adaptive divergence in both trait means and allele frequencies across populations.

Advances in genome-wide sequencing have enabled the investigation of genomic signals of local adaptation. For instance, Genome-Wide Association Studies (GWAS) are effective for identifying loci associated with specific phenotypic traits under selection across environments. GWAS employs linear mixed models to detect significant associations between genetic loci and phenotypic variation across large samples (Korte and Farlow 2013) and has been used to uncover genes influencing fitness-related traits in numerous taxa. Another key approach, Gene-Environment Association (GEA) analysis, is a phenotype-independent method combining landscape and population genomics to identify environmental variables driving adaptive genetic variation (Sork et al. 2013).

While studies on local adaptation to the breeding grounds of migratory animals are abundant, research on adaptation to non-breeding grounds is scarce. This gap stems from the challenges of tracking individuals and populations across vast distances and accurately quantifying their year-round climate exposure. However, advances in genome-wide sequencing and analytical methods now enable exploration of adaptation to both breeding and non-breeding grounds. For example, approaches that estimate allele frequency surfaces on breeding grounds allow for the prediction of geographic origins for individual birds captured on their wintering grounds (Ranola et al., 2014). These methods enable the determination of climatic variables

experienced by individual birds across their entire annual cycle, providing new insights into the selective pressures faced during migration and on non-breeding grounds.

Although many studies demonstrate patterns of local adaptation, fewer have identified specific agents of selection driving fitness trade-offs (Wadgymar et al. 2017). To fully characterize local adaptation, it is necessary to identify environmental drivers of selection, phenotypes under selection, and their genetic basis, while linking these components to fitness outcomes. Measuring fitness and physiological stress in wild, non-model species remains challenging, but telomeres provide a valuable proxy for lifespan and physiological stress, which I utilize throughout this dissertation.

Telomeres are nucleoprotein structures consisting of tandem arrays of repetitive sequence (5'-TTAGGG-3' in most vertebrates) and associated proteins that protect chromosome ends from degradation during cell replication and oxidative damage (Blackburn 1991, Blackburn 2005). Telomeres also prevent chromosomal termini from being detected as broken DNA ends and triggering inappropriate DNA damage responses, and so functional telomeres are essential for maintaining genome stability (De Lange 2005). In the absence or insufficiency of telomerase—the specialized reverse transcriptase capable of maintaining telomere length—telomeres shorten with each DNA replication cycle (Blackburn 2005). Telomere length also shortens with oxidative stress, inflammation, and a variety of lifestyle factors (e.g., Epel et al. 2004). Telomere shortening is associated with genomic instability, senescence and apoptosis (Aubert and Lansdorp 2008). Although the causal relationship between telomere length, disease, and survival is still debated, short telomeres have been linked to higher mortality risks across vertebrates (Boonekamp et al. 2013, Wilbourn et al. 2018, Whittemore et al. 2019).

Telomere dynamics provide an informative biomarker of somatic integrity (Schnee and Thompson 1984, Lopez-Otin, Blasco et al. 2013), predicting life-history traits such as lifespan (Heidinger et al. 2012, Bichet et al. 2020), lifetime reproductive success (Eastwood, Hall et al. 2019), and individual quality (Angelier et al. 2019, Rollings et al. 2019, Cheron et al. 2021). Stressful environments are known to accelerate telomere attrition (Epel et al. 2004, Monaghan 2014), with faster telomere shortening rates linked to increased mortality (Wilbourn et al. 2018, Whittemore et al. 2019). Environmental stressors such as competition, pollutants, and extreme weather events drive physiological and behavioral changes that prioritize immediate survival but incur physiological costs (Romero 2004, Casagrande and Hau 2019, Chatelain et al. 2020). Increased metabolic activity during stress elevates oxidative stress (Cadenas and Davies 2000), a major driver of telomere shortening (von Zglinicki 2002, Houben et al. 2008).

Telomere research in wild species has predominantly focused on avian taxa, largely due to the presence of nucleated blood cells, which facilitates telomere measurements from blood samples (Stier et al. 2015). Additionally, birds are extensively monitored and sampled across the globe, further contributing to their prominence in telomere studies. General patterns in avian species indicate that telomere length shortens with age (Heidinger et al., 2012; Bichet et al., 2020), that longer-lived species tend to have longer telomeres that shorten at a slower rate compared to shorter-lived species (Tricola et al., 2018), and that telomere dynamics exhibit heritability, though the degree of heritability varies among species (i.e., Reichert et al. 2015, Dugdale and Richardson 2018, Bauch et al. 2021). Moreover, studies have linked telomere length to lifetime reproductive success and individual quality across multiple avian species (e.g., Eastwood et al., 2019; Angelier et al., 2019).

Both field and laboratory research on birds suggest that much of the variation in telomere dynamics is driven by environmental factors such as weather conditions, disease exposure, urbanization, and predator pressure among many others (e.g., Mizutani et al. 2013, Asghar et al. 2015, Salmon and Burraco 2022, Kärkkäinen et al. 2019). However, while these influences have been well-documented at the individual and population levels, relatively little is known about how telomere length varies across broad spatial scales (but see Burraco et al. 2021). Understanding telomere dynamics in the context of geographic variation could therefore offer new insights into species' responses to environmental stressors, particularly in the face of climate change. Integrating telomere measurements with conservation genomics may further provide a powerful framework for assessing how maladaptation to shifting environmental conditions affects populations. To test if telomere dynamics could serve as a valuable tool in studies of local adaptation, offering a means to identify and validate fitness-related traits across taxa.

My dissertation tests the hypothesis that integrating telomere dynamics and conservation genomics would allow for the identification and validation of fitness-related traits in studies of local adaptation. To test this hypothesis, my dissertation integrates phenotypic measures, genotypes, environmental measures, and fitness metrics to assess local adaptation across the annual cycle of the yellow warbler.

LITERATURE CITED

Angelier, F., Weimerskirch, H., Barbraud, C., Chastel, O., & Hopkins, W. (2019). Is telomere length a molecular marker of individual quality? Insights from a long-lived bird. Functional Ecology, 33(6), 1076-1087. https://doi.org/10.1111/1365-2435.13307.

Asghar, M., Hasselquist, D., Hansson, B., Zehtindjiev, P., Westerdahl, H., & Bensch, S. (2015). Hidden costs of infection: chronic malaria accelerates telomere degradation and senescence in wild birds. *Science*, *347*(6220), 436-438.

Bichet, C., Bouwhuis, S., Bauch, C., Verhulst, S., Becker, P. H., & Vedder, O. (2020). Telomere length is repeatable, shortens with age and reproductive success, and predicts remaining lifespan in a long-lived seabird. Molecular Ecology, 29(2), 429-441.

Blackburn, E. H. (1991). Structure and function of telomeres. Nature, 350, 569-573.

Blackburn, E. H. (2005). Telomeres and telomerase: their mechanisms of action and the effects of altering their functions. FEBS Lett., 579, 859-862.

Blanquart, F., Kaltz, O., Nuismer, S. L., & Gandon, S. (2013). A practical guide to measuring local adaptation. Ecology letters, 16(9), 1195-1205.

Boonekamp, J. J., Simons, M. J., Hemerik, L., & Verhulst, S. (2013). Telomere length behaves as biomarker of somatic redundancy rather than biological age. Aging cell, 12(2), 330-332.

Burraco, P., Lucas, P. M., & Salmón, P. (2022). Telomeres in a spatial context: a tool for understanding ageing pattern variation in wild populations. Ecography, 2022(6), e05565.

Cadenas, E., & Davies, K. J. (2000). Mitochondrial free radical generation, oxidative stress, and

Casagrande, S., & Hau, M. (2019). Telomere attrition: metabolic regulation and signalling function?. Biol. Lett., 15, 20180885.

Chatelain, M., Drobniak, S. M., & Szulkin, M. (2020). The association between stressors and telomeres in non-human vertebrates: a meta-analysis. Ecol. Lett., 23, 381-398.

Cheron, M., Angelier, F., Ribout, C., & Brischoux, F. (2021). Clutch quality is related to embryonic development duration, hatchling body size and telomere length in the spined toad (Bufo spinosus). Biological Journal of the Linnean Society. https://doi.org/10.1093/biolinnean/blab035/6187432

Chirgwin, E., Monro, K., Sgro, C. M., & Marshall, D. J. (2015). Revealing hidden evolutionary capacity to cope with global change. Global Change Biology, 21(9), 3356-3366.

De Lange, T. (2005). Shelterin: the protein complex that shapes and safeguards human telomeres. Genes & development, 19(18), 2100-2110.

Epel, E. S., Blackburn, E. H., Lin, J., Dhabhar, F. S., Adler, N. E., Morrow, J. D., & Cawthon, R. M. (2004). Accelerated telomere shortening in response to life stress. Proceedings of the National Academy of Sciences, 101(49), 17312-17315.

Houben, J. M., Moonen, H. J., van Schooten, F. J., & Hageman, G. J. (2008). Telomere length assessment: biomarker of chronic oxidative stress? Free Radic. Biol. Med., 44, 235-246.

Kärkkäinen, T., Teerikorpi, P., Panda, B., Helle, S., Stier, A., & Laaksonen, T. (2019). Impact of continuous predator threat on telomere dynamics in parent and nestling pied flycatchers. Oecologia, 191, 757-766.

Kawecki, T. J., & Ebert, D. (2004). Conceptual issues in local adaptation. Ecology letters, 7(12), 1225-1241.

López-Otín, C., Blasco, M. A., Partridge, L., Serrano, M., & Kroemer, G. (2013). The hallmarks of aging. Cell, 153(6), 1194-1217.
Mizutani, Y., Tomita, N., Niizuma, Y., & Yoda, K. (2013). Environmental perturbations influence telomere dynamics in long-lived birds in their natural habitat. Biology Letters, 9(5), 20130511.
Monaghan, P. (2014). Organismal stress, telomeres and life histories. Journal of Experimental Biology, 217(1), 57-66.
Parmesan, C. (2006). Ecological and evolutionary responses to recent climate change. Annu. Rev. Ecol. Evol. Syst., 37(1), 637-669.
Ranola, J. M., Novembre, J., & Lange, K. (2014). Fast spatial ancestry via flexible allele frequency surfaces. Bioinformatics, 30(20), 2915-2922. https://doi.org/10.1093/bioinformatics/btu418
Rollings, N., Uhrig, E. J., Krohmer, R. W., Waye, H. L., Mason, R. T., Olsson, M.,…Friesen, C. R. (2017). Age-related sex differences in body condition and telomere dynamics of red-sided garter snakes. Proceedings of the Royal Society B: Biological Sciences, 284(1852), 20162146.
Romero, L. M. (2004). Physiological stress in ecology: lessons from biomedical research. Trends Ecol. Evol., 19, 249-255.
Savolainen, O., Lascoux, M., & Merilä, J. (2013). Ecological genomics of local adaptation. Nature Reviews Genetics, 14(11), 807-820.
Schnee, F. B., & Thompson Jr, J. N. (1984). Conditional polygenic effects in the sternopleural bristle system of Drosophila melanogaster. Genetics, 108(2), 409-424.
Somero, G. N. (2005). Linking biogeography to physiology: evolutionary and acclimatory adjustments of thermal limits. Frontiers in zoology, 2, 1-9.
Sork, V. L., Aitken, S. N., Dyer, R. J., Eckert, A. J., Legendre, P., & Neale, D. B. (2013). Putting the landscape into the genomics of trees: approaches for understanding local adaptation and population responses to changing climate. Tree Genetics & Genomes, 9, 901-911.
Urban, M. C. (2015). Accelerating extinction risk from climate change. Science, 348(6234), 571-573.
Valladares, F., Matesanz, S., Guilhaumon, F., Araújo, M. B., Balaguer, L., Benito-Garzón, M., ... & Zavala, M. A. (2014). The effects of phenotypic plasticity and local adaptation on forecasts of species range shifts under climate change. Ecology letters, 17(11), 1351-1364
Von Zglinicki, T. (2002). Oxidative stress shortens telomeres. Trends Biochem. Sci., 27, 339-344.
Wadgymar, S. M., Lowry, D. B., Gould, B. A., Byron, C. N., Mactavish, R. M., & Anderson, J. T. (2017). Identifying targets and agents of selection: innovative methods to evaluate the processes that contribute to local adaptation. Methods in Ecology and Evolution, 8(6), 738-749.
Waldvogel, A. M., Feldmeyer, B., Rolshausen, G., Exposito-Alonso, M., Rellstab, C., Kofler, R., ... & Pfenninger, M. (2020). Evolutionary genomics can improve prediction of species' responses to climate change. Evolution Letters, 4(1), 4-18.
Whittemore, K., Vera, E., Martínez-Nevado, E., Sanpera, C., & Blasco, M. A. (2019). Telomere shortening rate predicts species life span. Proceedings of the National Academy of Sciences, 116(30), 15122-15127.
Wilbourn, R. V., Moatt, J. P., Froy, H., Walling, C. A., Nussey, D. H., & Boonekamp, J. J. (2018). The relationship between telomere length and mortality risk in non-model vertebrate

systems: a meta-analysis. Philosophical Transactions of the Royal Society B: Biological Sciences, 373(1741), 20160447.

CHAPTER 1: GENETIC, PHENOTYPIC, ANF ENVIRONMENTAL DRIVERS OF LOCAL ADAPTATION AND CLIMATE-INDUCED MALADAPTATION IN A MIGRATORY SONGBIRD

Summary

Understanding processes driving local adaptation in wild species is a key goal in evolutionary biology, but linking genotype and phenotype to environmental drivers of natural selection remains challenging. Here we explore these connections on the breeding range of the yellow warbler (*Setophaga petechia*). First, we conduct genome-wide association studies (GWAS) to identify loci related to bill shape and individual quality. We then conduct a gene-environment association (GEA) analysis on resulting loci and find precipitation is underlying putative selection on bill shape. Finally, we test whether contemporary individuals whose bill shape deviates from historical relationships with precipitation, exhibit increased stress—measured by telomere length—resulting from maladaptation. Our results align with predictions from GWAS and GEA analyses, indicating birds with shallow bills in regions becoming drier experience higher stress (*i.e.* shorter telomeres) because of maladaptation. Overall, this study links genetic, phenotypic, and environmental data with stress biomarkers to improve understanding of the process of local adaptation and effects of climate change on biodiversity.

Introduction

Local adaption occurs when populations evolve in response to divergent selection across heterogeneous environments (Savolainen et al. 2013). While identifying local adaptation in wild populations remains a central goal of evolutionary biology, there remain very few examples where a complex genetic basis of a key phenotype and the environmental drivers of natural

Manuscript status: In preparation
Potential target journals: Proceedings of the National Academy of Sciences or Global Change Biology.

selection have been clearly identified (but see Lamichhaney et al. 2015, Cook et al. 2013, and Strickland et al. 2023). One of the most compelling examples of complex genetic architectures associated with phenotypes and environment exists in Darwin's finches (e.g. Lamichhaney et al. 2015, Grant and Grant 1993, and Lamichhaney et al. 2016) where beak size of the medium ground finch is known to increase in response to drought-induced decreases in the availability of smaller, softer seeds (Grant and Grant 1993, Lamichhaney et al. 2015). Genomic analysis has further shown that diversity at the HMGA2 and ALX1 genes are linked to beak size and shape and may allow for rapid evolution in the face of changes in precipitation (Grant and Grant 1993, Lamichhaney et al. 2016). As climate change continues to drive fluctuations in temperature and precipitation, understanding the genetic basis of phenotypes critical to local adaptation, along with the environmental drivers of natural selection, is becoming increasingly important for predicting how species may respond to global change.

In the era of Next-Generation Sequencing, genome-wide association studies (GWAS) have become a powerful approach for uncovering the genetic basis of traits linked to fitness and local adaptation (Santure and Garant 2018). A GWAS uses linear mixed models to find significant associations between loci associated with specific phenotypes across a large sample of individuals (Korte and Farlow 2013). This approach has been useful for identifying key genes underlying traits important to fitness across a variety of taxa, including autoimmune diseases in humans (Siminovitch 2004), reproductive behavior in steelhead trout (*Oncorhynchus mykiss;* Hess et al. 2016), and the genetic architecture of migratory direction in mule deer (*Odocoileus hemionus;* Bonar et al. 2022). In birds, bill shape is a good candidate phenotype for a GWAS because it often varies between populations, is highly heritable, and has established links to individual fitness across species (Lundregan et al. 2018, Bosse et al. 2017). Further, numerous

studies have connected bill morphology to climate, showing that larger bills are an adaptation to hot, dry conditions (Greenburg et al. 2012, Symonds and Tattersall 2010, Tattersall et a. 2017). After identifying genotype-phenotype links through a GWAS, a comprehensive understanding of the role of bill morphology in local adaptation necessitates examination of the environmental variables underlying natural selection.

Gene-environment association (GEA) methods are phenotype-free approaches that combine landscape and population genomics to identify environmental variables shaping adaptive genetic variation (Sork et al. 2013). For instance, recent studies have used GEA-based approaches to detect genomic signals of local adaptation to urban habitats in great tits (*Parus major*) across Europe (Salmón et al. 2021) and to snowpack in willow leaf beetles (*Chrysomela vigintipunctata*; Keller et al. 2023). In GEAs, the emphasis is put on selecting climate variables that may capture the drivers of selection at the correct spatial and temporal scale. Although both GWAS and GEA are commonly employed in studies of local adaptation, using them independently can limit their scope. Alternatively, combining these approaches allows researchers to gain a more comprehensive understanding of the genetic basis of traits important to local adaptation, and the environmental factors driving selection (e.g., De La Torre et al. 2021, Contina et al. 2023).

Perhaps the most critical and difficult step with identifying the genetic basis of traits important to local adaptation is validating the role of candidate genes in fitness and/or individual quality. Measuring individual quality is challenging in many species because it often requires monitoring offspring across multiple generations. Measuring telomere length, however, provides a promising and cost-effective alternative for assessing individual quality in species where offspring tracking is unfeasible. Telomeres are non-coding, specialized DNA sequences at the

ends of chromosomes that maintain chromosome stability and protect coding DNA from erosion (Blackburn 1984). Prior research has demonstrated that stressful environments can accelerate telomere attrition (Epel et al. 2004, Monaghan 2014), and faster rates of telomere shortening can predict mortality (Wilbourn et al. 2018, Whittemore et al. 2019). Telomere length is also known to vary with individual quality (i.e., Angelier et al. 2019, Le Vaillant et al. 2015) and fitness across a variety of taxa (e.g., Wilbourn et al, 2018, Chik et al. 2024, Froy et al. 2021). Comparative measures of telomere length between individuals can be used to test hypotheses about phenotypic traits important to local adaptation in species where field-intensive assessments of individual quality are impractical.

The yellow warbler (*Setophaga petechia*), a migratory songbird with a cross-continental breeding distribution, is a good system in which to identify the links between genotype, phenotype, and the environment because extensive prior research on all three aspects provides a strong foundation for generating testable hypotheses. Past work has shown a positive correlation between historical measures of bill depth and precipitation (Bay et al. 2021), offering a historical baseline from which to assess how deviations from this pre-climate change relationship may impact individual quality. Previous GEA analyses further suggest that precipitation is the primary driver of genetic variation across space and that recent population declines are linked to climate change-induced shifts in precipitation (Bay et al. 2018, Rodriguez et al. 2025). Collectively, these findings support the hypothesis that bill shape is critical to local adaptation in yellow warblers and that changes in precipitation may drive selection on this trait. Consequently, we predict that a failure to adjust bill shape in response to shifts in precipitation will lead to reduced individual quality and population declines.

To identify the links between genotype, phenotype, and environmental drivers of natural selection in the yellow warbler, and to test how climate change-induced mismatches may lead to maladaptation, we integrate measurements of bill shape (from both past and present) with a GWAS, GEA, and telomere length assessments across populations. We first conduct a GWAS in two populations to identify the genetic basis of bill shape and intersect these genes with a GWAS on telomere length (Fig. 1.1a) to focus on genes important to individual quality (Fig. 1.1b). To test if bill size mediates local adaptation to precipitation regimes, we then conduct a GEA on bill-linked loci identified through GWAS to determine the environmental drivers of variation in these subsets of putatively adaptive loci for 22 populations across the breeding range (Fig 1.1c). To investigate whether maladaptation may contribute to recent population declines, we examine how deviations from the pre-climate change baseline relationship between bill shape and precipitation impact individual quality (Fig. 1.1e-h). If recent population declines result from a failure to adjust bill size in response to changes in precipitation, we predict that populations exhibiting the greatest deviation from the pre-climate change relationship will experience the highest levels of stress and, consequently, have the shortest telomeres. Overall, our results enhance our understanding of the connections between phenotype, genotype, and the environmental drivers of natural selection, which are crucial for assessing the potential threats posed by global environmental change on this species and others.

Methods

Sample collection and DNA isolation

We collected samples from 121 yellow warblers from two reference populations in Michigan and Pennsylvania (Figure 1.1I). At each site, birds were captured using mist-netting, bill depth measurements were taken, and blood samples were collected via brachial venipuncture

and preserved in Queens lysis buffer. Further, we collected an additional 171 genetic samples from 22 sites across the yellow warbler breeding range to validate associations between allele frequencies and environmental variables in key loci. From the 171 samples, 63 samples with bill depth measurements from 10 sites across the breeding range were also used to validate the associations between bill depth and environmental variables. DNA from all samples was purified using the Qiagen™ Dneasy Blood and Tissue extraction kit and quantified using the Qubit dsDNA HS Assay kit (Thermo Fisher Scientific).

Whole-genome sequencing and variant calling

Whole genome sequencing libraries were prepared following modifications of Illumina's Nextera Library Preparation protocol (Schweizer et al. 2023) and were sequenced on NovaSeq6000 lanes at Duke University Sequencing and Genomic Technologies with a target sequencing depth of 2X per individual. To process sequence data, we used the workflow management system Snakemake to create a reproducible bioinformatics pipeline (Köster ad Rahmann 2012). We used the program Trimmomatic 0.39 (Bolger et al. 2014) to trim the sequence data to remove Illumina adapter sequences and polyG tails using a sliding window approach (SLIDINGWINDOW:4:20). We then mapped reads to the yellow warbler reference genome (NCBI BioProject PRJNA777222; Tsai et al. 2024) using BWA 0.7.17 (Li and Durbin 2009) with the bwa mem Snakemake wrapper (v1.23.3/bio/bwa/mem). After mapping, the resulting SAM files were sorted, converted to BAM files, and indexed using Samtools version 1.16 (Li et al. 2009). We used MarkDuplicates from Picard (http://broadinstitute.github.io/picard) to mark read duplicates and clipped overlapping reads with the clipOverlap function from bamUtil (Jun et al, 2015). To reduce sequencing depth variation, we used the downsample function from Picard (http://broadinstitute.github.io/picard)

to downsample reads from BAM files with greater than 3X coverage, to 3X coverage. This resulted in an average read depth of 2.7X coverage.

To identify genetic markers from low-coverage WGS data, we used the program HaplotypeCaller in the Genome Analysis Toolkit (GATK version 4.1.6.0; Van der Auwera) applying a minimum base quality score of 33 and a minimum mapping quality score of 20 to reduce lane effects (Lou and Therkildsen 2022). To parallel the genotype calling process, we generated genomic databases in ~3 Mb intervals across the genome and combined and indexed the genotyped VCF files with BCFtools 1.16 (Danecek et al. 2021). To remove systematic errors, we applied a hard filter to the subsequent VCF file with the following parameters, "QD < 2.0 || FS > 60.0 || MQ < 40.0 || MQRankSum < -12.5 || ReadPosRankSum < -8.0", filtering the indels separately with "QD < 2.0 || FS > 200.0 || ReadPosRankSum < -20.0". We then used BCFtools to keep biallelic sites (-m 2 -M 2) missing in fewer than 20% of the sampled individuals ('F_MISSING < 0.20'), with minor allele frequency of at least 0.05 (--min-af 0.05, --max-af 0.95), and with a sequencing quality score of at least 30 ('QUAL > 30'; Danecek et al. 2021). This filtering resulted in 2,999,708 variants in 298 individuals with an average of 21% missing data.

Telomere length measurement with WGS data

We measured telomere length from bam files using Telseq v0.0.2 (Ding et al. 2014), a widely used software developed specifically to calculate telomere length from whole-genome sequence data (Taub et al. 2022, Igoshin et al. 2023). Previous comparative analyses found that Telseq is highly correlated with qPCR measurements of telomere content on a panel of cell lines and cell strains, with R-squared values of 0.89 to 0.92 (Lee et al. 2017). Telseq was also previously validated using 260 leukocyte samples from the TwinsUK cohort, where its estimated

mean telomere length was compared to Telomere Restriction Fragment (TRF) estimates (Ding et al. 2014). Although TelSeq estimates were consistently shorter than TRF estimates, their correlation remined stable across a range of predefined numbers of telomeric repeats (Spearman's Q = 0.6).

Telomere length calculated from Telseq is the cumulative length of telomere repeats normalized based on the GC composition of total reads (48-52%), ensuring accurate telomere length estimation by accounting for GC bias. We modified parameters in the Telseq source code to adapt it to the yellow warbler genome, which includes changing the number of chromosomal ends, read length, and total GC content (bp). The parameters TELOMERE_ENDS, READ_LENGTH and GENOME_LENGTH_AT_TEL_GC were set equal to 62, 100, and 143831148, respectively. We calculated the latter by measuring the total length of 150 base pair windows in the yellow warbler genome with a GC content between 48% and 52%. We then calculated the residuals for a linear mixed model with telomere length as the response variable and sex and beak size as independent variables. This allowed for use to account for differences in sex and body size without identifying them as covariates, which we cannot do in the software for which our GWAS was conducted.

Genome-wide association analysis (GWAS) of bill depth and telomere length

We used a genome-wide association study (GWAS) to identify loci associated with bill depth and telomere length phenotypes (Figure 1.1a). We applied Bayesian sparse linear mixed models using GEMMA v0.98.3 (bslmm; Zhou et al. 2013) to identify single gene effects. Given that we do not know the genetic basis of bill depth or telomere phenotypes, the adaptive bslmm model allows us to infer it from the data. Bslmm combines both the linear mixed models (lmm) and Bayesian variable regression models (bsvr), giving the benefits of each when the underlying

genetic basis of the trait (i.e., many genes of small effect vs. few genes of large effect) is unknown. To statistically control for population structure, we incorporated a genetic kinship matrix generated with GEMMA using the 2,999,708 analyzed variants, where missing genotypes were imputed using beagle v. 4.1 (Browning and Browning 2016). We then ran the bslmm model with the kinship matrix, sampling for 5 million generations and a burn-in period of 500,000 iterations. Candidate SNPs associated with telomere length or bill morphology were retained when they had a posterior inclusion probability (PIP) threshold > 0.01. To calculate distance between loci, we placed the scaffold positions in the zebra finch (Taeniopygia guttata) chromosomal order using SatsumaSyteny2 (Grabherr et al. 2010) prior to the analyses. To identify genes located near outlier SNPs generated using GWAS, we downloaded Ensemble gene predictions for the zebra finch (taeGut3.2.4, GCF_000151805.1)). We then used the bedtools - closest (v2.30.0; Quinlan 2014) to find genes closest to the candidate variants and retained those that were within 50kb of the candidate loci (Figure 1.2b).

Environmental variables underlying bill-depth loci important to individual quality

To identify the environmental variables that best explained genetic variation underlying bill-depth and individual quality, we used gradient forest analysis with the R package gradientForest v0.1-34 (Figure 1.1c). The genetic data consisted of allele frequencies for 22 populations across on the yellow warbler range from 292,380 candidate loci with non-zero effects that overlapped from the GWAS on telomere length and bill depth. Climate and environmental data consisted of 19 WorldClim variables, as well as vegetation indices (NDVI and NDVIstd; Tree Cover; Carrol et al. 2004, Sexton et al. 2013), elevation data (https://www.usgs.gov/centers/eros/science/national-land-cover-database), and a measure of surface moisture characteristics (QuickSCAT from http:// scp.byu.edu). To create a ranked list of

environmental variables based on the relative predictive power of all environmental variables, we ran gradientforest over 100 trees. To visualize the predicted associations between genetic variation in bill depth loci important to individual quality and environmental variation across space, we used the resulting gradient forest model to predict the association between environmental variables at 100,000 random points across the yellow warbler breeding range and plotted the relationships using principal component analysis (PCA). To visualize the different adaptive environments across the breeding range, we assigned colors to the breeding range based on the top three principal component axes.

To validate the association between allele frequencies in bill-depth loci important to individual quality, we calculated the allele frequencies for the top loci that overlapped for bill depth and telomere length for each of our 22 sample locations. Standard linear regression was then used to test for associations between allele frequencies and environmental variation at the top four uncorrelated climate variables using the Benjamin and Hochberg false discovery rate procedure to correct for multiple testing for each locus (Figure 1.1d).

Effects of phenotype-environment mismatch on telomere length

To compare the current and pre-climate-change associations between phenotype and environment, we used data from Wiedenfeld (1991) which includes morphometric measurements from 153 yellow warblers captured between 1873 and 1987 (Figure 1.1I). As a body-size measurement was not included in the historic dataset, we instead used wing-chord as a proxy for body size to calculate body-size corrected bill depth in historic and current samples. Using locations of capture, we extracted historical monthly climate data from Worldclim CRU-TS 4.06 (Harris et al. 2020) downscaled with WorldClim 2.1 (Fick et al. 2017) for the breeding months of May, June, and July for each sample between the years of 1901 – 1950, which we then averaged.

As bioclim variables are not available for historic time-periods, we used an average that captured the most important environmental variable found in the GEA. We then used the 'lm' function in R version 3.5.3 (https://www.R-project.org) to fit linear models to test the association between bill depth and the environment for both our historic and contemporary samples (Figure 1.1e-f). We then calculated the residuals from the contemporary association to the historical line of best fit (Figure 1.1g). We used those residuals as a measure of change between the historic and contemporary relationship between bill depth and climate, where a larger residual means a bigger mismatch between bill depth and the environment, relative to what we assume is the pre-climate change optimal (Figure S1.1).

To test if the mismatch between bill depth and environment influences telomere length, which we use as a proxy for individual quality, we used an information theoretic approach for model selection and ranking (Burnham and Anderson 2002) using the package AICcmodavg v2.3-2 in R (Figure 1.1h). Using the 'lm' function, we constructed a set of linear models with telomere length as our response variable. Our candidate model set included a residual effect model, an environment effect model, and a bill depth effect model. As all our predictor variables have the potential for additive and interactive effects, all combinations of predictor variables were included in the candidate set. A null model was also included.

Results

Genome-wide association analysis (GWAS) of telomere length and bill depth phenotypes

In the bill depth GWAS, a median of 66% of phenotypic variation was explained by the genotype (95% CI 0.08 – 0.99), of which 45% was explained by SNPs with non-zero effects, but the credible intervals on both estimates were very high (95% CI 0.005 – 0.94). Approximately 40% of the variants had non-zero effects (n= 1,069,830), however 67 were considered to have

major effects. We defined the top candidate SNPs as those that were found with sparse effects in at least 1% of the Markov Chain Monte Carlo (MCMC) runs of a single chain (PIP>0.01), after controlling for population structure (Figure 1.2A). We identified five candidate SNPs, with the strongest statistical association observed for a SNP on chromosome 4, located within the intronic region of the CCDC109B gene (Table 1.1). One of the remaining four top candidate SNPs was found on chromosome 13 located within the intronic region of GABRB2, while the remaining three were found on chromosomes 2 and 18, within the intronic and regulatory regions of uncharacterized proteins. Of the 5 top candidate SNPs, only one overlapped with non-zero effect loci identified in the telomere GWAS, within the CCDC109B gene estimated (Table 1.1).

In the telomere length GWAS, a median of 68% of phenotypic variation was explained by the genotype (95% CI 0.22 - 0.99), of which 74% was explained by SNPs with non-zero effects, but the credible intervals on both estimates were very high (95% CI 0.24 – 0.98). Approximately 27% of the variants had non-zero effects (n=733,082), however only 24 were considered to have major effects. Twenty-nine variants were found with sparse effects in at least 1% of the MCMC runs (PIP>0.01), after controlling for population structure (Figure 1.2b). Of the 29 variants, 5 are associated with genes related to beak morphology or craniomorphology (Table 1.1). The strongest effect was found for a SNP on chromosome 3, within the ppp1cb gene. The remaining 28 top candidate SNPs were found spread across the genome. Of the other four SNPs associated with bill morphology or craniomorphology, the first two were found on chromosome 2, within the intronic regions of the Rims2 and SKAP2 genes. The third was found on chromosome 3, within the intronic region of ppp1cb gene, and the fourth was found on chromosome 7, within the intronic region of the MGAT5 gene. Of the 29 top candidate SNPs, 17 overlapped with non-zero effect loci identified in the bill-depth GWAS.

Environmental variables underlying bill-depth loci important to individual quality

While previous work has used gradient forest to rank which environmental variables are most important to describing patterns of genetic variation across space (e.g., Tigano et al. 2024, Ruegg et al. 2018), here we use gradient forest to identify environmental variables associated specifically with loci underlying bill depth and important to individual quality. To do this, we used the 292,380 overlapping SNPs with non-zero effects between the bill-depth and telomere length GWAS. This use of gradient forest allows us to focus on environmental drivers of local adaptation in a specific phenotype known to have important fitness effects.

Overall, our GEA analysis found a strong relationship between environmental variables and genomic variation underlying bill-depth loci important to individual quality. Precipitation variables did best at explaining genomic variation, with 6 of the 10 most important predictors in our model representing precipitation measurements (Figure 1.3a). The top four uncorrelated explanatory variables in our model were BIO18, BIO16, BIO14, and BIO3, which are precipitation of the warmest quarter, precipitation of the wettest quarter, precipitation of the driest month, and isothermality, respectively (Figure 1.3b). Spatial visualization of these variables indicated that the climate transitions to more precipitation of the warmest quarter with greater precipitation seasonality and less isothermality moving from East to West (Figure 1.3c).

We used the top-ranking SNPs from each GWAS that also had a non-zero effect in the other phenotype (1 for the bill-depth GWAS and 15 for the telomere length GWAS) to independently validate the association of top candidate SNPs with the top four uncorrelated environmental variables (Figure 1.4, Table S1.1-S1.4). Of the 16 top candidate SNPs, 3 had significant associations between allele frequency and one of the top environmental variables, and two of those were associated with a known gene (MGAT5 and RIMS2; Figure 1.4).

Effects of phenotype-environment mismatch on telomere length

To test if the mismatch between bill depth and environment influences telomere length, we used an information theoretic approach and found that the top ranked model, which also carried a majority of the model weight, included a three-way interaction between residuals, climate, and bill depth (Akaike; w_i=0.36; Table S1.5). To try and disentangle the 3-way interaction, we subset the data to only include negative residuals. As telomere length increases with increasing precipitation and increasing bill depth (Figure S1.2 and S1.3), we expected that in places that are drier and where bills are too shallow (samples with negative residuals), telomere length will be shortest. Focusing on the relationship between telomere length and residuals in the subset data, we found a significant negative association (p=0.013; Figure 1.5).

Discussion

In this study, we explore the connections between genetic, phenotypic, and environmental drivers of natural selection in the yellow warbler, a species with known linkages between climate change induced drying and population decline (Bay et al. 2018). Through GWAS, we identified candidate genes associated with bill morphology and individual quality, several of which have been linked to craniomorphology in other species. Additionally, GEA analyses showed that allele frequency variation within these candidate bill genes was strongly correlated with precipitation across the breeding range, with loci linked to larger bills more prevalent in dryer areas. Comparing current relationships between bill depth and precipitation with pre-climate change baselines revealed that contemporary birds with shallower bills in drier areas are experiencing more stress, as indicated by shorter telomeres. Together these findings indicate that climate change-induced drying may be exerting selective pressure on bill depth, especially in the drier regions of the range. Overall, our results support the hypothesis that bill depth mediates local

adaptation to varying precipitation regimes in yellow warblers, and that maladaptation resulting from climate change-induced drying may contribute to observed population declines.

In the first part of this study, we used GWAS to investigate the relationships between genotype and phenotype in the yellow warbler, focusing on bill shape and individual quality as the phenotypes (with telomere length as a proxy). The combined results from these analyses identified candidate genes associated with cranial morphology, thermoregulation, and bill shape. From these GWAS, we identified significant associations between genetic variation and our phenotypes of interest in 5 genes, 1 of which, ppp1cb, is associated with craniomorphology in humans (Lin et al. 2018, Vaneynde et al. 2022). We also identified significant associations with the SKAP2 gene, which is linked to beak shape and diversification across 72 bird species (Yusef et al. 2020), Rims2, which is associated with craniomorphology in birds (Abernathy 2021, and MGAT5 which is associated with craniomorphology in humans (Timberlake et al. 2023). Additionally, we identified the CCDC109B gene, which is thought to be involved in metabolic processes (e.g., Gherardi et al. 2020, Houlihan 2013), feeding efficiency (Salleh et al. 2018), and stress induced thermoregulation (Moisiadis et al. 2017). Such associations may indirectly influence bill morphology through the efficiency with which a bird can exploit available food sources (e.g., Grant and Grant 1993) and/or thermoregulate through the surface area of their bill when faced with heat stress (e.g., Tattersal et al. 2017). While further research is needed to confirm the roles these genes play in shaping bill morphology, the fact that our candidate genes were identified in both the bill shape and individual quality (telomere) GWAS adds additional support to the idea that these genes are not only involved in bill morphology but also important to fitness.

While the first part of our study focused on identifying genes associated with bill shape and individual quality in 121 individuals from two breeding populations, the second part identified environmental variables potentially driving patterns of genetic variation in these genes across 22 populations spanning the breeding range. Our landscape genomic analysis revealed that the top five environmental predictors of genetic variation at bill-linked loci were associated with precipitation, with the top predictor being precipitation of the warmest quarter (BIO18; Fig. 3A). If bill shape plays a role in local adaptation as has been suggested by past work in this system (Bay et al. 2021), we predicted that genetic variation in bill-linked loci would correlate with precipitation across the range. Consistent with this prediction, we found that allele frequency variation was significantly associated with precipitation in 3 of the 17 bill-linked loci identified via GWAS. While past research has shown an association between genome-wide genetic variation and precipitation in yellow warblers (Bay et al. 2018), here we take this one step further by identifying the association between precipitation and genetic variation in genes specifically linked to bill morphology in the yellow warbler. Specifically, allele frequency in MGAT5 and Rims2, genes known to be associated with craniomorphology, are significantly associated with precipitation of the warmest quarter (BIO18) and isothermality (BIO3), respectively (Fig. 2.3). The link between precipitation and genetic variation at genes putatively affecting bill morphology lends further support to the idea that changes in precipitation place selective pressure on yellow warblers across time and space.

The link between precipitation and genetic variation in bill-linked loci make sense considering other research showing that bill morphology plays an important role in heat retention and dissipation as well as water retention in arid environments (e.g., Symonds and Tattersall 2010, Tattersall et al. 2017, Greenberg et al. 2012). In small endotherms with high metabolic

rates, such as yellow warblers, water loss due to evaporation from the skin and respiratory tract can be very high (Speakman and Król 2010). Beaks, however, are impermeable to evaporative water loss due to their keratin covering and are therefore more effective at dry heat dissipation than other body parts. Hence, larger bills allow for more water savings as more dry heat is dissipated. For example, in song sparrows, a 13.1% increase in bill surface area was estimated to reduce water loss requirements by 7.7% Greenberg et al. 2012). Similarly, in California savannah sparrows, a 7.37% increase in bill size resulted in an estimated 16.2% reduction in water loss (Benham and Bowie 2021). Thus, one likely explanation for the link between genetic variation in bill-linked loci and precipitation described herein is that bill depth in the yellow warbler is important for dissipating heat and retaining water in the hottest and driest areas.

Our modern-historical bill size comparison illustrates that climate-change-induced disruptions to the relationships between genotype (bill-linked loci), phenotype (bill depth) and the environment (precipitation) may lower individual quality and result in population declines. Although there are few cases where testing historical associations between morphology and climate are possible, the availability of historical bill measurements of yellow warblers across the breeding range allowed us to compare pre-climate change and contemporary associations between bill depth and breeding season precipitation. We predicted that if bill shape is important to local adaptation and climate change has resulted in maladaptation, then deviations from the pre-climate change optima would correlate with decreases in individual quality. In keeping with this prediction, our results support the idea that in areas that have gotten drier over time, individuals with shallower bills than expected based on the pre-climate change baselines are experiencing significantly more stress (had shorter telomeres) (Fig. 2.5). As telomeres are suggestive of individual quality, these results support the idea that yellow warblers in areas that

have gotten drier may be unable to adapt rapidly enough to keep pace with drying environments, which may increase stress and lower fitness. Overall, the impact of climate change induced drying on individual quality may help explain why an increase in drying is associated with population decline in this species (Bay et al. 2018). Overall, these results lend further support to the idea that larger bills are an adaptation to arid environments through their functioning in heat dissipation and water retention, and that climate change induced increases in aridity may result in maladaptation.

Conclusion

Clear examples of the links between genotype, phenotype, and the environmental drivers of local adaptation are rare in wild populations, and examples of the effects of maladaptation are even rarer. Here, we combine GWAS and GEA analyses to identify genes underlying bill shape in the yellow warbler and examine the role of precipitation in explaining genetic variation within a subset of these bill-linked genes. Using telomere length as a proxy for individual quality, we show that rapid, climate change-induced drying, without corresponding shifts in bill depth, increases stress and likely contributes to observed population declines. Overall, this study represents an important test of the putative links between genotype, phenotype, and the environmental drivers of natural selection. As changes in climate continue to disrupt patterns of local adaptation, this research can serve as a model for assessing the impacts of such disruptions in free-living species where field-based assessments of individual quality are not feasible.

Figures and Tables

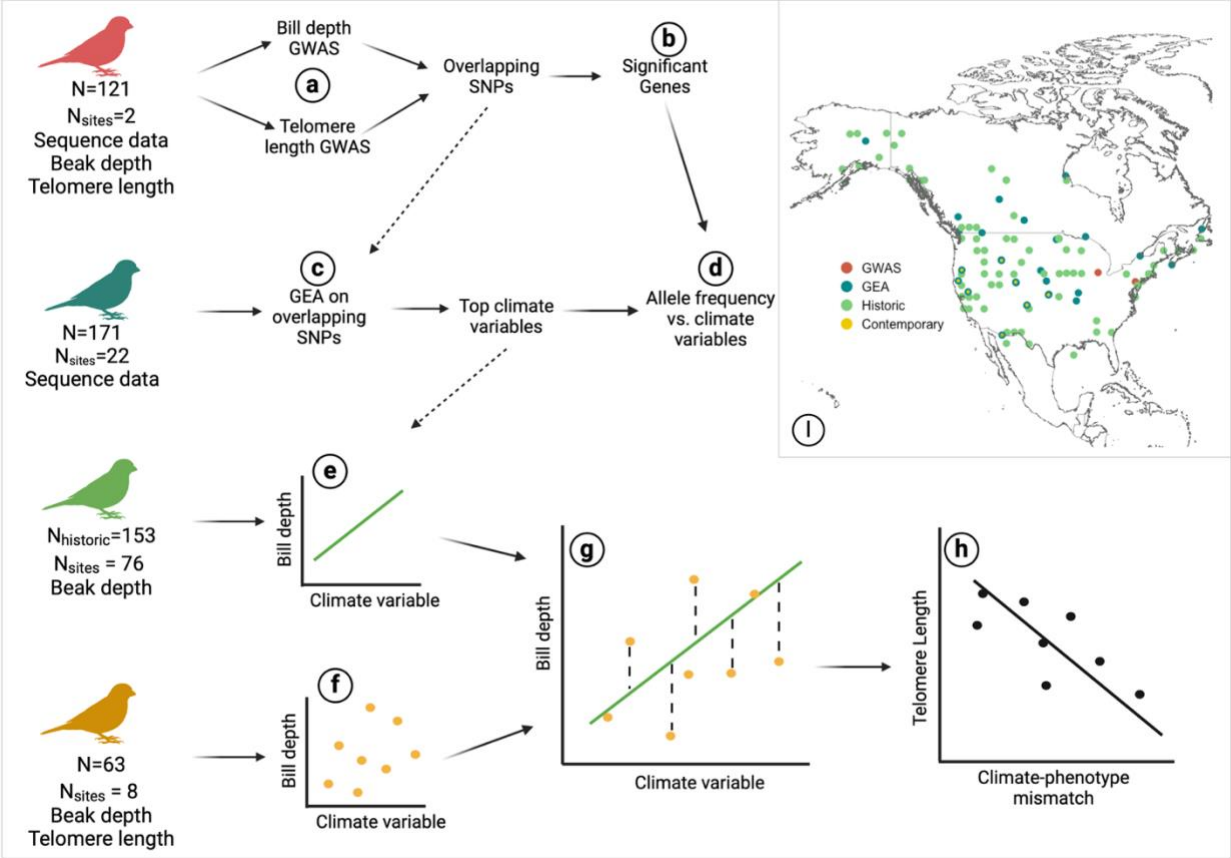

Figure 1.1. Workflow for study connecting the genotype, phenotype, and environmental components of local adaptation in the yellow warbler (Setophaga petechia), as well effects of maladaptation to climate change. A) We first conduct two separate genome-wide association studies (GWAS) on 121 reference individuals from one genetically distinct population to identify a suite of loci related to both bill depth and telomere length. B) Using the results of the GWAS, we find overlapping SNPs with non-zero effects on both bill depth and telomere length. For SNPs with significant effects on at least one of the phenotypes of interest, we then investigate associated genes. C) On the overlapping SNPs from both GWAS, we then run a gene-environment analysis (GEA) on 171 individuals from across the yellow warbler range to find environmental variables associated with bill depth and telomere length-associated genomic variation. D) We then aim to validate the significant genes found in B by looking at the relationship between allele frequencies and values of the top climate variables found in C. E) Using 153 historic yellow warbler samples from across the breeding range, we then analyzed the relationship between bill depth and the top climate variable from C, to find the line of best fit. F) Similarly, we looked at 63 contemporary yellow warbler samples from across the breeding range (samples overlap from C) and analyzed the relationship between bill depth and the top climate variable from C. G) We then measured the distance from the line of best fit in E to each point in F to quantify climate-phenotype mismatch. H) Finally, we analyze the association between climate-phenotype mismatch and telomere length to find if distance from the optimal climate-phenotype association is negatively associated with individual quality as we predict. I) Samples

span the breeding range of the yellow warbler. The map shows the distribution of the samples for each of associated analysis. The contemporary samples are yellow with a blue border as they are samples also used in the GEA.

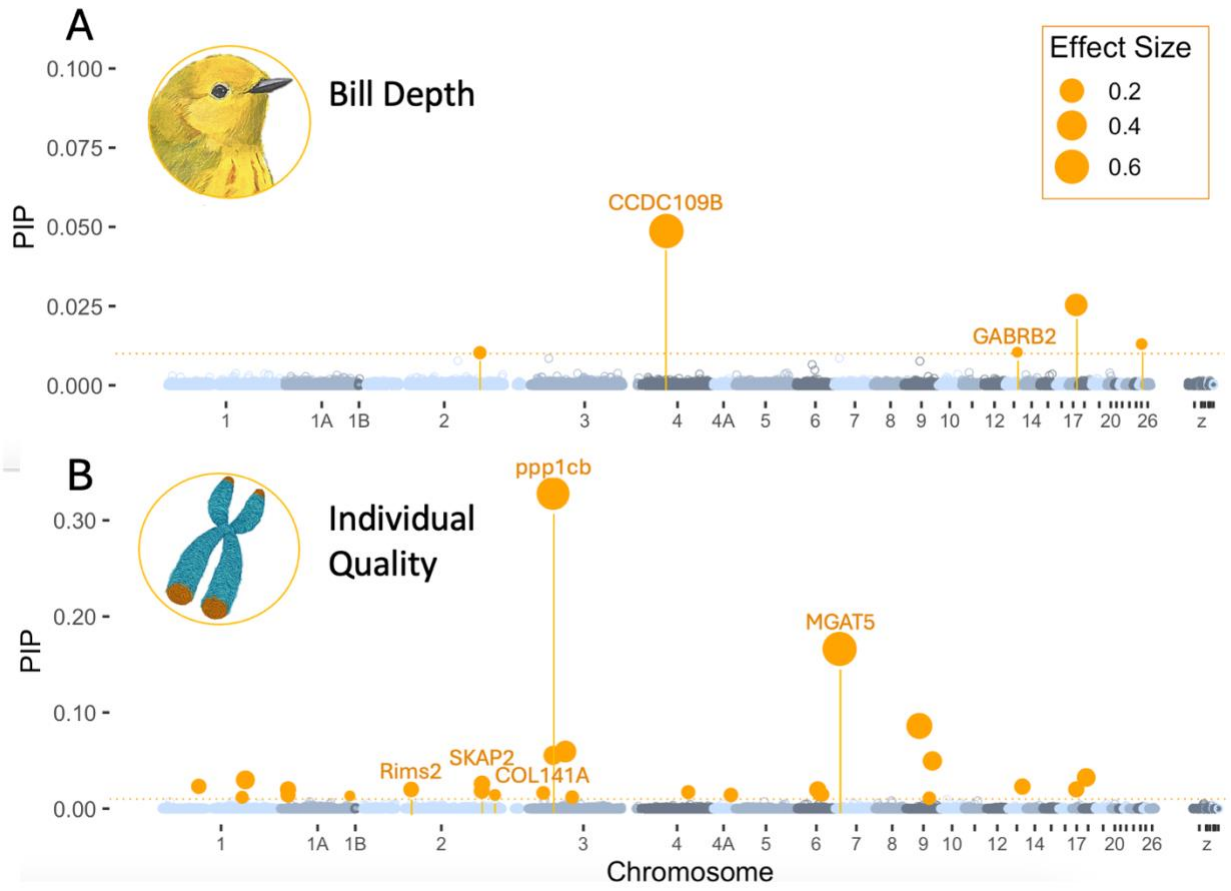

Figure 1.2. Manhattan plots of genome-wide association results. (A) GWAS results for bill depth with SNPs associated with known genes labelled. (B) GWAS results for telomere length (a proxy for individual quality), with genes related to bill morphology and/or craniomorphology labelled. Orange highlights the top candidate SNPs found with sparse effects in at least 1% of the MCMC runs (PIP>0.01), after controlling for population structure. The size of the top candidate SNPs indicates the effect size. Alternating blue and gray colors indicate chromosomes.

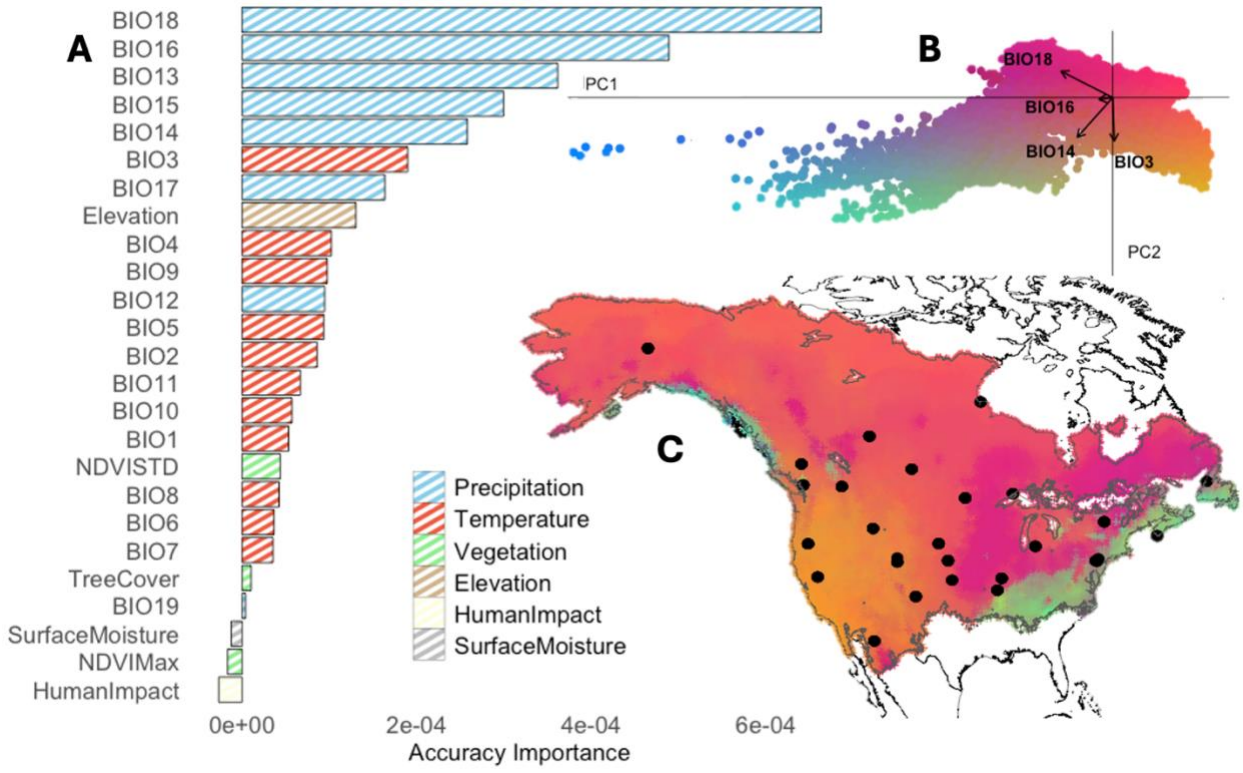

Figure 1.3. (A) Ranked importance of environmental variables based on gradient forest analysis shows that climate, especially precipitation, strongly explains genomic variation related to bill-depth-linked loci important to individual quality. (B) Principal components analysis (PCA) of transformed climate where arrows show the loading of the top 4 uncorrelated climate variables: BIO18 (precipitation of warmest quarter), BIO16 (precipitation of wettest quarter), BIO14 (precipitation of driest month), and BIO3 (isothermality). (C) Gradient forest-transformed climate variables show climate adaptation across the breeding range. Points on map reflect sampled locations. Colors are based on the PCA in panel B, and show genetic variation is generally associated with drier conditions in the western portion of the yellow warbler breeding range and wetter conditions in the eastern portion of the breeding range.

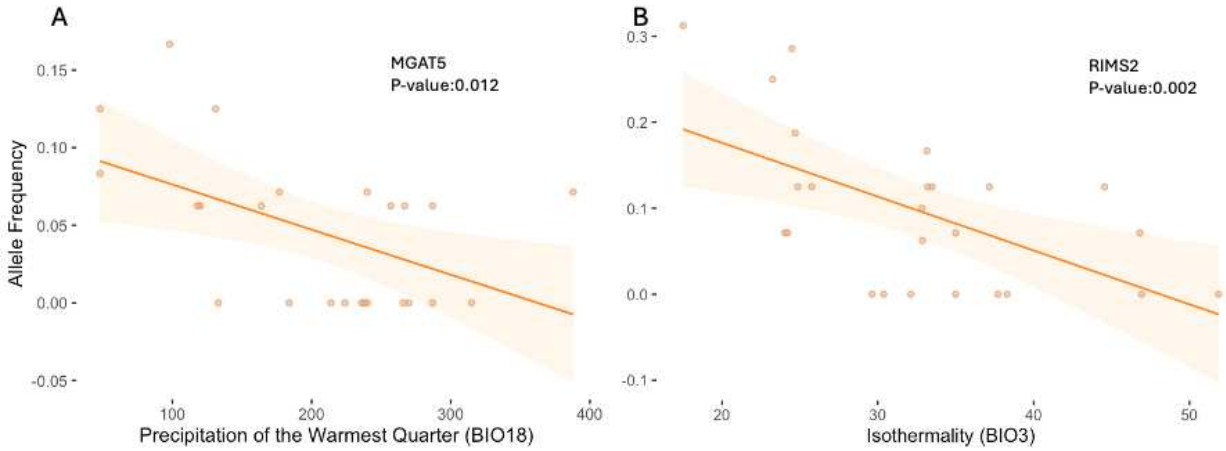

Figure 1.4. Associations between top candidate environmental variables and allele frequencies of genes important to bill depth and individual quality. (A) Association between allele frequency of MGAT5 gene and precipitation of the warmest quarter (BIO18). (B) Association between Rims2 gene and isothermality (BIO3).

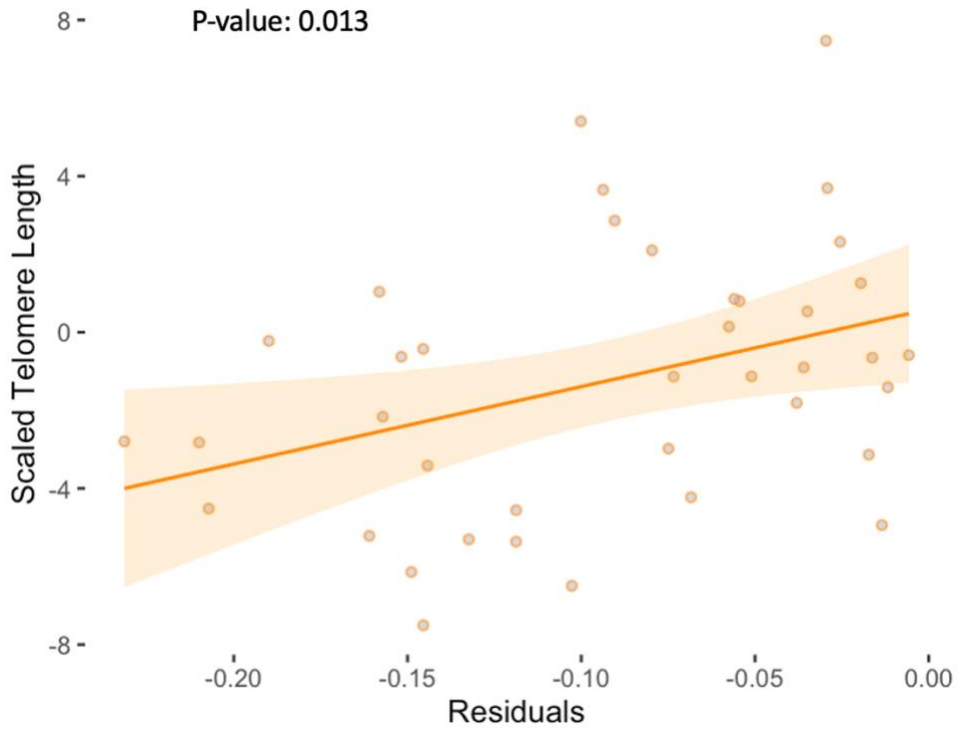

Figure 1.5. Subset data looking at association between telomere length and residuals of association between precipitation and bill depth between pre-climate and contemporary data. Data from Wiedenfeld (1991) was used to determine the pre-climate change association between bill depth and breeding-season precipitation, which we then compared to our contemporary data. We then calculated residuals from contemporary data to the line of best fit from the pre-climate data, which we used as way to measure the distance from the optimal association between precipitation and bill depth. Data was subset to only include negative residuals, which represent drying areas.

Table 1.1. Candidate genes identified from results of two GWAS analyses. In the bill depth GWAS, candidate SNPs were retained if they had sparse effects in at least 1% of the MCMC runs (PIP> 0.01). In the telomere length GWAS, candidate SNPs were retained if they had sparse effects in at least 1% of the MCMC runs and were associated with genes related to beak morphology or craniomorphology. Bslmm was used to estimate effect size and PIP.

Phenotype	Chromosome	Marker position (bp)	Gene name	Region	Distance to region	Effect size	PIP	Function	References
Bill depth	4	25876083	CCDC109B	Intron 1	0	0.007	0.049	Metabolic processes, feeding efficiency, thermoregulation	Gherardi et al. 2020, Houlihan et al. 2013, Salleh 2018, Moisiadis et al. 2017
Bill depth	18	7991726	Unknown	Regulatory	605	0.002	0.025	Unknown	
Bill depth	27	2283880	Unknown	Intron 2	0	0.001	0.013	Unknown	
Bill depth	13	11897325	GABRB2	Intron 5	0	0.001	0.010	Neurotransmission, anxiety-related behavior	Barki & Xue 2022, Fallahsharoudi et al. 2017
Bill depth	2	115455185	Unknown	Intron 1	0	0.001	0.010	Unknown	
Telomere length	3	31237157	PPP1CB	Intron 8	0	0.102	0.055	Head and neck squamous cell carcinoma, morphological adaptation in great tits	Gašperov et al. 2020, Spurgin et al. 2020
Telomere length	2	52445219	SKAP2	Intron 1	0	0.042	0.020	Elevated rates of protein evolution associated with hot- spots of beak shape morphological diversification. Craniofacial development.	Yusuf et al. 2020, Wilderman et al. 2024
Telomere length	2	119754048	RIMS2	Intron 2	0	0.053	0.026	Periodontitis. Head and neck squamous cell carcinoma.	Kim et al. 2021, Stransky et al. 2011
Telomere length	7	4037108	MGAT5	Intron 2	0	0.713	0.166	Craniosyntosis.	Dudakovic et al. 2021, Timberlake et al. 2023
Telomere length	8	334380	DNM3	Intron 2	0	0.011	0.006	Hypoxic adaptation in chickens. Crest cushion formation in ducks. Skeletal formation in humans.	Raynes 2023, Ashraf et al. 2015, Lefroy et al. 2018

LITERATURE CITED

Abernathy, E. (2021). The Genomic Basis of Population and Adaptive Divergence in Buteo Sister Species Across Multiple Evolutionary and Geographic Scales. University of California, Davis.

Angelier, Frédéric, et al. "Is telomere length a molecular marker of individual quality? Insights from a long-lived bird." Functional Ecology 33.6 (2019): 1076-1087.

Bay, R. A., Harrigan, R. J., Underwood, V. L., Gibbs, H. L., Smith, T. B., & Ruegg, K. (2018). Genomic signals of selection predict climate-driven population declines in a migratory bird. Science, 359(6371), 83-86.

Bay, R. A., Karp, D. S., Saracco, J. F., Anderegg, W. R., Frishkoff, L. O., Wiedenfeld, D., ... & Ruegg, K. (2021). Genetic variation reveals individual-level climate tracking across the annual cycle of a migratory bird. Ecology Letters, 24(4), 819-828.

Benham, P. M., & Bowie, R. C. (2021). The influence of spatially heterogeneous anthropogenic change on bill size evolution in a coastal songbird. Evolutionary Applications, 14(2), 607-624.

Blackburn, E. H., & Szostak, J. W. (1984). The molecular structure of centromeres and telomeres. Annual review of biochemistry, 53(1), 163-194.

Bolger, A. M., Lohse, M., & Usadel, B. (2014). Trimmomatic: a flexible trimmer for Illumina sequence data. Bioinformatics, 30(15), 2114-2120.

Bonar, M., Anderson, S. J., Anderson Jr, C. R., Wittemyer, G., Northrup, J. M., & Shafer, A. B. (2022). Genomic correlates for migratory direction in a free-ranging cervid. Proceedings of the Royal Society B, 289(1988), 20221969.

Bosse, M., Spurgin, L. G., Laine, V. N., Cole, E. F., Firth, J. A., Gienapp, P., ... & Slate, J. (2017). Recent natural selection causes adaptive evolution of an avian polygenic trait. Science, 358(6361), 365-368.

Browning, B. L., & Browning, S. R. (2016). Genotype imputation with millions of reference samples. The American Journal of Human Genetics, 98(1), 116-126.

Burnham KP, Anderson DR (2002) Model selection and multimodel inference: a practical information-theoretic approach, 2nd edn. Springer, New York.

Carroll, M. L., DiMiceli, C. M., Sohlberg, R. A., & Townshend, J. R. G. (2004). 250m MODIS normalized difference vegetation index. University of Maryland, College Park, Maryland.

Chik, H. Y. J., Mannarelli, M. E., Dos Remedios, N., Simons, M. J., Burke, T., Schroeder, J., & Dugdale, H. L. (2024). Adult telomere length is positively correlated with survival and lifetime reproductive success in a wild passerine. Molecular Ecology, e17455.

Contina, A., Bossu, C. M., Allen, D., Wunder, M. B., & Ruegg, K. C. (2023). Genetic and ecological drivers of molt in a migratory bird. Scientific reports, 13(1), 814.

Cook, L. M., & Saccheri, I. J. (2013). The peppered moth and industrial melanism: evolution of a natural selection case study. Heredity, 110(3), 207-212.

Danecek, P., Bonfield, J. K., Liddle, J., Marshall, J., Ohan, V., Pollard, M. O., ... & Li, H. (2021). Twelve years of SAMtools and BCFtools. Gigascience, 10(2), giab008.

De La Torre, A. R., Wilhite, B., Puiu, D., St. Clair, J. B., Crepeau, M. W., Salzberg, S. L., ... & Neale, D. B. (2021). Dissecting the polygenic basis of cold adaptation using genome-wide association of traits and environmental data in Douglas-fir. Genes, 12(1)

Ding, Z., Mangino, M., Aviv, A., UK10K Consortium, Spector, T., & Durbin, R. (2014). Estimating telomere length from whole genome sequence data. Nucleic acids research, 42(9), e75-e75.
Epel, E. S., Blackburn, E. H., Lin, J., Dhabhar, F. S., Adler, N. E., Morrow, J. D., & Cawthon, R. M. (2004). Accelerated telomere shortening in response to life stress. Proceedings of the National Academy of Sciences, 101(49), 17312-17315.
Fick, S.E. and R.J. Hijmans, 2017. WorldClim 2: new 1km spatial resolution climate surfaces for global land areas. International Journal of Climatology 37 (12): 4302-4315.
Froy, H., Underwood, S. L., Dorrens, J., Seeker, L. A., Watt, K., Wilbourn, R. V., ... & Nussey, D. H. (2021). Heritable variation in telomere length predicts mortality in Soay sheep. Proceedings of the National Academy of Sciences, 118(15), e2020563118.
Gherardi, G., Monticelli, H., Rizzuto, R., & Mammucari, C. (2020). The mitochondrial Ca2+ uptake and the fine-tuning of aerobic metabolism. Frontiers in physiology, 11, 554904.
Grabherr, M. G., Russell, P., Meyer, M., Mauceli, E., Alföldi, J., Di Palma, F., & Lindblad-Toh, K. (2010). Genome-wide synteny through highly sensitive sequence alignment: Satsuma. Bioinformatics, 26(9), 1145-1151.
Grant, B. R., & Grant, P. R. (1993). Evolution of Darwin's finches caused by a rare climatic event. Proceedings of the Royal Society of London. Series B: Biological Sciences, 251(1331), 111-117.
Greenberg, R., Cadena, V., Danner, R. M., & Tattersall, G. (2012). Heat loss may explain bill size differences between birds occupying different habitats. PloS one, 7(7), e40933.
Greenberg, R., Danner, R., Olsen, B., & Luther, D. (2012). High summer temperature explains bill size variation in salt marsh sparrows. Ecography, 35(2), 146-152.
Harris, I., Osborn, T.J., Jones, P.D., Lister, D.H. (2020). Version 4 of the CRU TS monthly high-resolution gridded multivariate climate dataset. Scientific Data 7: 109.
Hess, J. E., Zendt, J. S., Matala, A. R., & Narum, S. R. (2016). Genetic basis of adult migration timing in anadromous steelhead discovered through multivariate association testing. Proceedings of the Royal Society B: Biological Sciences, 283(1830), 20153064.
Houlihan, P. R. (2013). The role of mitochondrial restructuring in neuronal calcium homeostasis and excitotoxicity (Doctoral dissertation, University of Iowa).
Igoshin, A. V., Yudin, N. S., Romashov, G. A., & Larkin, D. M. (2023). A multibreed genome-wide association study for cattle leukocyte telomere length. Genes, 14(8), 1596.
Jun, G., Wing, M. K., Abecasis, G. R., & Kang, H. M. (2015). An efficient and scalable analysis framework for variant extraction and refinement from population-scale DNA sequence data. Genome research, 25(6), 918-925.
Keller, A. G., Dahlhoff, E. P., Bracewell, R., Chatla, K., Bachtrog, D., Rank, N. E., & Williams, C. M. (2023). Multi-locus genomic signatures of local adaptation to snow across the landscape in California populations of a willow leaf beetle. Proceedings of the
Korte, A., & Farlow, A. (2013). The advantages and limitations of trait analysis with GWAS: a review. Plant methods, 9, 1-9.
Köster, J., & Rahmann, S. (2012). Snakemake—a scalable bioinformatics workflow engine. Bioinformatics, 28(19), 2520-2522.
Lamichhaney, S., Berglund, J., Almén, M. S., Maqbool, K., Grabherr, M., Martinez-Barrio, A., ... & Andersson, L. (2015). Evolution of Darwin's finches and their beaks revealed by genome sequencing. Nature, 518(7539), 371-375.

Lamichhaney, S., Han, F., Berglund, J., Wang, C., Almén, M. S., Webster, M. T., ... & Andersson, L. (2016). A beak size locus in Darwin's finches facilitated character displacement during a drought. Science, 352(6284), 470-474.

Le Vaillant, M., Viblanc, V. A., Saraux, C., Le Bohec, C., Le Maho, Y., Kato, A., ... & Ropert-Coudert, Y. (2015). Telomere length reflects individual quality in free-living adult king penguins. Polar Biology, 38, 2059-2067.

Lee, M., Napier, C. E., Yang, S. F., Arthur, J. W., Reddel, R. R., & Pickett, H. A. (2017). Comparative analysis of whole genome sequencing-based telomere length measurement techniques. Methods, 114, 4-15.

Li, H., & Durbin, R. (2009). Fast and accurate short read alignment with Burrows–Wheeler transform. bioinformatics, 25(14), 1754-1760.

Li, H., Handsaker, B., Wysoker, A., Fennell, T., Ruan, J., Homer, N., ... & 1000 Genome Project Data Processing Subgroup. (2009). The sequence alignment/map format and SAMtools. bioinformatics, 25(16), 2078-2079.

Lin, C. H., Lin, W. D., Chou, I. C., Lee, I. C., Fan, H. C., & Hong, S. Y. (2018). Epileptic spasms in PPP1CB-associated Noonan-like syndrome: a case report with clinical and therapeutic implications. BMC neurology, 18, 1-6.

Lou, R. N., & Therkildsen, N. O. (2022). Batch effects in population genomic studies with low-coverage whole genome sequencing data: Causes, detection and mitigation. Molecular Ecology Resources, 22(5), 1678-1692.

Lundregan, S. L., Hagen, I. J., Gohli, J., Niskanen, A. K., Kemppainen, P., Ringsby, T. H., ... & Jensen, H. (2018). Inferences of genetic architecture of bill morphology in house sparrow using a high-density SNP array point to a polygenic basis. Molecular ecology, *27*(17), 3498-3514.

Moisiadis, V. G., Constantinof, A., Kostaki, A., Szyf, M., & Matthews, S. G. (2017). Prenatal glucocorticoid exposure modifies endocrine function and behaviour for 3 generations following maternal and paternal transmission. Scientific reports, 7(1), 11814.

Monaghan, P. (2014). Organismal stress, telomeres and life histories. Journal of Experimental Biology, 217(1), 57-66.

Quinlan, A. R. (2014). BEDTools: the Swiss-army tool for genome feature analysis. Current protocols in bioinformatics, 47(1), 11-12.

Rodriguez, M. D., Bay, R. A., & Ruegg, K. C. (2025). Telomere Length Differences Indicate Climate Change-Induced Stress and Population Decline in a Migratory Bird. Molecular Ecology, e17642.

Ruegg, K., Bay, R. A., Anderson, E. C., Saracco, J. F., Harrigan, R. J., Whitfield, M., ... & Smith, T. B. (2018). Ecological genomics predicts climate vulnerability in an endangered southwestern songbird. Ecology letters, 21(7), 1085-1096.

Salleh, M. S., Mazzoni, G., Nielsen, M. O., Løvendahl, P., & Kadarmideen, H. (2018). Identification of expression QTLs targeting candidate genes for residual feed intake in dairy cattle using systems genomics. Journal of Genetics and Genome Research, 5(1).

Salmón, P., Jacobs, A., Ahrén, D., Biard, C., Dingemanse, N. J., Dominoni, D. M., ... & Isaksson, C. (2021). Continent-wide genomic signatures of adaptation to urbanisation in a songbird across Europe. Nature Communications, 12(1), 2983.

Santure, A. W., & Garant, D. (2018). Wild GWAS—association mapping in natural populations. Molecular ecology resources, 18(4), 729-738.

Savolainen, O., Lascoux, M., & Merilä, J. (2013). Ecological genomics of local adaptation. Nature Reviews Genetics, 14(11), 807-820.
Schweizer, T. M., & DeSaix, M. G. (2023). Cost-effective library preparation for whole genome sequencing with feather DNA. Conservation Genetics Resources, 15(1), 21-28.
Sexton, J. O., Song, X. P., Feng, M., Noojipady, P., Anand, A., Huang, C., ... & Townshend, J. R. (2013). Global, 30-m resolution continuous fields of tree cover: Landsat-based rescaling of MODIS vegetation continuous fields with lidar-based estimates of error.
Siminovitch, K. A. (2004). PTPN22 and autoimmune disease. Nature genetics, 36(12), 1248-1249.
Sork, V. L., Aitken, S. N., Dyer, R. J., Eckert, A. J., Legendre, P., & Neale, D. B. (2013). Putting the landscape into the genomics of trees: approaches for understanding local adaptation and population responses to changing climate. Tree Genetics & Genomes, 9,
Speakman, J. R., & Król, E. (2010). The heat dissipation limit theory and evolution of life histories in endotherms—time to dispose of the disposable soma theory?. Integrative and comparative biology, 50(5), 793-807.
Strickland, K., Räsänen, K., Kristjánsson, B. K., Phillips, J. S., Einarsson, A., Snorradóttir, R. G., ... & Jónsson, Z. O. (2023). Genome-phenotype-environment associations identify signatures of selection in a panmictic population of threespine stickleback.
Symonds, M. R., & Tattersall, G. J. (2010). Geographical variation in bill size across bird species provides evidence for Allen's rule. The American Naturalist, 176(2), 188-197.
Tattersall, G. J., Arnaout, B., & Symonds, M. R. (2017). The evolution of the avian bill as a thermoregulatory organ. Biological Reviews, 92(3), 1630-1656.
Taub, M. A., Conomos, M. P., Keener, R., Iyer, K. R., Weinstock, J. S., Yanek, L. R., ... & Mathias, R. A. (2022). Genetic determinants of telomere length from 109,122 ancestrally diverse whole-genome sequences in TOPMed. Cell Genomics, 2(1).
Tigano, A., Weir, T., Ward, H. G., Gale, M. K., Wong, C. M., Eliason, E. J., ... & Russello, M. A. (2024). Genomic vulnerability of a freshwater salmonid under climate change. Evolutionary Applications, 17(2), e13602.
Timberlake, A. T., McGee, S., Allington, G., Kiziltug, E., Wolfe, E. M., Stiegler, A. L., ... & Kruszka, P. (2023). De novo variants implicate chromatin modification, transcriptional regulation, and retinoic acid signaling in syndromic craniosynostosis. The Amer
Tsai, W. L., Escalona, M., Garrett, K. L., Terrill, R. S., Sahasrabudhe, R., Nguyen, O., ... & Bay, R. A. (2024). A highly contiguous genome assembly for the Yellow Warbler (Setophaga petechia). Journal of Heredity, 115(3), 317-325.
Van der Auwera, G. A., Carneiro, M. O., Hartl, C., Poplin, R., Del Angel, G., Levy-Moonshine, A., ... & DePristo, M. A. (2013). From FastQ data to high-confidence variant calls: the genome analysis toolkit best practices pipeline. Current protocols in bioinforma
Vaneynde, P., Verbinnen, I., & Janssens, V. (2022). The role of serine/threonine phosphatases in human development: Evidence from congenital disorders. Frontiers in cell and developmental biology, 10, 1030119.
Whittemore, K., Vera, E., Martínez-Nevado, E., Sanpera, C., & Blasco, M. A. (2019). Telomere shortening rate predicts species life span. Proceedings of the National Academy of Sciences, 116(30), 15122-15127.
Wiedenfeld, D. A. (1991). Geographical morphology of male Yellow Warblers. The Condor, 93(3), 712-723.

Wilbourn, R. V., Moatt, J. P., Froy, H., Walling, C. A., Nussey, D. H., & Boonekamp, J. J. (2018). The relationship between telomere length and mortality risk in non-model vertebrate systems: a meta-analysis. Philosophical Transactions of the Royal Society B: Bi

Yusuf, L., Heatley, M. C., Palmer, J. P., Barton, H. J., Cooney, C. R., & Gossmann, T. I. (2020). Noncoding regions underpin avian bill shape diversification at macroevolutionary scales. Genome research, 30(4), 553-565.

Zhou, Xiang, Peter Carbonetto, and Matthew Stephens. "Polygenic modeling with Bayesian sparse linear mixed models." PLoS genetics 9.2 (2013): e1003264.

CHAPTER 2: TELOMERE LENGTH DIFFERENCES INDICATE CLIMATE CHANGE-INDUCED STRESS AND POPULATION DECLINE IN A MIGRATORY BIRD*

Summary

Genomic projections of (mal)adaptation under future climate change, known as genomic offset, faces limited application due to challenges in validating model predictions. Individuals inhabiting regions with high genomic offset are expected to experience increased levels of physiological stress as a result of climate change, but documenting such stress can be challenging in systems where experimental manipulations are not possible. One increasingly common method for documenting physiological costs associated with stress in individuals is to measure the relative length of telomeres – repetitive regions that "cap" the ends of chromosomes – which shortens at faster rates with more adverse conditions. Here we combine models of genomic offsets with measures of telomere shortening in a migratory bird, the yellow warbler (*Setophaga petechia*), and find a strong correlation between genomic offset, telomere length, and population decline. While further research is needed to fully understand these links, our results support the idea that birds in regions where climate change is happening faster are experiencing more stress and that such negative effects may help explain the observed population declines.

Introduction

The ability of populations to persi*st when threatened by climate change depends on their capacity for range shift (Tingley et al. 2009) or adaptation to climate in place (Beever et al. 2016,

* Rodriguez, M. D., Bay, R. A., & Ruegg, K. C. (2025). Telomere Length Differences Indicate Climate Change-Induced Stress and Population Decline in a Migratory Bird. *Molecular Ecology*, e17642.

Nicotra et al. 2015, Nogues-Bravo et al. 2018). In the past, assessments of vulnerability to climate change mostly focused on forecasting distributional changes using ecological niche modeling approaches (e.g., Cianfrani et al. 2018, Saunders et al. 2020, Thuiller et al. 2005), but such approaches do not consider the capacity for organisms to adapt (Beever et al. 2016, Nicotra et al. 2015, Rellstab 2021). In contrast, landscape genomic approaches like genomic offset use the difference between current gene-environment relationships and those modeled under future climate change scenarios to identify which populations will have the most difficulty adapting to changing climate conditions (Bay et al. 2018, Capblancq et al. 2020, Ruegg et al. 2018). These approaches use associations between genomic variation and climate variables measured where individuals are sampled to determine the genomic variation needed to adapt to current climate conditions. These associations are then projected across future predicted climate scenarios to determine the genetic shift that would be needed by populations to adapt to future conditions. The amount of genetic shift needed is the genomic offset measure, where regions with the highest genomic offset are predicted to experience the most climate induced stress in the future, and in some cases, may have already experienced population declines (Bay et al. 2018). While genomic offset methods are becoming increasingly popular for predicting climate change responses, their broadscale utility is often limited by the inability to validate model predictions.

One of the biggest challenges with genomic offset approaches is the difficulty with validating the predicted costs associated with maladaptation. In plant systems, past genomic offset studies have validated fitness effects by using phenotypic data in common garden or reciprocal transplant studies (e.g., Borrel et al. 2020, Fitzpatrick et al. 2021). For example, Borrell et al. (2019) measured fitness-related phenotypic traits in a common garden and found a significant negative relationship between genomic offset and reproductive output in *Betula nana*. Similarly,

Fitzpatrick et al. (2021) showed a negative association between genomic offset and performance in two common garden experiments. They also found that genomic offset was ultimately a better predictor of performance than differences in climate alone. Despite their value for validating genomic offset predictions, common garden studies are infeasible for many wild non-model organisms. Thus, a method for validating the predicted negative effects of genomic offset in non-model organisms would help increase its broadscale utility.

An increasingly common method for assessing the relative influence of stress on individuals across taxa that has not yet been applied to test predictions from genomic offset models is telomere length. Telomeres are protective structures that "cap" the ends of linear chromosomes and consist of tandem arrays of repetitive sequence (5'-TTAGGG-3' in vertebrates), as well as a host of associated proteins (Blackburn 1991, Blackburn 2005) REFs. Telomeres shorten with cell division (Blackburn 2005) and thus with aging. Telomeres also shorten with oxidative stress, inflammation, and a variety of lifestyle factors (REFs). Telomere shortening is associated with stress and can be accelerated by stress experienced by the individual, also known as allostatic load (McEwen and Wingfield 2003). Many environmental factors can be labeled as stressors in that they cause a physiological and behavioral change that prioritizes survival at the expense of a physiological cost (Romero 2004). Acute and chronic stress is associated with increased metabolic rate, which in turn is associated with increased mitotic and mitochondrial activity (Silverin 1986, McEwen and Wingfield 2003, Boonstra 2004, Haase et al. 2016). This increased mitochondrial activity is responsible for increased oxidative stress (Cadenas and Davies 2000), which has been labeled as one of the main drivers of telomere shortening (von Zglinicki 2000, 2002, Sozou and Kirkwood 2001, Houben et al. 2008). For example, factors such as intra and interspecies competition, pollutant exposure, and severe weather events are a few examples of

adverse environmental factors that trigger an environmentally-induced stress response (Casagrande and Hau 2019, Chatelain et al. 2020, Reichert and Stier 2017, Von Zglinicki 2002).

Telomere length is increasingly being used as a biomarker for important life-history traits such as lifespan (Bichet et al. 2020, Heidinger et al. 2012), lifetime reproductive success (Eastwood et al. 2019), and individual quality (Angelier et al. 2019, Cheron et al. 2021, Rollings et al. 2017) across a variety of taxa, from humans, to birds, to small mammals. Telomeres seem to be particularly sensitive to environmental variation at early life stages, including prior to birth/hatching (Casagrande et al. 2020, Hausmann et al. 2012, Noguera et al. 2022) via maternal effects and parental life histories (Haussmann et al. 2012, McLennan et al. 2018). Consequently, in wild populations, environmental conditions experienced during early life can generate long-lasting cohort effects on telomere length and may even have a larger impact on telomere length than current conditions (Debes et al. 2016). Thus, telomere length may represent both generational and contemporary effects of the stress induced by maladaptation to the changing climate and can serve as a method for validating predictions from genomic offset models.

The objective of this study is to expand the application of genomic offset as a tool for predicting the impacts of climate change by developing methods that can be used to test key model predictions. To achieve this, we will investigate the relationship between genomic offset, telomere length, and population decline in the yellow warbler (*Setophaga petechia)*. The yellow warbler is a migratory songbird that breeds in various habitats throughout North America and is an excellent system for this study because earlier work by Bay et al. (2018) identified patterns of genomic offset across the species range. The researchers then used the correlation between genomic offset and past population declines (1970s to present) to suggest that climate change is negatively affecting populations. However, as noted by Fitzpatrick et al. (2018), a key

assumption of this work is that past population declines resulted from past climate change-induced stress. The authors, however, failed to provide a metric for documenting such stress and did not establish the necessary correlation between past and future climate change.

In this study, we aim to test the hypothesis that genomic offset can help identify regions where climate change is negatively impacting wild populations using telomere length as a biomarker for the impacts of climate induced stress. To test this hypothesis, we measure telomere length and approximate past population trends in yellow warbler populations across regions of high and low genomic offset. If telomere length, genomic offset, and population declines are strongly correlated even after accounting for other important variables that can influence telomere shortening (such as age, sex, body size, and population level effects), then we can conclude that genomic offset results in increases in adverse conditions. Additionally, we will investigate the specific climate factors contributing to shorter telomeres and population declines in the yellow warbler system and test the relationship between past and future climate change. We focus on precipitation because previous research indicates that precipitation was highly weighted in genomic offset predictions (Bay et al. 2018). If precipitation is a main driver climate-induced stress, both population trends and telomere length should also be correlated with past precipitation. Overall, this study will help test assumptions at the core of many genomic offset predictions, thereby increasing their utility for predicting climate change impacts in wild populations.

Methods

Study Design and Sampling

We used genotypes derived from restriction-site associated DNA sequencing (RAD-Seq) data from Bay et al. (2018) on 229 individuals from 21 locations across the yellow warbler

breeding range. To estimate genomic offset, we then ran gradient forest (Fitzpatrick et al. 2021), a machine-learning regression tree-based approach implemented in the R package gradientforest (Ellis et al. 2012) on a subset of 1694 unlinked candidate single-nucleotide polymorphisms (SNPs) that were significantly associated with climatic variables based on LFMM analysis from Bay et al. (2018). We built a gradient forest model with average monthly precipitation, temperature maximum, temperature minimum, latitude, and longitude values for the months of May through July (breeding months for the yellow warbler) as environmental response variables and the candidate SNPs as predictors. Precipitation data was obtained from the CRU-TS 4.06 dataset (Harris et al., 2020) downscaled with WorldClim 2.1 (Fick and Hijmans, 2017). We then used the predict function within gradient forest to weight the environmental response variables for both current (2021-2040) and future (2041-2060) predicted climates at 10,000 random locations across the yellow warbler breeding range. We then interpolated across the entire breeding range to form a continuous map of genomic offset (Figure 2.1).

We selected sample sites for telomere measurements by using the continuous map of genomic offset and choosing areas across a gradient of genomic offset in addition to precipitation and elevation. Estimates of genomic offset were then calculated for each specific sample site. We collected blood samples for telomere measurements from each sample location spanning the breeding range of the yellow warbler once over the course of 2020 and 2021 breeding seasons. Birds were captured via mist-nets and once in hand, individuals were banded, morphological measurements were taken, and age and sex were recorded. Age was determined using plumage characteristics outlined in Pyle (1997). Due to rapid telomere shortening and variation in telomere length during early life, hatch year birds were not included in the study. Between 10 µl and 30 µl of blood was collected using brachial venipuncture and stored in Queen's lysis buffer

on ice until reaching the lab where they were stored in -20°C until extraction, which occurred within 6 months of collection (Criscuolo et al. 2009). Birds that could not be sexed in the field were sexed using PCR with the primer set CHD1F and CHD1R (Cakmak et. al 2017). Our sampling resulted in blood samples from 416 yellow warblers spanning 39 sample sites across the breeding range of the species (Figure 2.1).

Telomere Length Measurement

DNA was extracted from yellow warbler whole blood samples using DNeasy Blood and Tissue kits (Qiagen, Valencia, California) following the manufacturer's protocol. Telomere length analysis was conducted within three months following DNA extraction. A NanoDrop 8000 spectrophotometer (Thermo Scientific) was used to measure DNA concentration and quality on the same day as the telomere analysis took place. The average ratio of absorbance at 260 nm over 280 nm was used to check for protein contamination and the average ratio of absorbance at 260 nm over 230 nm was used to check for salt contamination. If either ratio of absorbance was < 1.8, the extract was excluded from further analysis (Morinha et al. 2020). DNA integrity was visually assessed on an agarose gel as recommended by Seeker (2016). Following the protocol of Criscuolo et al. (2009), telomere length was determined by quantitative real-time polymerase chain reaction (qPCR). Telomere length was calculated as the ratio (T/S) of telomere repeat copy number (T) to a control single gene copy number (S), which was standardized to a reference sample and then expressed as relative telomere length.

Glyceraldehyde-3-phosphate dehydrogenase (GAPDH) was employed as the single copy control gene. The primer sequences used to amplify the telomere track were as follows: Tel1b (5'-CGGTTTGTTTGGGTTTGGGTTTGGGTTTGGGTTTGGGTT-3') and Tel2b (5'-

GGCTTGCCTTACCCTTACCCTTACCCTTACCCTTACCCT-3'); and for amplification of GAPDH, GADPH-F (5'-GGTAGATGGGAGTTCAGTTGTG-3') and GAPDH-R (5'-AGAAACAAAGCACTGTCAGGG-3') specific primers were utilized. Multiplexed qPCR was performed using 3 µl of sample DNA at 3 ng/µl, Tel1b/Tel2b primers at a concentration of 900 nM, and GAPDH-F/GAPDH-R primers at a concentration of 400 nM in a final volume of 25µl containing 10µl of GoTaq qPCR Master Mix (Promega, Madison, Wisconsin, USA). Telomere qPCR reactions were run on a CFX96 Touch Real-Time PCR Detection System machine (Bio-Rad) using the following conditions:10 min at 95˚C followed by 30 cycles of 15 s at 95˚C, 30 s at 54.5˚C and 30 s at 72˚C. For the GAPDH amplification, 10 min at 95˚C was followed by 40 cycles of 15 s at 95˚C, 30 s at 60.5˚C and 30 s at 72˚C. DNA samples were run in triplicate and a reference sample was run on every plate to compare measurements between plates. QPCR plates included serial dilutions (0.2, 0.4, 2, 10, 30, and 50 ng) of DNA from the same reference bird to create a reference curve to control for amplifying efficiency of the qPCR. All plates had standard curves within acceptable ranges. One yellow warbler sample from our study site (but not included in our study) served as the reference sample. Overall, 416 samples across 22 qPCR plates were included. Samples were randomly distributed across plates, and sample triplicates were all run on the same plate. Coefficient of determination was > 0.99 and efficiencies within 100 ±10% (Telomere standard curve: mean = 1.99, standard deviation = 0.02; GAPDH standard curve: mean = 1.99, standard deviation = 0.02). Within sample triplicates, if the coefficient of variation was > 0.14 for a sample, one triplicate was dropped. Samples were excluded if the remaining sample duplicate coefficient of variation was still > 0.14 (Nettle et al. 2019). Average repeatability (standard deviation) of T/S values was 0.067 across all samples and was 0.045 for

reference samples across plates. Interplate repeatability based on samples measured across plates was 1.02 (95% CI [1.0026,1.0334]).

Following the methods described in Kärkkäinen et al. (2021), we validated the use of our qPCR approach at the between-population level by evaluating whether populations varied in control single gene Cq, in addition to qPCR efficiencies for both control single gene and telomere assays (Table S1.1). Control gene Cq values differed across populations ($F_{38,337} = 8.137$, $p < 0.001$), as did both control gene and telomere assay efficiencies (Control gene: $F_{38,377} = 9.95$, $p<0.001$; Telomere: $F_{38,377} = 7.527$, $p<0.001$). Thus, we added qPCR plate as a random effect in all downstream telomere analyses. In addition, relative telomere length (T/S) was calculated based on plate-specific efficiencies (Table S2.2) using the mathematical model presented in Pfaffl (2001).

Statistical Analysis

Statistical analyses were carried out using R 4.1.2 (R Core Team, 2021). The findings reported in the Bay et al. (2018) study suggest a connection between genomic offset and the decline in yellow warbler populations. To validate this assertion, it is crucial to investigate the correlation between past and future climate changes. To test this assumption, we analyzed the correlation between historic and future changes in climate for the top three uncorrelated climate variables found to be associated with yellow warbler genomic variation according to Bay et al. (2018). These climate variables were bio18 (mean monthly precipitation amount of the warmest quarter), bio15 (precipitation seasonality), and bio13 (precipitation amount of the wettest month).

The distribution of relative telomere length was right-skewed, so log relative telomere length was used in subsequent analyses. Log relative telomere length was then standardized with z-transformation using the scale()-function in R to facilitate comparison to future studies

(Verhulst 2020). We first tested for variation in telomere length across sample populations by fitting a linear mixed model with telomere length as the dependent variable, sample population as the independent variable, and qPCR plate as a random effect. We then examined whether potential population differences in telomere length could be explained by genomic offset, by using an Information-Theoretic framework in R. We used estimates of genomic offset calculated for each sample location. For this analysis, we constructed a global model consisting of variables that could be influencing telomere length within and across populations of yellow warblers on their breeding range. These predictor variables included genomic offset, age class, sex, elevation, latitude, tarsus length, and date. Our candidate model set consisted of linear mixed effects models (lmer in lme4; Bates et al. 2015) where we included study site and qPCR plate as random effects in each model.

As all our predictor variables have potential for additive effects, all combinations of the predictor variables included in the global model were compared and ranked based on AICc using the package MUMIN (Barton 2015). Two-way interactions were only included in the global model if such relationships were considered plausible a priori. A null model was included in the candidate model set. Akaike weights were used to assess the support for each model. All continuous predictors were centered and scaled but were back-transformed for plotting. Prior to model comparison, to determine independence of predictor variables, correlations between all predictor variables were checked and variance inflation factors (VIF) of the global model were checked to assess multicollinearity: all VIFs were less than 3 (Fox and Weisberg 2011). Model residuals of the global models were assessed to confirm compliance with model assumptions. The top model was estimated using maximum likelihood and the Kenward-Roger method was

used to calculate degrees of freedom of fixed factors and to assess parameter estimates and their standard errors.

To test the assumption that historical changes in precipitation are associated with population trends and telomere length, we again used an information-Theoretic framework. A global model was constructed, which consisted of variables that could be influencing yellow warbler abundance trends and telomere length across populations on their breeding range. These variables included the top three uncorrelated BIOCLIM variables found to be important to yellow warbler local adaptation in Bay et al. (2018). BIOCLIM measures are a collection of monthly climate variables made to capture environmentally important climate variation (Fick and Hijman 2017). The predictor variables were historic changes of precipitation amount of the wettest month (bio13), precipitation seasonality (bio15), and mean monthly precipitation amount of the warmest quarter (bio18), in addition to elevation and latitude variables. In analyzing telomere length, our candidate model set consisted of linear mixed effects models (lmer in lme4; Bates et al. 2015) where we included sample site as a random effect in each model. In analyzing abundance trends, our candidate model set consisted of linear models. Each candidate model set included a null model. Global model construction and model selection was conducted using the same methods described above. Yellow warbler abundance trend values for each sample location were extracted from Breeding Bird Survey (BBS) data (Ziolkowski et al. 2022).

Finally, we test the association between telomere length and abundance trends across yellow warbler populations to explore whether populations in decline also have shorter average telomere length. To do this, we analyzed the correlation between abundance trends and average telomere length across sample sites.

Results

Since genomic offset is based on future climate, and Bay et al. (2018) used future climate in their model, and current stress and past population declines are a result of past climate, we tested the assumption that past and future climates are correlated. To do this, changes in each of the top climate variables in Bay et al (2018) were compared and significant correlations found among two of the three primary bioclimatic variables (bio13, r-squared 0.76; bio15, r-squared 0.76), as well as a positive trend in the third bioclimatic variable (bio18, r-squared 0.08; Figure 2.2).

Telomere length, genomic offset, and population trends

Significant variation in telomere length across sampled populations of breeding yellow warblers ($F_{38,331} = 0.996$, $p<0.001$, Figure S2.1) was observed. Moreover, significant population differences in telomere length could be explained by genomic offset. Using an information theoretic approach, the top ranked model, which also carried a majority of the model weight, included interactive effects of genomic offset and elevation along with an additive effect of tarsus length (Akaike; w_i=0.46; Table S2.3). Conducting a standard linear regression on telomere length versus genomic offset revealed evidence of a significant decline in telomere length with increasing genomic offset estimates (p=<0.018, Figure 2.3). The interaction between genomic offset and elevation (p=0.002) provides evidence that in high elevation areas with high genomic offset, telomere length is shorter than in low elevation areas (Figure S2.2). The additive effect of tarsus length is likely related to body size differences, supporting the idea that larger birds with longer tarsi have shorter telomeres relative to smaller birds with shorter tarsi (Figure S2.3). Despite the influence of body size and elevation on telomere length, results support the idea that genomic offset is significantly linked to telomere length. Overall, while factors such as

population, elevation, and body size influence telomere length, their remains a strong correlation between telomere length and genomic offset in the direction predicted, indicating that birds in locations with high genomic offset may be experiencing more climate-induced stress.

Association between precipitation, population trends, and telomere length

To test the assumption that changes in climate are associated with abundance trends, AIC model selection was conducted. The top ranked model was an interactive model between bio15 (precipitation seasonality) and latitude (Akaike; w_i=0.33; Table S2.4), suggesting a significant decline in abundance trends with increasing precipitation seasonality (between the years 1960 – 2021) and latitude (R^2=0.38, p-value=0.044; Figure 2.4a). AIC model selection was also utilized to identify the most important climate variables associated with telomere length and, similar to the analysis on abundance, the top-ranking model was an interactive model between bio15 (precipitation seasonality) and latitude (Akaike; w_i=0.14; Table S2.5), suggesting a significant decline in telomere length with increasing precipitation seasonality (years 1960 – 2021) and latitude (R^2=0.41, p-value=0.03; Figure 2.4b). Finally, the association between telomere length and abundance trends across yellow warbler populations was tested and a significant positive correlation was observed, with abundance trends increasing with increasing telomere length (p=0.005; Fig. S2.4).

Discussion

The integration of adaptation into models of vulnerability to climate change, known as genomic offset (e.g., Hoffman et al. 2021, Layton et al. 2021, Ruegg et al. 2018), faces limitations in its widespread application due to challenges associated with validating model predictions. Specifically, organisms inhabiting regions predicted to experience high genomic offset are also projected to encounter increased climate-induced stress and decreased fitness due to climate

change, but estimating such responses is challenging in most systems. Our findings suggest that yellow warblers in regions predicted to undergo significant climate change are situated in areas that have historically encountered substantial climate change. Furthermore, birds in these regions have experienced the most significant declines in abundance and have the shortest telomeres, consistent with increased levels of stress. Overall, this work provides a valuable framework for validating assumptions at the core of genomic offset models in cases where reciprocal transplants are not possible. Results support the notion that while genomic offset models predict how organisms will fare under future climate change, they can also be used to identify regions where populations may already be experiencing climate change-induced stress in cases where past and future climate changes are correlated.

Previous studies that have used telomere shortening to assess the impacts of climate change often concentrated on single populations or lacked essential information about environmental variables crucial for local adaptation. Our approach represents a noteworthy advance for the field because it deliberately considers specific variables recognized as important for climate adaptation. For instance, studies by Zhang et al. (2018) and Eastwood et al. (2022) identified associations between temperature and telomere length within specific populations, but did not establish whether temperature is a significant factor in local adaptation, nor did they investigate how local adaptation across the landscape is predicted to change in the future. In contrast, our strategy links telomere length to precipitation, which we know from our analyses is the environmental variable most strongly associated with genomic variation across space in yellow warbler. As such, we have a strong reason to expect that variation in precipitation across the landscape helps shape patterns of local adaptation in the yellow warbler and, correspondingly, changes in precipitation over the last 30 years may result in elevated stress if

populations are unable to evolve fast enough to keep pace with such changes. Additionally, unlike past research, we show that telomere length is not only associated with changes in precipitation - the environmental variable most likely important to local adaptation in yellow warblers - but also with past population declines. While further work is needed, the finding that populations in decline also have shorter telomeres supports the idea that climate-induced stress may have long-term fitness effects in the yellow warbler. Overall, we demonstrate that measuring telomere length alongside genomic offset provides a robust framework for evaluating the impacts of climate change across diverse populations.

In birds, changes in precipitation have frequently been linked to population declines (e.g., Cruz-McDonnell et al. 2016, Iknayan and Beissinger 2018, Senapathi et al. 2011), but reasons for these association remain unclear. Precipitation plays a vital role in determining the availability of food resources for birds (e.g., Ferger et al. 2014, Wagner et al. 2020, Zhu et al. 2014), and when precipitation patterns deviate from optimal conditions, populations may experience reduced reproductive success and subsequent population declines (Anctil et al. 2014, Coe et al. 2015, Conrey et al. 2016). Building upon findings in other bird species for the relationship between precipitation, resource availability, and fitness, one hypothesis to explain our results would be that climate change induced increases in aridity across the yellow warbler breeding grounds have led to shifts in the insect and plant communities upon which yellow warblers depend for survival. While further work is necessary, such shifts in food availability may be placing increased selective pressure on bill morphology, which previous work suggests is correlated with precipitation across the breeding range in this species (Bay et al 2021). To further investigate these linkages, future research will focus on identifying recent changes in the

food resources crucial for yellow warblers during the breeding season and determining whether such changes may be placing selective pressure on bill size.

In addition to illustrating a negative association between telomere length and genomic offset, our results provide evidence for an effect of elevation, where high elevation populations in high genomic offset regions have the shortest telomeres. While the negative relationship between telomere length and elevation has been found in prior research (Stier et al. 2016), the interaction between genomic offset and elevation could be explained by mountainous areas being considered as climate "hotspots," where effects of climate change can be amplified or accelerated (Pepin et al. 2022). Therefore, yellow warbler populations that are unable to adapt to climate change may be facing even higher fitness consequences at high elevation where changes in climate are occurring more rapidly. Further, we demonstrate that genomic offset may be used to identify current regions of climate-induced stress, in cases where past and future climate change are correlated, as is the case with the yellow warbler. In addition to validating the genomic offset concept, these results support the use of genomic offset as an important tool for understanding impacts of climate change on current and future populations and informing conservation efforts.

Climate change has been observed to impact the fitness of various wild species (e.g., Benito Garzón et al. 2018, Huang and Pike 2011, Lane et al. 2012), but identifying specific ecological drivers of fitness loss can be challenging. Overall, our work supports the idea that combining telomere length measurements with data on past population trends and changes in environmental variables important to local adaptation provides a framework for assessing the impacts of climate change on wild populations. Future work will aim to clarify the relationships between genotype, phenotype, and natural selection by identifying the genes underlying bill

morphology and assessing whether genetic variation within these genes has shifted due to recent climate change.

Figures

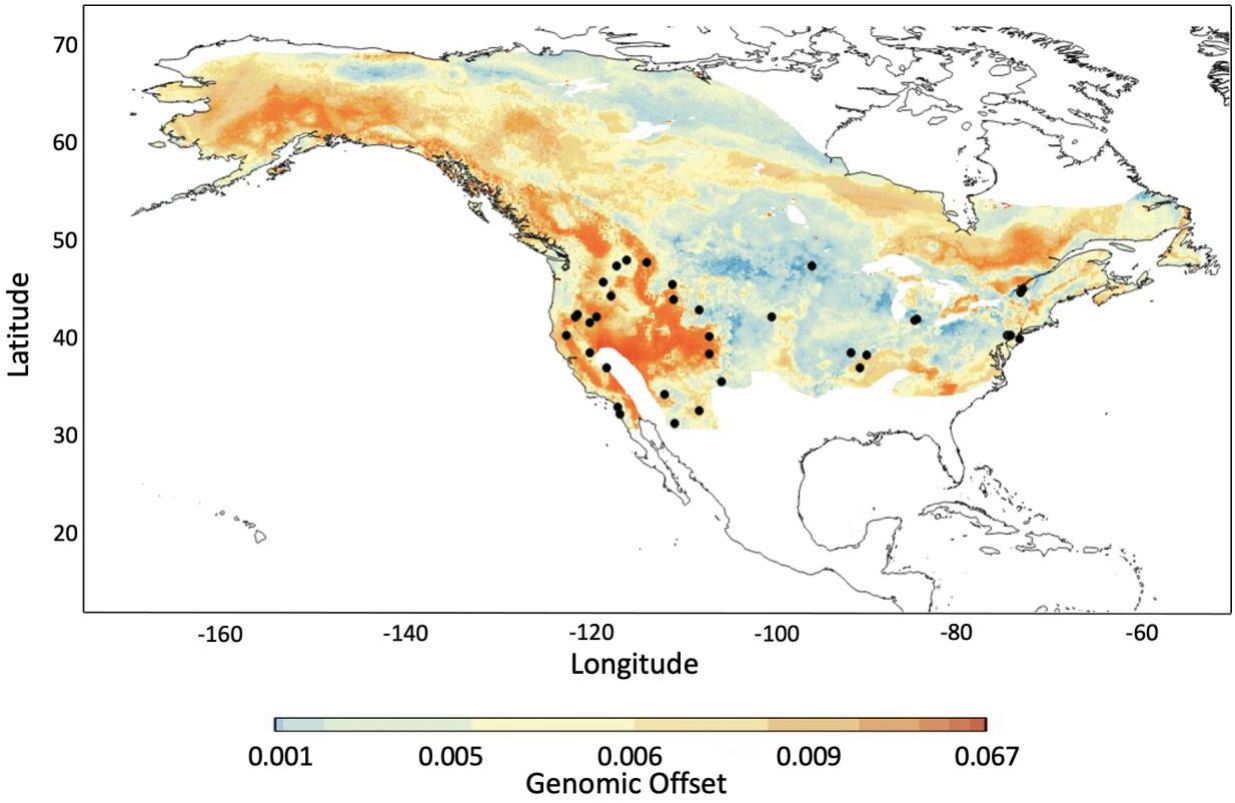

Figure 2.1. Map of the yellow warbler breeding distribution showing estimates of genomic offset based on 2050 SSP 885 projections, where cool colors indicate low genomic offset and warm colors indicate high genomic offset. Black dots are yellow warbler sampling locations.

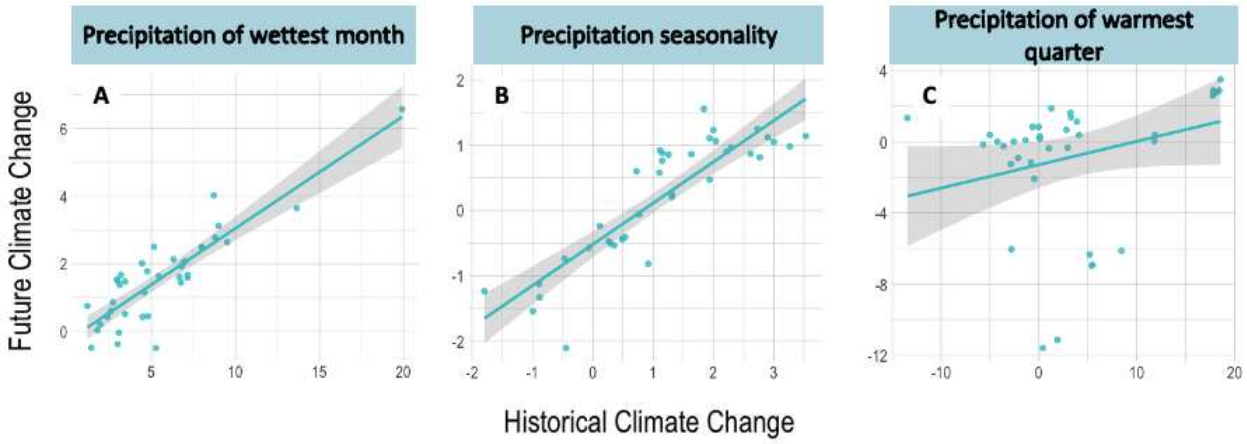

Figure 2.2. Correlation between historic and future changes in climate at 39 yellow warbler sample sites for bioclimatic variables associated with yellow warbler genomic variation of the breeding grounds. Historical climate change was calculated by subtracting historic bioclimatic variables (1970-2000) from those bioclimatic variables calculated for 2021-2040. Similarly, future changes were calculated by subtracting bioclimatic variables from 2021-2040 from future bioclimatic variables (2041-2060). We show that a) changes in historical precipitation amounts of the wettest month are associated with future projected changes (R^2=0.76, p-values=<0.001), b) changes in historical precipitation seasonality are associated with future projected changes (R^2= 0.76, p-value=<0.001), and c) changes in precipitation of the warmest quarter have an insignificant but positive trending association with future projected changes (R^2=0.08, p-value=0.078).

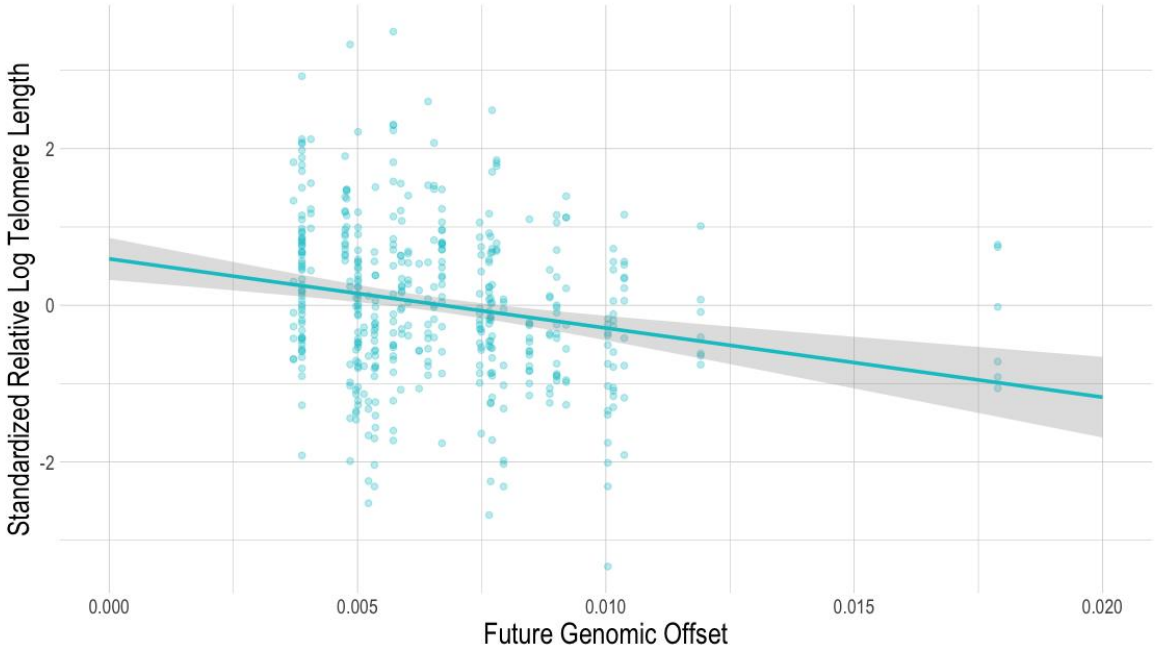

Figure 2.3. Yellow warblers (n=416) sampled in areas with high genomic vulnerability had lower standardized relative telomere length compared to those in areas of low genomic vulnerability (R^2=0.35).

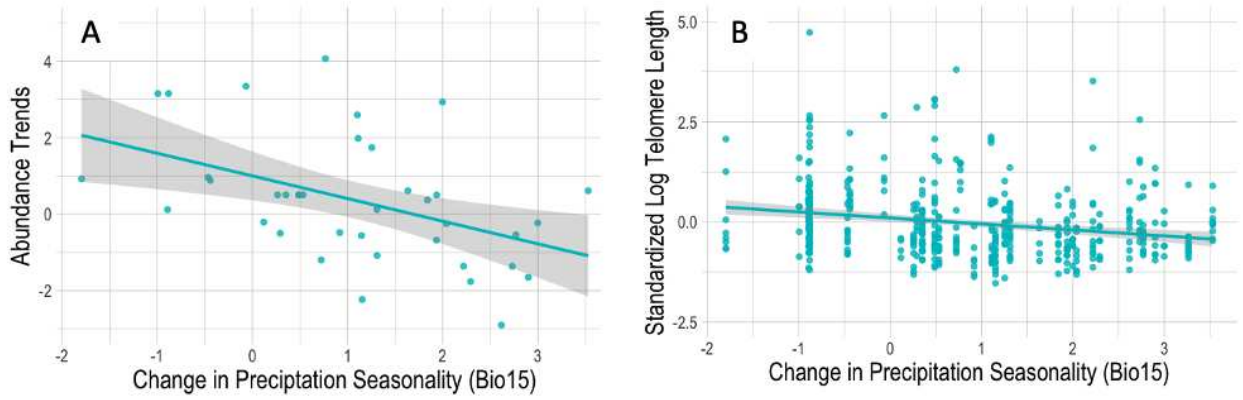

Figure 2.4. Yellow warbler abundance trends and telomere length in response to historical climate change using bioclimatic variables associated with genomic variation on the breeding grounds. a) a significant negative association between abundance trends and historical changes in precipitation seasonality across 39 sample sites (R^2=0.38, p-value=0.044). b) a significant negative association between historic changes in precipitation seasonality and telomere length in 451 yellow warbler samples across 39 sample sites (R^2=0.41, p-value=0.03).

LITERATURE CITED

Anctil, A., Franke, A., & Bêty, J. (2014). Heavy rainfall increases nestling mortality of an arctic top predator: experimental evidence and long-term trend in peregrine falcons. *Oecologia*, *174*, 1033-1043.

Angelier, F., Weimerskirch, H., Barbraud, C., & Chastel, O. (2019). Is telomere length a molecular marker of individual quality? Insights from a long-lived bird. *Funct. Ecol.*, *33*, 1076-1087.

Bartoń, K. (2009). MuMIn: Multi-model inference (R package version 0.12.2)

Bates D, Mächler M, Bolker B, Walker S (2015). Fitting Linear Mixed-Effects Models Using lme4. *J. Stat. Softw.*, 67, 1–48.

Bay, R. A., Harrigan, R. J., Underwood, V. L., Gibbs, H. L., Smith, T. B., & Ruegg, K. (2018). Genomic signals of selection predict climate-driven population declines in a migratory bird. *Science*, *359*, 83-86.

Bay, R. A., Karp, D. S., Saracco, J. F., Anderegg, W. R., Frishkoff, L. O., Wiedenfeld, D. et al. (2021). Genetic variation reveals individual-level climate tracking across the annual cycle of a migratory bird. *Ecol. Lett.*, *24*, 819-828.

Beever, E.A., O'leary, J., Mengelt, C., West, J.M., Julius, S., Green, N. et al. (2016). Improving conservation outcomes with a new paradigm for understanding species' fundamental and realized adaptive capacity. *Conserv. Lett.*, *9*, 131-137.

Benito Garzón, M., González Muñoz, N., Wigneron, J. P., Moisy, C., Fernández-Manjarrés, J., & Delzon, S. (2018). The legacy of water deficit on populations having experienced negative hydraulic safety margin. *Glob. Ecol. Biogeogr.*, *27*, 346-356.

Bichet, C., Bouwhuis, S., Bauch, C., Verhulst, S., Becker, P. H., & Vedder, O. (2020). Telomere length is repeatable, shortens with age and reproductive success, and predicts remaining lifespan in a long-lived seabird. *Molec. Ecol., 29*, 429-441.

Blackburn, E. H. (1991). Structure and function of telomeres. *Nature*, *350*, 569-573.

Blackburn, E. H. (2005). Telomeres and telomerase: their mechanisms of action and the effects of altering their functions. *FEBS Lett.*, *579*, 859-862.

Boonstra, R. (2004). Coping with changing northern environments: the role of the stress axis in birds and mammals. *Integr. Comp. Biol.*, 44, 95-108.Borrell, J. S., Zohren, J., Nichols, R. A., & Buggs, R. J. (2020). Genomic assessment of local adaptation in dwarf birch to inform assisted gene flow. *Evol. Appl.*, *13*, 161-175.

Cadenas, E., & Davies, K. J. (2000). Mitochondrial free radical generation, oxidative stress, and aging. *Free Radic. Biol. Med.*, 29, 222-230.

Çakmak, E., Akın Pekşen, Ç., & Bilgin, C. C. (2017). Comparison of three different primer sets for sexing birds. *J. Vet. Diagn. Invest.*, *29*, 59-63.

Capblancq, T., Fitzpatrick, M. C., Bay, R. A., Exposito-Alonso, M., & Keller, S. R. (2020). Genomic prediction of (mal) adaptation across current and future climatic landscapes. *Annu. Rev. Ecol. Evol. Syst.*, *51*, 245-269.

Casagrande, S., & Hau, M. (2019). Telomere attrition: metabolic regulation and signalling function?. *Biol. Lett.*, *15*, 20180885.

Casagrande, S., Stier, A., Monaghan, P., Loveland, J. L., Boner, W., Lupi, S. et al. (2020). Increased glucocorticoid concentrations in early life cause mitochondrial inefficiency and short telomeres. *J. Exp. Biol.*, *223*, jeb222513.

Chatelain, M., Drobniak, S. M., & Szulkin, M. (2020). The association between stressors and telomeres in non-human vertebrates: a meta-analysis. *Ecol. Lett.*, *23*, 381-398.

Cheron, M., Angelier, F., Ribout, C., & Brischoux, F. (2021). Clutch quality is related to embryonic development duration, hatchling body size and telomere length in the spined toad (Bufo spinosus). *Biol. J. Linn. Soc.*, *133*, 135-142.

Cianfrani, C., Broennimann, O., Loy, A., & Guisan, A. (2018). More than range exposure: Global otter vulnerability to climate change. *Biol. Conserv.*, *221*, 103-113.

Coe, B. H., Beck, M. L., Chin, S. Y., Jachowski, C. M., & Hopkins, W. A. (2015). Local variation in weather conditions influences incubation behavior and temperature in a passerine bird. *J. Avian Biol.*, *46*, 385-394.

Conrey, R. Y., Skagen, S. K., Yackel Adams, A. A., & Panjabi, A. O. (2016). Extremes of heat, drought and precipitation depress reproductive performance in shortgrass prairie passerines. *Ibis*, *158*, 614-629.

Criscuolo, F., Bize, P., Nasir, L., Metcalfe, N. B., Foote, C. G., Griffiths, K. et al. (2009). Real-time quantitative PCR assay for measurement of avian telomeres. *J. Avian Biol.*, *40*, 342-347.

Cruz-McDonnell, K. K., & Wolf, B. O. (2016). Rapid warming and drought negatively impact population size and reproductive dynamics of an avian predator in the arid southwest. *Glob. Change Biol.*, *22*, 237-253.

Debes, P. V., Visse, M., Panda, B., Ilmonen, P., & Vasemägi, A. (2016). Is telomere length a molecular marker of past thermal stress in wild fish? *Molec. Ecol.*, *25*, 5412-5424.

Eastwood, J. R., Connallon, T., Delhey, K., Hall, M. L., Teunissen, N., Kingma, S. A. et al. (2022). Hot and dry conditions predict shorter nestling telomeres in an endangered songbird: Implications for population persistence. *Proc. Natl. Acad. Sci. U.S.A.*, *119*, e2122944119.

Eastwood, J. R., Hall, M. L., Teunissen, N., Kingma, S. A., Hidalgo Aranzamendi, N., Fan, M. et al. (2019). Early-life telomere length predicts lifespan and lifetime reproductive success in a wild bird. *Molec. Ecol.*, *28*, 1127-1137.

Ellis, N., Smith, S. J., & Pitcher, C. R. (2012). Gradient forests: calculating importance gradients on physical predictors. *Ecology*, *93*, 156-168.

Ferger, S. W., Schleuning, M., Hemp, A., Howell, K. M., & Böhning-Gaese, K. (2014). Food resources and vegetation structure mediate climatic effects on species richness of birds. *Glob. Ecol. Biogeogr.*, *23*, 541-549.

Fick, S.E. and R.J. Hijmans, 2017. WorldClim 2: new 1km spatial resolution climate surfaces for global land areas. *Int. J. Climatol., 37, 4302-4315*.

Fitzpatrick, M. C., Chhatre, V. E., Soolanayakanahally, R. Y., & Keller, S. R. (2021). Experimental support for genomic prediction of climate maladaptation using the machine learning approach Gradient Forests. *Mol. Ecol. Resour.*, *21*, 2749-2765.

Fitzpatrick, M. C., Keller, S. R., & Lotterhos, K. E. (2018). Comment on "Genomic signals of selection predict climate-driven population declines in a migratory bird". *Science*, *361*, eaat7279.

Fox, J., & Weisberg, S. (2011). *An R companion to applied regression*. Sage publications, Thousand Oaks, California, USA.

Haase, C. G., Long, A. K., & Gillooly, J. F. (2016). Energetics of stress: linking plasma cortisol levels to metabolic rate in mammals. *Biol. Lett.*, *12*, 20150867.
Harris, I., Osborn, T.J., Jones, P.D., Lister, D.H. (2020). Data from: Version 4 of the CRUTS monthly high-resolution gridded multivariate climate dataset. Scientific Data 7: 109. Available at: https://crudata.uea.ac.uk/cru/data/hrg/
Haussmann, M. F., Longenecker, A. S., Marchetto, N. M., Juliano, S. A., & Bowden, R. M. (2012). Embryonic exposure to corticosterone modifies the juvenile stress response, oxidative stress and telomere length. *Proc. Royal Soc. B.*, *279*, 1447-1456.
Heidinger, B. J., Blount, J. D., Boner, W., Griffiths, K., Metcalfe, N. B., & Monaghan, P. (2012). Telomere length in early life predicts lifespan. *Proc. Natl. Acad. Sci.*, *109*, 1743-1748.
Hoffmann, A. A., Weeks, A. R., & Sgrò, C. M. (2021). Opportunities and challenges in assessing climate change vulnerability through genomics. *Cell*, *184*, 1420-1425.
Houben, J. M., Moonen, H. J., van Schooten, F. J., & Hageman, G. J. (2008). Telomere length assessment: biomarker of chronic oxidative stress? *Free Radic. Biol. Med.*, *44*, 235-246.
Huang, W. S., & Pike, D. A. (2011). Climate change impacts on fitness depend on nesting habitat in lizards. *Funct. Ecol.*, *25*, 1125-1136.
Iknayan, K. J., & Beissinger, S. R. (2018). Collapse of a desert bird community over the past century driven by climate change. *Proc. Natl. Acad. Sci.*, *115*, 8597-8602.
Kärkkäinen, T., Laaksonen, T., Burgess, M., Cantarero, A., Martínez-Padilla, J., Potti, J., Moreno, J., Thomson, R.L., Tilgar, V. and Stier, A. (2022). Population differences in the length and early-life dynamics of telomeres among European pied flycatchers. *Molec. Ecol.*, *31*, 5966-5978.
Lane, J. E., Kruuk, L. E., Charmantier, A., Murie, J. O., & Dobson, F. S. (2012). Delayed phenology and reduced fitness associated with climate change in a wild hibernator. *Nature*, *489*, 554-557.
Layton, K. K. S., Snelgrove, P. V. R., Dempson, J. B., Kess, T., Lehnert, S. J., Bentzen, P., ... & Bradbury, I. R. (2021). Genomic evidence of past and future climate-linked loss in a migratory Arctic fish. *Nat. Clim. Change*, *11*, 158-165.
McEwen, B. S., & Wingfield, J. C. (2003). The concept of allostasis in biology and biomedicine. *Horm. Behav*., 43, 2-15.
McLennan, D., Armstrong, J. D., Stewart, D. C., McKelvey, S., Boner, W., Monaghan, P., & Metcalfe, N. B. (2018). Links between parental life histories of wild salmon and the telomere lengths of their offspring. *Mol. Ecol.*, *27*, 804-814.
Nettle, D., Seeker, L., Nussey, D., Froy, H., & Bateson, M. (2019). Consequences of measurement error in qPCR telomere data: A simulation study. *PLoS One*, *14*, e0216118.
Nicotra, A. B., Beever, E. A., Robertson, A. L., Hofmann, G. E., & O'Leary, J. (2015). Assessing the components of adaptive capacity to improve conservation and management efforts under global change. *Conserv. Biol.*, *29*, 1268-1278.
Noguera, J. C., da Silva, A., & Velando, A. (2022). Egg corticosterone can stimulate telomerase activity and promote longer telomeres during embryo development. *Mol. Ecol.*, *31*, 6252-6260.
Nogués-Bravo D, Rodríguez-Sánchez F, Orsini L, de Boer E, Jansson R, Morlon H, Fordham D. A., Jackson S. T. (2018). Cracking the code of biodiversity responses to past climate change. *Trends Ecol. Evol.*, *33*, 765-776.

Pepin, N. C., Arnone, E., Gobiet, A., Haslinger, K., Kotlarski, S., Notarnicola, C. et al. (2022). Climate changes and their elevational patterns in the mountains of the world. *Rev. Geophys.*, *60*, e2020RG000730.

Pfaffl, M. W. (2001). A new mathematical model for relative quantification in real-time RT–PCR. *Nucleic Acids Res.*, *29*, e45-e45.

Pyle, P. (1997). Molt limits in North American passerines. *North American Bird Bander*, *22*, 1.

Reichert, S., & Stier, A. (2017). Does oxidative stress shorten telomeres in vivo? A review. *Biol. Lett.*, *13*, 20170463.

Rellstab, C. (2021). Genomics helps to predict maladaptation to climate change. *Nat. Clim. Change*, *11*, 85-86.

Rollings, N., Uhrig, E. J., Krohmer, R. W., Waye, H. L., Mason, R. T., Olsson, M., ... & Friesen, C. R. (2017). Age-related sex differences in body condition and telomere dynamics of red-sided garter snakes. *Proc. Royal Soc. B.*, *284*, 20162146.

Romero, L. M. (2004). Physiological stress in ecology: lessons from biomedical research. *Trends Ecol. Evol.*, *19*, 249-255.

Ruegg, K., Bay, R. A., Anderson, E. C., Saracco, J. F., Harrigan, R. J., Whitfield, M. et al. (2018). Ecological genomics predicts climate vulnerability in an endangered southwestern songbird. *Ecol. Lett.*, *21*, 1085-1096.

Saunders, S. P., Michel, N. L., Bateman, B. L., Wilsey, C. B., Dale, K., LeBaron, G. S., & Langham, G. M. (2020). Community science validates climate suitability projections from ecological niche modeling. *Ecol. Appl.*, *30*, e02128.

Seeker, L. A., Holland, R., Underwood, S., Fairlie, J., Psifidi, A., Ilska, J. J., ... & Nussey, D. H. (2016). Method specific calibration corrects for DNA extraction method effects on relative telomere length measurements by quantitative PCR. *PloS one*, *11*(10), e0164046.

Senapathi, D., Nicoll, M. A., Teplitsky, C., Jones, C. G., & Norris, K. (2011). Climate change and the risks associated with delayed breeding in a tropical wild bird population. *Proc. Royal Soc. B.*, *278*, 3184-3190.

Silverin, B. (1986). Corticosterone-binding proteins and behavioral effects of high plasma levels of corticosterone during the breeding period in the pied flycatcher. *Gen. Comp. Endocrinol. 64*(1), 67-74.

Sozou, P. D., & Kirkwood, T. B. (2001). A stochastic model of cell replicative senescence based on telomere shortening, oxidative stress, and somatic mutations in nuclear and mitochondrial DNA. *J. theor. Biol.*, *213*, 573-586.

Stier, A., Delestrade, A., Bize, P., Zahn, S., Criscuolo, F., & Massemin, S. (2016). Investigating how telomere dynamics, growth and life history covary along an elevation gradient in two passerine species. *J. Avian Biol.*, *47*, 134-140.

Thuiller, W., Lavorel, S., & Araújo, M. B. (2005). Niche properties and geographical extent as predictors of species sensitivity to climate change. *Glob. Ecol. Biogeogr.*, *14*, 347-357.

Tingley, M. W., Monahan, W. B., Beissinger, S. R., & Moritz, C. (2009). Birds track their Grinnellian niche through a century of climate change. Proc. Natl. Acad. Sci. U.S.A., 106, 19637-19643.

Verhulst, S. (2020). Improving comparability between qPCR-based telomere studies. *Mol. Ecol. Resour.,* 20, 11-13.

Wagner, D. L. (2020). Insect declines in the Anthropocene. *Annu. Rev. Entomol.*, *65*, 457-480.

Von Zglinicki, T. (2000). Role of oxidative stress in telomere length regulation and replicative senescence. *Ann. N.Y. Acad. Sci.*, *908*, 99-110.

Von Zglinicki, T. (2002). Oxidative stress shortens telomeres. *Trends Biochem. Sci.*, *27*, 339-344.

Zhang, Q., Han, X.Z., Burraco, P., Hao, X., Teng, L.W., Liu, Z.S. et al. (2023). Telomere length, oxidative stress and their links with growth and survival in a lizard facing climate warming. *Sci. Total Environ.*, *891*, 164424.

Zhu, H., Wang, D., Wang, L., Fang, J., Sun, W., & Ren, B. (2014). Effects of altered precipitation on insect community composition and structure in a meadow steppe. *Ecol. Entomol.*, *39*, 453-461.

Ziolkowski, D.J., Lutmerding, M., English, W.B., Aponte, V.I., and Hudson, M-A.R., (2023), Data from: North American Breeding Bird Survey Dataset 1966 - 2022: U.S. Geological Survey data release. Available at: https://doi.org/10.5066/P9GS9K64.

CHAPTER 3: CLIMATE ADAPTATION ACROSS SEASONAL HABITAT IN A MIGRATORY SONGBIRD, THE YELLOW WARBLER (SETOPHAGA PETECHIA)

Summary

Local adaptation shapes the environmental variation populations can tolerate, thereby influencing species distributions and responses to climate change. While well-documented on breeding grounds, local adaptation to non-breeding grounds in migratory species remains largely unexplored. Using whole-genome sequencing, we investigated local adaptation to non-breeding grounds in the yellow warbler (*Setophaga petechia*), a Neotropical migratory songbird. We assigned non-breeding individuals to breeding locations by estimating allele frequency surfaces across the breeding range and used genotype-environment association analyses to identify climate-linked genetic variation across the annual cycle. Our results reveal distinct genomic signals of local adaptation to non-breeding climate, primarily associated with temperature variables. In contrast, adaptation on the breeding grounds was driven by precipitation. Although genomic signals of adaptation were stronger on the breeding grounds, we identified shared candidate genes linked to climate adaptation across both phases. We also tested whether climate tracking—a behavior aligning migration with consistent climatic conditions—reflects local adaptation across the annual cycle by testing for increased physiological stress with lower levels of climate tracking. Contrary to expectation, we found no correlation between climate tracking and telomere length, a biomarker for physiological stress, suggesting that climate tracking is not driven by adaptation to similar climates across the annual cycle, but may instead be a consequence of other processes. These findings highlight the complexity of selective pressures experienced by migratory species across their annual cycles and challenge assumptions about the

Manuscript status: In preparation
Potential target journals: Ecology Letters, Nature Communications, or Diversity and Distributions

adaptiveness of climate tracking. By providing novel insights into local adaptation on non-breeding grounds, this study advances our understanding of the evolutionary ecology of migratory birds.

Introduction

Local adaptation plays a pivotal role in driving ecological and evolutionary dynamics by shaping the environmental variation a population can withstand, influencing its geographic distribution, and impacting its response to anthropogenic climate change (Kawecki & Ebert, 2004, Kirkpatrick & Barton 1997; Savolainen et al. 2007). Identifying local adaptation is therefore a fundamental focus of evolutionary biology and has been documented across a wide array of taxonomic groups (DuBois et al. 2022, Jackson et al. 2020; Liu et al. 2021, Mahony et al., 2020, Peterson et al. 2014, Ruiz Minano et al. 2022, Sanford & Worth 2010). Despite this progress, local adaptation in migratory species to their nonbreeding environments remains largely unexplored. For example, birds are one of the most widely studied taxonomic groups of migratory animals, spending majority of the year on their nonbreeding grounds, however, most of our knowledge regarding their ecology and evolution is restricted to the breeding areas (Webster and Marra 2005). Investigating local adaptation in migratory birds is particularly challenging because these organisms experience varying selective pressures across different geographic locations throughout the year, which may even conflict between the breeding and nonbreeding grounds (Webster & Marra, 2005). This limited focus has led to a significant knowledge gap, as conditions on the wintering grounds are increasingly being recognized as key drivers of survival, migration timing, and fitness, collectively shaping population dynamics (Rockwell et al. 2017, Ryan Norris & Marra 2007, Webster et al. 2002).

Theoretical predictions suggest that the extent of local adaptation to the nonbreeding grounds is influenced by the strength of migratory connectivity, defined as the level to which individuals breeding in one area also winter together in a particular location (Turbek et al. in prep, Webster et al. 2002, Webster and Marra 2004). Strong migratory connectivity is expected to promote local adaptation to the wintering areas via reduced gene flow between populations, while weak migratory connectivity is expected to increase gene flow, potentially hindering local adaptation (Webster et al. 2002). Theoretical models further predict that in species with strong migratory connectivity, local adaptation will be accelerated if populations experience similar environmental conditions, and thus similar selection pressures, across the annual cycle (Webster et al. 2002). In addition to the role of migratory connectivity, these theoretical frameworks highlight how environmental conditions throughout the annual cycle can shape patterns of local adaptation. Consequently, understanding the relative importance of breeding and nonbreeding climates to local adaptation is essential in uncovering the selective forces that shape migratory species.

Contrary to resident species who are often subject to dramatic seasonal differences in environmental conditions, migratory species may encounter selective pressures that are more constant over the annual cycle. This is due to the ability of migratory birds to select nonbreeding areas with similar environmental conditions to their breeding grounds, a phenomenon known as climate tracking (Joseph 2003, Joseph and Stockwell 2000). Climate tracking has often been interpreted as indirect evidence for local adaptation to nonbreeding grounds, as maintaining consistent climatic associations suggests that shared selection pressures operate across the breeding and nonbreeding phases (Fandos et al. 2020; Illán et al. 2022, Zurell et al. 2018, Bay et al. 2021). However, the extent to which tracking is adaptive has yet to be tested due to the

difficulty of tracking individuals across vast distances and accurately quantifying their climate exposure across the annual cycle. If climate tracking is adaptive, individuals that effectively track climate would be expected to exhibit signals of local adaptation to the same climate variables on the breeding and nonbreeding grounds, and to experience reduced physiological stress compared to those that track less effectively or switch climates between seasons.

Alternatively, variation in seasonal climate tracking may result from other processes influencing migration patterns. Recent studies suggest that migratory behavior is primarily influenced by the need to optimize resource availability and minimize movement costs, rather than by direct response to climate (Somveille et al. 2021, Somveille et al. 2024). Under this scenario, migration patterns may include both climate-tracking and climate-switching populations, with distributions shaped more by geographical chance than by climatic adaptation. If migration patterns are primarily driven by energy efficiency rather than climate tracking, individuals that switch climate across the annual cycle would not experience significantly higher stress than those that track climates. One way to test the consequences of the climate tracking hypothesis is to use telomere length as an informative biomarker of physiological stress.

Telomeres, tandem arrays of repetitive DNA sequence and associated proteins that "cap" the ends of eukaryotic chromosomes, are essential for maintaining genome stability as they serve to protect coding DNA from erosion and prevent inappropriate DNA damage responses (Blackburn 1991, Blackburn 2005). Telomeres progressively shorten with each DNA replication cycle and thus with aging, and this process can be accelerated by environmental stress, often referred to as allostatic load (Blackburn 1991, McEwen & Wingfield 2003). Environmental stressors, factors that trigger physiological and behavioral changes to prioritize survival, often come at a physiological cost (Romero 2004). These stressors increase metabolic rates, oxidative

stress, and mitotic activity, all of which are linked to accelerated telomere attrition (Cadenas & Davies 2000, Houben et al. 2008, Sozou & Kirkwood, 2001, von Zglinicki 2000, Von Zglinicki 2002). As a result, telomere length has emerged as a particularly useful biomarker for key life-history traits, including lifespan (Bichet et al. 2020, Heidinger et al. 2012), lifetime reproductive success (Eastwood et al. 2019), and individual quality (Angelier et al. 2019, Cheron et al., 2021, Rollings et al. 2017) across diverse taxa.

To investigate the potential for local adaptation to non-breeding habitats, our chosen model species is the yellow warbler (Setophaga petechia). Extensive prior research on migratory connectivity and local adaptation to breeding climates in this species facilitates the generation of testable hypotheses regarding the potential role of the nonbreeding grounds in the process of divergence. Previous work identified moderate levels of migratory connectivity in the yellow warbler, as well as individual and population-level precipitation tracking (Bay et al. 2021, Gomez et al. 2016, Somevielle et al. 2023). Thus, if the strength of migratory connectivity is linked to the strength of local adaptation on the wintering grounds in migratory birds, we predict moderate levels of migratory connectivity will result in moderate levels of local adaptation to the non-breeding grounds. Further, if tracking of habitats is adaptive across breeding and non-breeding grounds, we predict that the same environmental variables will be under selection on breeding and wintering grounds, and further that individuals that fail to track similar climates will experience increased physiological stress.

To test these hypotheses, we use landscape genomic approaches to quantify local adaptation on breeding and non-breeding grounds, combined with analysis telomere length to quantify physiological stress in individuals relative to their degree of climate tracking. We begin by using genetic assignment tests (Ranola et al. 2014) to predict the breeding origins of

individuals captured during the non-breeding season. This method allows us to describe the climate individuals experience across the annual cycle and directly compare the relative importance of breeding and non-breeding climate variables to local adaptation. Next, we investigate whether climate tracking is adaptive by testing whether the same climate variables show evidence of selection on both breeding and non-breeding grounds, and whether individuals that failed to track similar climates showed increased signs of physiological stress as indicated by telomere shortening. Overall, this study is among the first to explore the role of local adaptation across the full annual cycle of a migratory species and our findings provide a foundation for better understanding of how migratory birds may respond to future climate change.

Methods

Whole-genome sequencing and variant calling

We collected blood samples from 106 yellow warblers across 17 populations on the nonbreeding grounds for assignment to the breeding grounds (Figure 3.1a). Additionally, 159 blood samples from 18 populations on the breeding region were collected for model training and validation (Figure S3.1). Birds were captured using mist-nets, and blood samples were collected via brachial venipuncture, then preserved in Queen's lysis buffer. DNA was extracted using the Qiagen™ DNeasy Blood and Tissue Kit and quantified with the Qubit dsDNA HS Assay Kit (Thermo Fisher Scientific).

Whole genome sequencing libraries were prepared following modifications of Illumina's Nextera Library Preparation protocol (Schweizer & DeSaix 2023) and were sequenced on NovaSeq6000 lanes at Duke University Sequencing and Genomic Technologies with a target sequencing depth of 2X per individual. To process sequence data, the workflow management system Snakemake was used to create a reproducible bioinformatics pipeline (Köster and

Rahmann 2012). The program Trimmomatic 0.39 (Bolger et al. 2014) was used to trim the sequence data to remove Illumina adapter sequences and polyG tails using a sliding window approach (SLIDINGWINDOW:4:20). Reads were then mapped to the yellow warbler reference genome (NCBI BioProject PRJNA777222; Tsai et al. 2024) using BWA 0.7.17 (Li & Durbin, 2009) with the bwa mem Snakemake wrapper (v1.23.3/bio/bwa/mem). After mapping, the resulting SAM files were sorted, converted to BAM files, and indexed using Samtools version 1.16 (Li et al., 2009). MarkDuplicates from Picard (http://broadinstitute.github.io/picard) were utilized to mark read duplicates and clipped overlapping reads with the clipOverlap function from bamUtil (Jun et al. 2015). To reduce sequencing depth variation, the downsample function from Picard (http://broadinstitute.github.io/picard) was used to downsample reads from BAM files with greater than 3X coverage, to 3X coverage. This resulted in an average read depth of 2.7X coverage.

To identify genetic markers from low-coverage WGS data, the HaplotypeCaller program in the Genome Analysis Toolkit (GATK version 4.1.6.0) (Van der Auwera et al. 2013) was employed, applying a minimum base quality score of 33 and a minimum mapping quality score of 20 to reduce lane effects (Lou & Therkildsen 2022). To parallel the genotype calling process, genomic databases in ~3 Mb intervals across the genome were generated and combined, and the genotyped VCF files indexed with BCFtools 1.16 (Danecek et al. 2021). To remove systematic errors, a hard filter was applied to the subsequent VCF file with the following parameters, "QD < 2.0 || FS > 60.0 || MQ < 40.0 || MQRankSum < -12.5 || ReadPosRankSum < -8.0", filtering the indels separately with "QD < 2.0 || FS > 200.0 || ReadPosRankSum < -20.0". We then used BCFtools to keep biallelic sites (-m 2 -M 2) missing in fewer than 20% of the sampled individuals ('F_MISSING < 0.20'), with minor allele frequency of at least 0.05 (--min-af 0.05, --

max-af 0.95), and with a sequencing quality score of at least 30 ('QUAL > 30') (Danecek et al. 2021). This filtering resulted in 2,999,708 variants in 298 individuals with an average of 21% missing data.

Telomere length measurement

Telomere length was quantified from bam files using Telseq v0.0.2 (Ding et al., 2014), a widely used software developed specifically to calculate telomere length from whole-genome sequence data (Igoshin et al. 2023, Taub et al., 2022). Telomere length calculated from Telseq is the cumulative length of telomere repeats normalized based on the GC composition of total reads (48-52%), ensuring accurate telomere length estimation by accounting for GC bias. Parameters in the Telseq source code were customized to adapt it to the yellow warbler genome, which included changing the number of chromosomal ends, read length, and total GC content (bp). The parameters TELOMERE_ENDS, READ_LENGTH and GENOME_LENGTH_AT_TEL_GC were set equal to 62, 100, and 143831148, respectively. The latter was calculated by measuring the total length of 150 base pair windows in the yellow warbler genome with a GC content between 48% and 52%.

Individual breeding location assignment

Each of the 106 non-breeding yellow warblers was assigned to a breeding location by generating probability surfaces using the R package OriGen (Ranola et al. 2014). OriGen creates continuous allele frequency surfaces across a species' breeding range but is typically designed for smaller datasets, such as panels of 96 genotyped SNPs, and cannot directly handle whole-genome sequencing data. To optimize its performance for our larger dataset, breeding sample data was subsetted and the program tested with different numbers of SNPs to identify the subset that produced the most accurate assignments.

For the training dataset,191 samples captured on the breeding grounds, each with a known breeding location, were used. To validate the assignment process, 10% of the samples from each site was withheld for independent testing, leaving 159 samples for model training. As these samples were included in Turbek et al. (in prep), we used the study's assignment of each sample to distinct genetic breeding cluster, which was done using PCAngsd and WGSassign (Meisner and Albrechtsen 2018, DeSaix et al. 2023). Pairwise Fst outlier analyses between the five genetic clusters was performed, resulting in 10 pairwise comparisons. To optimize the SNP subset for accurate assignment, the top 10, 15, 20, 50, and 100 SNPs from each pairwise Fst analysis was selected. After removing duplicates, SNP subsets for each selection threshold were created. For each subset, OriGen was trained on the 159 training samples and then estimated the breeding location for the 32 validation samples.

Using OriGen, continuous allele frequency surfaces across the yellow warbler breeding range were created for each SNP subset. These surfaces estimated the probability that an individual belonged to a given grid cell within the breeding range, with grids spanning approximately 1.5° longitude by 0.5° latitude. The grids were trimmed to the known breeding range of the yellow warbler, and probabilities were rescaled to sum to one. To determine which SNP subset most accurately assigned individuals to their breeding location, we calculated the Euclidean distance between the actual sampling location and the grid cell with the highest assignment probability for each validation sample (Figure S3.2). The subset with the smallest average distance was selected, resulting in a final subset of 410 SNPs (the top 50 SNPs per pairwise Fst comparison). The average assignment distance for this subset was 718 km. The accuracy of the climate predictions based on the Origen assignment was then tested by comparing the known and expected mean annual precipitation and mean annual temperature,

which resulted in associations of R=0.8 and R=0.57, respectively. (Figure S3.3). Using the optimized subset of 410 SNPs, each of the 106 nonbreeding individuals was assigned to their breeding location. OriGen was used to create continuous allele frequency surfaces for each nonbreeding individual as described above, providing probability grids for breeding location assignment (Figure 3.1b, S3.4).

Extracting climate variables

To characterize the climatic conditions across the yellow warbler's breeding and non-breeding ranges, climate data from WorldClim (Fick & Hijmans 2017) was gathered. This dataset provides high-resolution global climate layers, and all 19 BioClim variables for the years 1970-2000 were extracted. Given the inherent uncertainty in assigning individuals to specific breeding locations, spatial variability was accounted for by defining a radius around the grid cell with the highest assignment probability, which was then used to extract climate variables. Assignment probabilities were scaled so that the highest probability within the grid was set to one by normalizing values across all grid cells for each individual. The average radius encompassing a cumulative assignment probability of 0.99 was calculated across all individuals, resulting in a radius of 114 km (Figure S3.5). This radius served as the extraction zone for climate data around the top-assigned breeding grid cell for each individual. For each individual, the mean value of each BioClim variable within the 114 km radius on the breeding grounds was calculated using the package raster in R version 3.5.3 (https://www.R-project.org). Similarly, for known nonbreeding locations, the mean value of each BioClim variable within a 114 km radius from the point of sampling was calculated.

Genotype-environment association analyses

Redundancy analysis (RDA) was used to identify climate variables most strongly associated with genomic variation across the breeding and nonbreeding grounds of yellow warblers; specifically, a partial RDA using the R package vegan and genotype data from individuals sampled on the nonbreeding grounds. To account for population structure, Moran eigenvector maps (MEM) were calculated as spatial predictors using the R package adespatial (Dray et al. 2018). Spatial coordinates were transformed into distance matrices, and MEMs were derived using eigen decomposition. The one significant MEM based on a p-value threshold of 0.05 was retained and included as a conditioning variable in the RDA. Environmental variables highly correlated with the MEM ($r > 0.7$) were excluded from the analysis.

After confirming an association with the environment when accounting for population structure (Table S3.1), the RDA was rerun without the conditioning variable to identify putatively adaptive SNPs. Individual SNPs with loadings greater than three standard deviations from the mean on the constrained axes explaining the most variance were classified as candidate SNPs (two-tailed p-value = 0.0027; Forester et al., 2016). Duplicate detections were removed, and the environmental variable most strongly correlated with each candidate SNP determined.

To assess the strength of local adaptation on the breeding versus non-breeding grounds, the number of SNPs most strongly associated with breeding versus nonbreeding climate variables were compared, and Pearson's correlation coefficients (r) calculated between candidate SNPs and their associated environmental variables on the breeding and nonbreeding grounds.

Identification of candidate genes

In order to focus on the most relevant climate-linked genetic markers, candidate SNPs with correlations below 0.4 were excluded, and only the most highly correlated SNPs retained.

To calculate distance between loci, scaffold positions in the zebra finch (Taeniopygia guttata) were placed in chromosomal order using SatsumaSyteny2 (Grabherr et al. 2010) prior to analyses. To identify genes located near SNPs identified through RDA, Ensemble gene predictions for the zebra finch (taeGut3.2.4, GCF_000151805.1) were downloaded. To find genes located within 25 kb upstream or downstream of each candidate SNP, bedtools - closest (v2.30.0) (Quinlan, 2014) was employed; this range is thought to encompass the genomic region within which linkage disequilibrium typically breaks down (Backström et al. 2006). Duplicates were identified based on SNP coordinates and gene annotations and were subsequently removed. Genes without functional annotations were excluded from further analysis. The degree of overlap between genes associated with candidate SNPs identified on the breeding and non-breeding grounds was then assessed.

To investigate the potential functional relevance of climate-linked SNPs, a list of candidate genes was compiled from the literature with gene ontology (GO) terms associated with thermal tolerance, bill morphology, and feather color (Table S3.2). The GO list was derived using annotations from AmiGO (Carbon et al. 2009) and curated manually from literature. We then cross-referenced the genes located near climate-linked SNPs with published candidate genes and those with relevant GO terms. This allowed examination of potential functions of the identified SNPs and their relationship to traits associated with climatic adaptation.

Climate tracking and telomere variation analysis

To quantify the level of climate matching for each individual, we first identified the environmental variables most strongly associated with SNPs on the breeding and non-breeding grounds, respectively. Each variable was then standardized (mean 0, standard deviation 1) to facilitate direct comparisons between the breeding and nonbreeding grounds. Assuming that

perfect climate tracking across the annual cycle would result in a regression line with a slope of 1, the distance between each data point in the regression and the line of perfect tracking was calculated (Figure 3.2). This distance served as a measure of climate tracking, where smaller values indicated closer adherence to perfect tracking (i.e., greater climate matching), and larger values indicated less tracking.

To test whether climate tracking is adaptive, the lm function in R was utilized to fit a linear model and assess the relationship between climate tracking and telomere length, which provided a biological indicator of stress. This analysis allowed determination of whether individuals with higher levels of climate tracking experienced reduced physiological stress compared to those with lower tracking levels.

Results

Genotype-environment association analyses

Redundancy analysis (RDA) identified candidate SNPs associated with climate across the breeding and non-breeding grounds (Figure 3.3). A total of 29,481 candidate loci were identified, with 7,065 loci (~24%) associated with nonbreeding climate variables and 22,416 loci (~76%) associated with breeding climate variables (Figure 3.4a). The mean correlation strength between candidate SNPs and their associated environmental variables was 0.26 (± 0.07) for the non-breeding grounds and 0.40 (± 0.12) for the breeding grounds (Figure 3.4b).

On the non-breeding grounds, RDA identified 2,193 candidate loci associated with mean annual temperature (BIO1) and 2,790 loci associated with maximum temperature of the warmest month (BIO5), which were the strongest associations observed on the nonbreeding grounds and collectively accounted for ~17% of the total candidate loci identified. In contrast, on the breeding grounds RDA identified precipitation of the warmest quarter (BIO18) as the strongest

association, with 12,437 candidate loci identified, representing ~42% of the total candidate loci (Figure 4c). The mean correlation strength was 0.27 (± 0.08) for nonbreeding BIO1, 0.27 (± 0.07) for nonbreeding BIO5, and 0.47 (± 0.09) for breeding BIO18.

Identification of candidate genes

Of the candidate SNPs with correlations to environmental variables above 0.4, 938 were linked to known genes and were associated with the breeding grounds, while 119 were linked to known genes and associated with the nonbreeding grounds. Forty-nine associated candidate genes that overlapped between the non-breeding and breeding seasons were identified. One key gene, GLI3, was also present in the candidate gene list. The SNPs associated with GLI3 had a correlation of 0.40 with BIO1 (mean annual temperature) and 0.55 with BIO18 (precipitation of the warmest quarter). The GLI3 gene is associated with heat adaptation, bill morphology, respiratory system processes, and melanocyte differentiation (Bosse et al. 2017, Xu et al. 2022) (Table 3.1). The SNPs linked to GLI3 were located in intronic regions of the gene.

Climate matching and telomere analysis

A significant correlation between nonbreeding and breeding climate was observed only for precipitation of the warmest quarter ($p=0.001$; $R = 0.414$), providing evidence for moderate precipitation tracking in yellow warblers (Figure 3.5e). In contrast, there was no support for temperature tracking, with very low correlations for mean annual temperature ($p=0.462$; $R =0.005$) and maximum temperature of the warmest quarter ($p=0.930$; $R = 0.000$) between the nonbreeding and breeding seasons (Figure 3.5a,c).

After calculating the distance to perfect tracking for each individual for each of the 3 climate variables, which was used as a level of climate tracking, we then compared these distances to the telomere length of that individual bird (Figure 3.2). There was no significant

relationship between the level of climate tracking and telomere length for any of the three climate variables, with all p-values exceeding 0.05 (Figure 53.b,d,f). The correlations between telomere length and tracking levels for mean annual temperature, maximum temperature of the warmest quarter, and precipitation of the warmest quarter were 0.055, 0.015, and 0.0414, respectively.

Discussion

In this study, we provide some of the first evidence for local adaptation across seasonal habitats in migratory birds, marking a significant advancement in understanding selection pressures throughout the annual cycle. We first tested the theoretical prediction that migratory connectivity influences local adaptation to the nonbreeding grounds. While yellow warblers, which exhibit moderate migratory connectivity, show genomic variation linked to nonbreeding climate, selection pressures on nonbreeding grounds were markedly weaker with nearly three times less loci associated with nonbreeding climate compared to breeding climate. There were also fewer than 50 of the 1008 candidate genes that showed overlapping selection across both seasons, highlighting that breeding and nonbreeding selection pressures are largely distinct and as such, act on separate sets of genes. Additionally, there was no evidence that climate tracking is adaptive, as signals of local adaptation were linked to different climate variables across breeding and nonbreeding grounds. Furthermore, results indicate that there is no physiological cost of reduced climate tracking, as telomere length did not differ with varying levels of climate tracking.

The identification of climate-associated loci on the nonbreeding grounds is an important finding, as most studies of local adaptation in migratory species focus exclusively on the breeding grounds (Ruegg et al. 2018, Tigano et al 2017, Wauchope et al.). Approximately 24%

of the candidate loci identified were associated with non-breeding climate variables, demonstrating that the nonbreeding climate exerts distinct and measurable selective pressures on yellow warblers. However, the extent of local adaptation to nonbreeding climate is likely influenced by the strength of migratory connectivity (Webster and Marra 2005, Webster et al. 2002). Yellow warblers exhibit moderate migratory connectivity, resulting in some gene flow between populations exposed to different environmental conditions on the nonbreeding grounds (Bay et al. 2021). This gene flow may dilute signals of local adaptation to the nonbreeding grounds by introducing alleles from other populations experiencing divergent selection. Consequently, this could explain why the majority of candidate loci were associated with breeding climate, as well as why only 49 SNPs were linked to genes associated with climate on both the breeding and nonbreeding grounds. This pattern is further supported by a lower average correlation coefficient between candidate SNPs and nonbreeding climate variables compared to breeding climate variables. From a conservation perspective, moderate migratory connectivity and weaker signals of local adaptation to the nonbreeding grounds may help maintain standing genetic diversity, which could facilitate future adaptation to changing climates. However, the extent to which these factors influence climate adaptation on the nonbreeding grounds remains unclear and warrants further investigation.

Our findings suggest that the strongest associations between genomic variation and climate variables differ on the breeding and nonbreeding grounds. These results challenge the assumption that climate tracking reflects uniform selective pressures across the annual cycle. On the nonbreeding grounds, we find that yellow warblers exhibit genomic variation mostly associated with temperature variables such as mean annual temperature and maximum temperature of the warmest month. On the breeding grounds, however, we find that precipitation

of the warmest quarter was associated with the majority of candidate loci, consistent with previous studies on local adaptation of yellow warbler to their breeding grounds (Bay et al., 2018 Rodriguez et al. 2025). Past studies have often assumed that birds who track their climate between the breeding and nonbreeding ranges are dependent on the same climatic variables across their annual cycle (Fandos et al., 2020, Illán et al. 2022, Zurell et al., 2018, Bay et a. 2021). However, in yellow warblers, a species that exhibits climate tracking at the individual, regional, and population levels, we find that birds are adapted to different climatic variables on the breeding and nonbreeding grounds.

This distinction between seasonal selection pressures is further reflected in our analysis of climate-linked SNPs. To investigate the potential functional relevance of candidate climate-linked SNPs, we first identified genes from the literature that are linked to thermal tolerance, bill morphology (related to insect availability and heat dissipation), and feather color (related to thermal effects; Table S3.1). Although 938 candidate genes were linked to SNPs associated with breeding climate and 119 were associated with nonbreeding climate, the GLI3 gene was the only gene from our predetermined list associated with candidate SNPs linked to climate on both the nonbreeding and breeding grounds. GLI3 has been implicated in heat adaptation in chickens, bill morphology involved in local adaptation in great tits, and is associated with GO terms related to respiratory system processes and melanocyte differentiation (Bosse et al. 2017, Xu et al., 2022). These diverse functions suggest that GLI3 plays a multifaceted role in facilitating adaptation to climate across the annual cycle, potentially enabling yellow warblers to respond to selective pressures in both their breeding and nonbreeding habitats. However, the fact that no other genes were linked to traits associated with climate adaptation overlapping between the seasons further

reinforces our findings that selection is acting on different traits in each phase of the annual cycle.

We also find that higher levels of climate tracking do not correlate with reduced physiological stress. Previously (Chapter 1), we demonstrated that telomere length decreases with increasing phenotype-environment mismatch, supporting its use as an informative biological indicator of maladaptation. Based on these findings, if climate tracking were adaptive, individuals with lower tracking levels would be expected to exhibit shorter telomeres. However, no differences in telomere length were observed between individuals who track climate more closely and those who track it less for the three climate variables, with the strongest genomic associations across the breeding and nonbreeding grounds. These results challenge the assumption that climate tracking reflects local adaptation and instead suggest that it is likely driven by other factors, such as resource availability or energetic trade-offs, as proposed by Somveille et al. (2021). Since our results focus on climate tracking at the individual level, further research is needed at regional and population scales to determine whether its adaptiveness is scale-dependent.

Conclusion

Despite significant advances in understanding local adaptation on the breeding grounds of migratory birds, the non-breeding season remains comparatively understudied, leaving critical gaps in our knowledge of how selection pressures shape populations across the full annual cycle. In this study, we address this disparity by leveraging whole-genome sequencing to identify genomic signals of local adaptation in yellow warblers throughout their annual cycle. Our findings demonstrate that in accordance with our predictions, yellow warblers experience distinct selective pressures on their non-breeding grounds, although signals of local adaptation on the

breeding grounds are stronger. Furthermore, we find no evidence that climate tracking is adaptative. Different climate variables were important to local adaptation on the breeding versus the wintering grounds and climate tracking was not correlated with reduced physiological stress, as indicated by telomere length. These results challenge assumptions about the adaptiveness of climate tracking and suggest that other ecological or energetic factors may drive this behavior.

By directly comparing the climatic drivers of adaptation across breeding and non-breeding phases at the individual level, our study highlights the complexity of selective pressures experienced by migratory species across their annual cycles. These findings contribute to a growing understanding of the evolutionary ecology of migratory birds and provide a foundation for future studies aiming to predict population responses to climate change in migratory bird species.

Figures and Tables

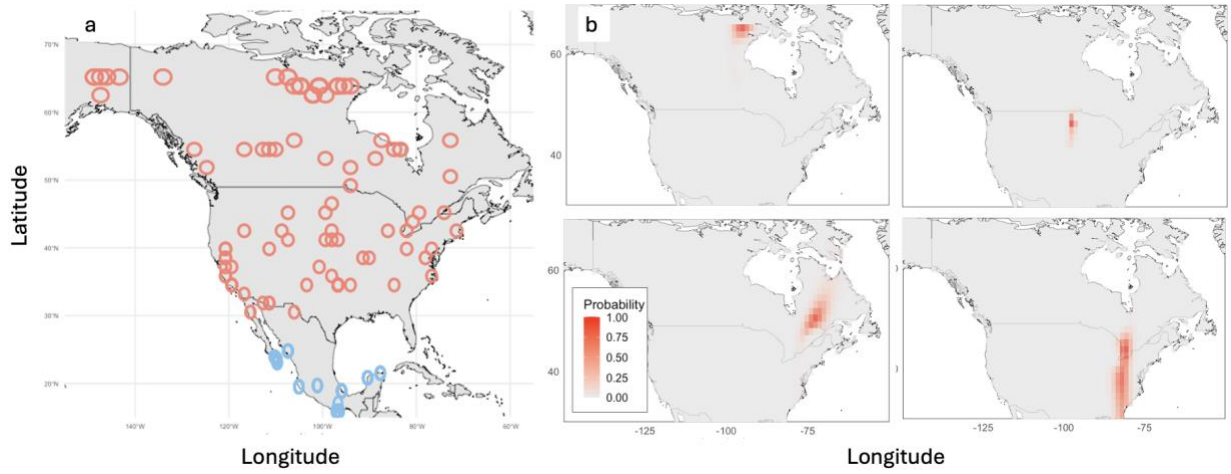

Figure 3.1. A) Map of 106 yellow warblers from 17 populations sampled on the nonbreeding grounds (blue) and their corresponding location on the breeding grounds that had the highest probability of assignment (red). Climate variables were extracted from a 114 km radius around each point, corresponding to the average radius for which the assignment probability was 0.99. The extraction radius for each sample is represented by each circle on the map. B) Examples of breeding assignment probability plots for four different individuals. Nonbreeding birds were assigned breeding locations by estimating allele frequency surfaces across the breeding range using whole-genome sequencing data from birds sampled on the breeding range.

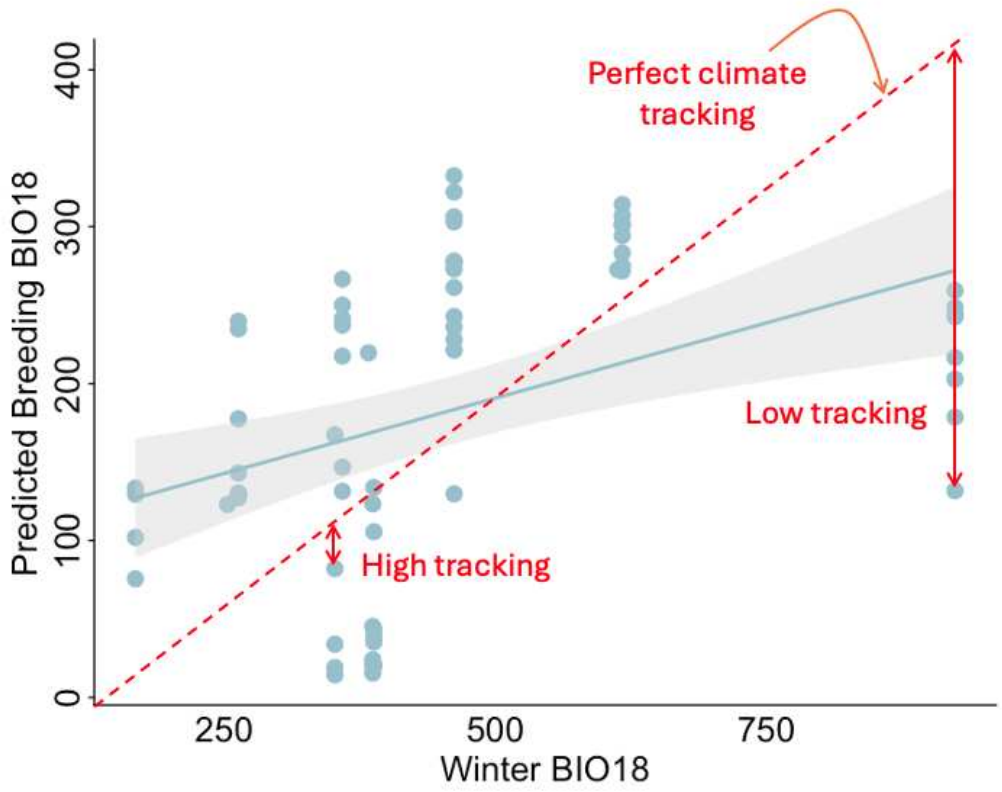

Figure 3.2. Level of tracking was determined by calculating the distance between each data point in the climate regression and the expected line of perfect tracking. The climate regression shows the relationship between winter climate and predicted breeding climate. In calculating climate tracking, smaller values indicated closer adherence to perfect tracking (i.e., greater climate matching), and larger values indicated less tracking.

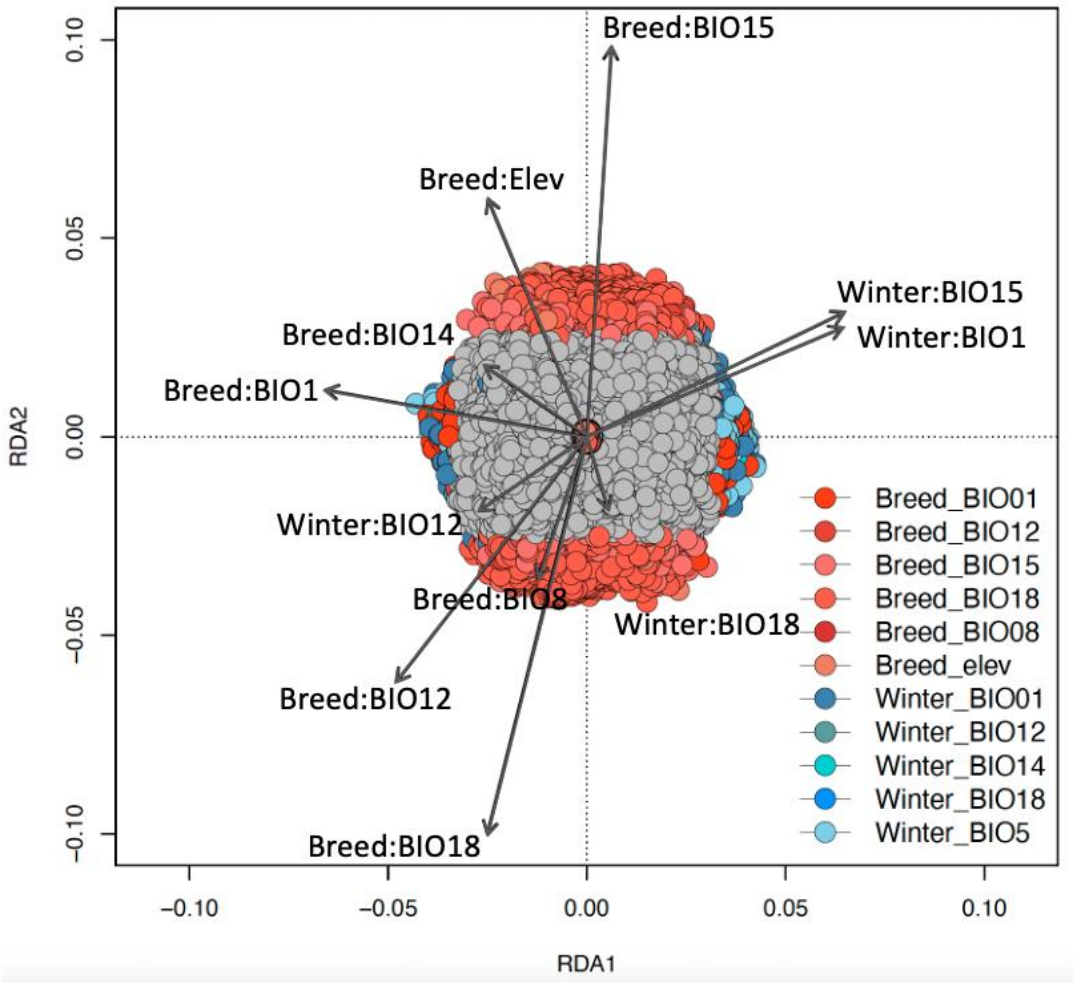

Figure 3.3. Redundancy analysis (RDA) was used to identify the climate variables most strongly associated with genomic variation across the annual cycle of the yellow warbler. Each circle represents a single nucleotide polymorphism (SNP), while the length and direction of arrows correspond to the strength and direction of the association with each climate variable. Cooler colors represent SNPs most strongly associated with nonbreeding climate, while warmer colors represent SNPs most strongly associated with the breeding climate.

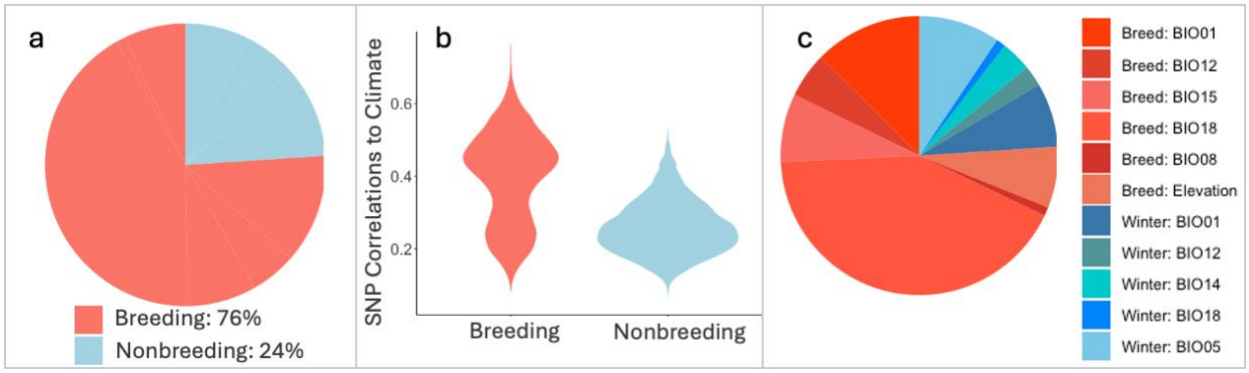

Figure 3.4. Redundancy analysis (RDA) was used to identify candidate SNPs associated with climate across the breeding and non-breeding grounds. a) Of the 29,481 candidate loci identified, 7,065 loci were associated with non-breeding climate variables and 22,416 loci were associated with breeding climate variables. b) The mean correlation strength between candidate SNPs and their associated environmental variables was 0.26 (± 0.07) for the non-breeding grounds and 0.40 (± 0.12) for the breeding grounds. C) candidate SNPs associated with climate variables across the breeding and non-breeding grounds. Colors represent the proportion of SNPs most associated with each bioclim variable, where warmer colors represent breeding climate variables and cooler colors represent nonbreeding climate variables. Variables include mean annual temperature (BIO1), annual precipitation (BIO12), precipitation seasonality. (BIO15), precipitation of the warmest quarter (BIO18), precipitation of the driest month (BIO14), and max temperature of the warmest month (BIO5).

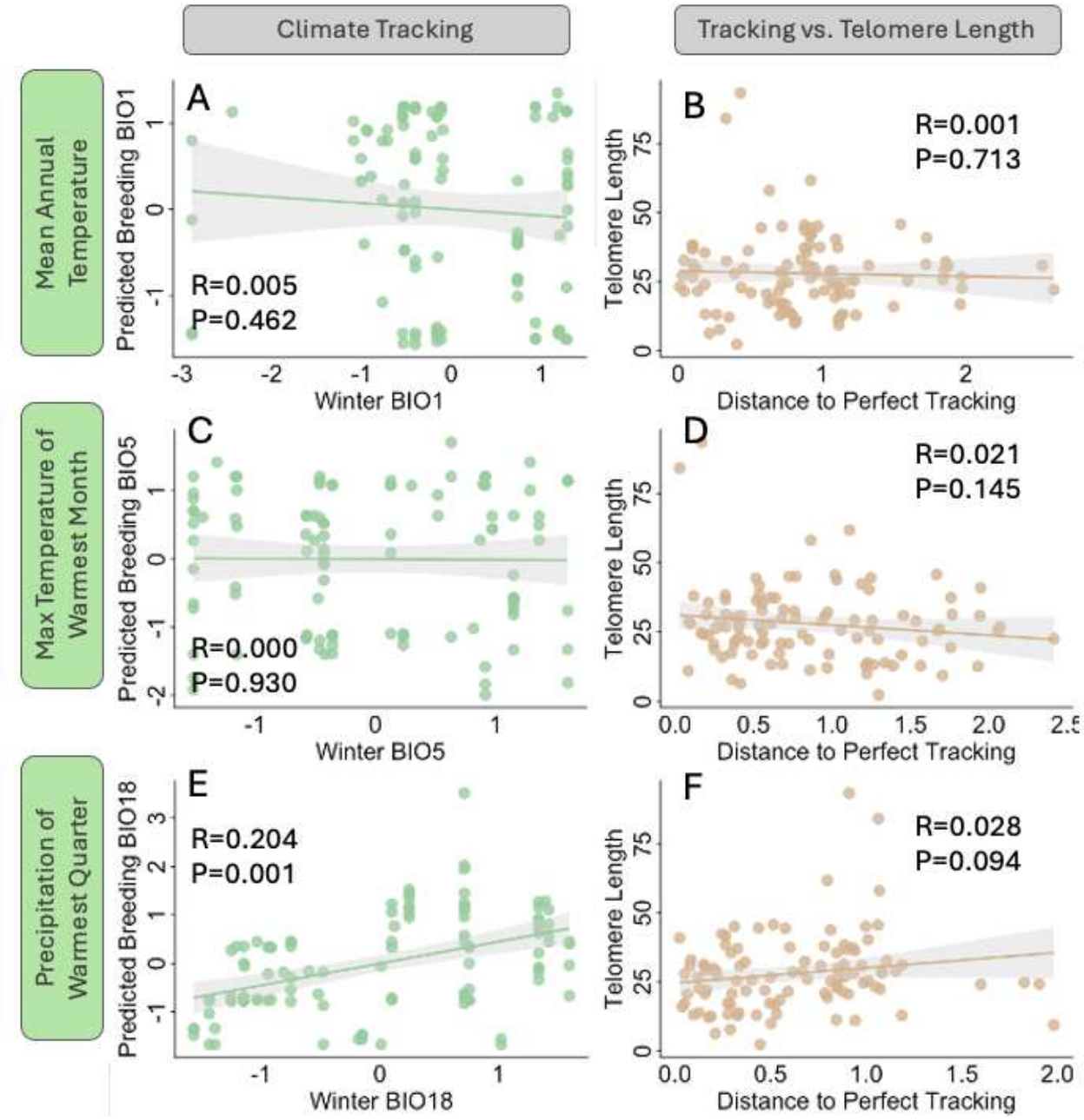

Figure 3.5. Climate tracking and telomere length measurements in 106 yellow warblers for the top climate variables on the nonbreeding and breeding grounds. Based on the redundancy analysis (RDA), mean annual temperature (BIO1) and max temperature of the warmest month (BIO5) were the most important climate variables for the nonbreeding grounds, while precipitation of the warmest quarter (BIO18) was most important for the breeding grounds. Climate tracking was calculated by first looking at the association between standardized nonbreeding and predicted breeding climate (A, C, E). Assuming perfect climate tracking results in a regression line with a slope of 1, we calculated the distance between each data point and the line of perfect tracking. The adaptiveness of climate tracking was then tested for by looking at

the relationship between telomere length and climate tracking to find if less tracking was associated with more physiological stress (B, D, F).

Table 3.1. Candidate SNPs identified by redundancy analyses (RDA) with correlations to environmental variables above 0.4 and overlapping with genes on our predetermined candidate SNP list (Table S1). Season refers to whether the SNP associated with the gene was linked to climate on the breeding or nonbreeding grounds (or both). Climate variables are the noncorrelated bioclim variables associated with the SNP of interest.

Season	Climate Variable	Chromosome	Marker position (bp)	Gene name	Region	Distance to region	Correlation	Function	References
Breeding	BIO15	SCAF_1	23234914	DISC1	Intron 10	7887	0.41238985	Cold tolerance	Fedorova et al. 2022 Romanov et al. 2023
Breeding	BIO18	SCAF_1	25450622	RYR2	Intron 8	3820	0.42438008	Cold tolerance	Fedorova et al. 2022
Breeding	BIO15	SCAF_10	2094105	OTUD7A	Intron 11	770	0.41720393	Heat adaptation	Xu et al. 2023
Breeding	BIO15	SCAF_13	15087136	PTPRG	Intron 1	1029	0.42579788	Heat adaptation	Xu et al. 2024
Breeding	BIO18	SCAF_2	4480172	EXOC2	Intron 19	748	0.42481232	Heat adaptation; heat stress	Carvalho et al. 2021 Zhuang et al. 2019
Breeding	Elevation	SCAF_2	42453195	CHD7	Intron 4	3786	0.48335897	Roof of mouth development	GO term
Breeding	Elevation	SCAF_2	56153204	VPS13B	Intron 79	2048	0.40576423	Bill morphology	Lamichhaney et al. 2015 Bosse et al. 2017
Breeding	BIO18	SCAF_20	3037327	TENM2	Intron 8	30951	0.43339884	Climate adaptation	Fleming et al. 2016
Breeding	BIO18	SCAF_3	51643412	SOX10	Upstream gene variant	649	0.4628383	Melanocyte differentiation	GO term

Breeding	BIO18	SCAF_38	3763273	INHBA	Intron 1	1561	0.43769745	Roof of mouth development	GO term
Breeding	BIO18	SCAF_38	3897986	GLI3	Intron 4	1264	0.51655566	Climate adaptation, bill morphology, melanocyte differentiation	Xu et al. 2023 Bosse et al. 2017 GO term
Breeding	BIO18	SCAF_38	3942219	PPARGC1A	Intron 1	320	0.40112588	Cold tolerance heat stress	Romanov et al. 2023 Wang et al. 2020
Breeding	BIO18	SCAF_4	15851321	WFIKKN2	Exon 1	0	0.49273517	Roof of mouth development	GO term
Breeding	BIO18	SCAF_40	4924209	SPAG9	Intron 13	24	0.51704097	Cold tolerance	Fedorova et al. 2022 Romanov et al. 2023
Breeding	BIO18	SCAF_40	5038277	BCOR	Intron 6	2789	0.41424086	Roof of mouth development	GO term
Breeding	BIO18	SCAF_48	747218	MGAT4C	Intron 2	462	0.56760685	Bill morphology	Lawson et al. 2017
Breeding	BIO18	SCAF_49	1977502	TGFBR2	Intron 1	306	0.45189447	Cold tolerance	Romanov et al. 2023
Non-breeding	BIO1	SCAF_6	31437959	GLI3	Intron 4	1130	0.41415481	Climate adaptation, bill morphology, melanocyte differentiation	Xu et al. 2023 Bosse et al. 2017 GO term
Non-breeding	BIO1	SCAF_47	2698312	RGS6	Intron 4	2813	0.40675387	Heat adaptation	Xu et al. 2023

Non-breeding	BIO5	SCAF_8	27827115	USP13	Intron 11	425	0.41149311	Melanocyte differentiation	GO term

LITERATURE CITED

Angelier, F., Weimerskirch, H., Barbraud, C., Chastel, O., & Hopkins, W. (2019). Is telomere length a molecular marker of individual quality? Insights from a long-lived bird. Functional Ecology, 33(6), 1076-1087. https://doi.org/10.1111/1365-2435.13307.

Backström, N., Qvarnström, A., Gustafsson, L., & Ellegren, H. (2006). Levels of linkage disequilibrium in a wild bird population. Biology letters, 2(3), 435-438.

Bay, R. A., Harrigan, R. J., Underwood, V. H., Gibbs, H. L., Smith, T. B., & Ruegg, K. C. (2018). Genomic signals of selection predict climate-driven population declines in a migratory bird. Science, 359, 83-86.

Bay, R. A., Karp, D. S., Saracco, J. F., Anderegg, W. R. L., Frishkoff, L. O., Wiedenfeld, D.,…Ruegg, K. (2021). Genetic variation reveals individual-level climate tracking across the annual cycle of a migratory bird. Ecol Lett, 24(4), 819-828. https://doi.org/10.1111/ele.13706

Bichet, C., Bouwhuis, S., Bauch, C., Verhulst, S., Becker, P. H., & Vedder, O. (2020). Telomere length is repeatable, shortens with age and reproductive success, and predicts remaining lifespan in a long-lived seabird. Molecular Ecology, 29(2), 429-441.

Blackburn, E. H. (1991). Structure and function of telomeres. Nature, 350(6319), 569-573.

Blackburn, E. H. (2005). Telomeres and telomerase: their mechanisms of action and the effects of altering their functions. FEBS Lett, 579(4), 859-862. https://doi.org/10.1016/j.febslet.2004.11.036

Bolger, A. M., Lohse, M., & Usadel, B. (2014). Trimmomatic: a flexible trimmer for Illumina sequence data. Bioinformatics, 30(15), 2114-2120.

Bosse, M., Spurgin, L. G., Laine, V. N., Cole, E. F., Firth, J. A., Gienapp, P.,…Slate, J. (2017). Recent natural selection causes adaptive evolution of an avian polygenic trait. Science.

Cadenas, E., & Davies, K. J. (2000). Mitochondrial free radical generation, oxidative stress, and aging. Free radical biology and medicine, 29(3-4), 222-230.

Carbon, S., Ireland, A., Mungall, C. J., Shu, S., Marshall, B., Lewis, S.,…Group, W. P. W. (2009). AmiGO: online access to ontology and annotation data. Bioinformatics, 25(2), 288-289.

Cheron, M., Angelier, F., Ribout, C., & Brischoux, F. (2021). Clutch quality is related to embryonic development duration, hatchling body size and telomere length in the spined toad (Bufo spinosus). Biological Journal of the Linnean Society. https://doi.org/10.1093/biolinnean/blab035/6187432

Danecek, P., Bonfield, J. K., Liddle, J., Marshall, J., Ohan, V., Pollard, M. O.,…Davies, R. M. (2021). Twelve years of SAMtools and BCFtools. Gigascience, 10(2), giab008.

DeSaix, M. G., Rodriguez, M. D., Ruegg, K. C., & Anderson, E. C. (2024). Population assignment from genotype likelihoods for low-coverage whole-genome sequencing data. *Methods in Ecology and Evolution*, *15*(3), 493-510.

Ding, Z., Mangino, M., Aviv, A., Consortium, U. K., Spector, T., & Durbin, R. (2014). Estimating telomere length from whole genome sequence data. Nucleic acids research, 42(9), e75-e75.

Dray, S., Blanchet, G., Borcard, D., Guenard, G., Jombart, T., Larocque, G.,…Dray, M. S. (2018). Package 'adespatial'. R package, 2018, 3-8.

DuBois, K., Pollard, K. N., Kauffman, B. J., Williams, S. L., & Stachowicz, J. J. (2022). Local adaptation in a marine foundation species: Implications for resilience to future global change. Glob Chang Biol, 28(8), 2596-2610. https://doi.org/10.1111/gcb.16080

Eastwood, J. R., Hall, M. L., Teunissen, N., Kingma, S. A., Hidalgo Aranzamendi, N., Fan, M.,…Peters, A. (2019). Early-life telomere length predicts lifespan and lifetime reproductive success in a wild bird. Mol Ecol, 28(5), 1127-1137. https://doi.org/10.1111/mec.15002

Fandos, G., Rotics, S., Sapir, N., Fiedler, W., Kaatz, M., Wikelski, M.,…Zurell, D. (2020). Seasonal niche tracking of climate emerges at the population level in a migratory bird. Proc Biol Sci, 287(1935), 20201799. https://doi.org/10.1098/rspb.2020.1799

Fick, S. E., & Hijmans, R. J. (2017). WorldClim 2: new 1-km spatial resolution climate surfaces for global land areas. International journal of climatology, 37(12), 4302-4315.

Forester, B. R., Jones, M. R., Joost, S., Landguth, E. L., & Lasky, J. R. (2016). Detecting spatial genetic signatures of local adaptation in heterogeneous landscapes. Molecular ecology, 25(1), 104-120.

Gomez, C., Tenorio, E. A., Montoya, P., & Cadena, C. D. (2016). Niche-tracking migrants and niche-switching residents: evolution of climatic niches in New World warblers (Parulidae). Proc Biol Sci, 283(1824). https://doi.org/10.1098/rspb.2015.2458

Grabherr, M. G., Russell, P., Meyer, M., Mauceli, E., Alföldi, J., Di Palma, F., & Lindblad-Toh, K. (2010). Genome-wide synteny through highly sensitive sequence alignment: Satsuma. Bioinformatics, 26(9), 1145-1151.

Heidinger, B. J., Blount, J. D., Boner, W., Griffiths, K., Metcalfe, N. B., & Monaghan, P. (2012). Telomere length in early life predicts lifespan. Proc Natl Acad Sci U S A, 109(5), 1743-1748. https://doi.org/10.1073/pnas.1113306109

Houben, J. M., Moonen, H. J., van Schooten, F. J., & Hageman, G. J. (2008). Telomere length assessment: biomarker of chronic oxidative stress? Free radical biology and medicine, 44(3), 235-246.

Igoshin, A. V., Yudin, N. S., Romashov, G. A., & Larkin, D. M. (2023). A multibreed genome-wide association study for cattle leukocyte telomere length. Genes, 14(8), 1596.

Illán, J. G., Wang, G., King, D. T., & Cunningham, F. L. (2022). Seasonal variation and tracking of climate niche of a migratory bird. Global Ecology and Conservation, 37. https://doi.org/10.1016/j.gecco.2022.e02155

Jackson, J. M., Pimsler, M. L., Oyen, K. J., Strange, J. P., Dillon, M. E., & Lozier, J. D. (2020). Local adaptation across a complex bioclimatic landscape in two montane bumble bee species. Mol Ecol, 29(5), 920-939.

Joseph, L. (2003). Predicting distributions of South American migrant birds in fragmented environments: a possible approach based on climate. In How landscapes change: human disturbance and ecosystem fragmentation in the Americas (pp. 263-283). Berlin, Heidelberg: Springer Berlin Heidelberg.

Joseph, L., & Stockwell, D. (2000). Temperature-based models of the migration of Swainson's Flycatcher (Myiarchus swainsoni) across South America: A new use for museum specimens of migratory birds. Proceedings of the Academy of Natural Sciences of Philadelphia, 293-300.

Jun, G., Wing, M. K., Abecasis, G. R., & Kang, H. M. (2015). An efficient and scalable analysis framework for variant extraction and refinement from population-scale DNA sequence data. Genome research, 25(6), 918-925.

Kawecki, T. J., & Ebert, D. (2004). Conceptual issues in local adaptation. Ecology Letters, 7(12), 1225-1241. https://doi.org/10.1111/j.1461-0248.2004.00684.x
Kirkpatrick, M., & Barton, N. H. (1997). Evolution of a species' range. The American Naturalist, 150(1), 1-23.
Köster, J., & Rahmann, S. (2012). Snakemake—a scalable bioinformatics workflow engine. Bioinformatics, *28*(19), 2520-2522.
Li, H., & Durbin, R. (2009). Fast and accurate short read alignment with Burrows-Wheeler transform. Bioinformatics, 25(14), 1754-1760. https://doi.org/10.1093/bioinformatics/btp324
Li, H., Handsaker, B., Wysoker, A., Fennell, T., Ruan, J., Homer, N.,…Genome Project Data Processing, S. (2009). The Sequence Alignment/Map format and SAMtools. Bioinformatics, 25(16), 2078-2079. https://doi.org/10.1093/bioinformatics/btp352
Liu, Q., Liu, H., Shi, L., Gan, M., Zhao, X., Lyu, L. D.,…Gao, Q. (2021). Local adaptation of Mycobacterium tuberculosis on the Tibetan Plateau. Proc Natl Acad Sci U S A, 118(17). https://doi.org/10.1073/pnas.2017831118
Lou, R. N., & Therkildsen, N. O. (2022). Batch effects in population genomic studies with low-coverage whole genome sequencing data: Causes, detection and mitigation. Molecular Ecology Resources, 22(5), 1678-1692.
Mahony, C. R., MacLachlan, I. R., Lind, B. M., Yoder, J. B., Wang, T., & Aitken, S. N. (2020). Evaluating genomic data for management of local adaptation in a changing climate: A lodgepole pine case study. Evol Appl, 13(1), 116-131. https://doi.org/10.1111/eva.12871
McEwen, B. S., & Wingfield, J. C. (2003). The concept of allostasis in biology and biomedicine. Horm Behav, 43(1), 2-15. https://doi.org/10.1016/s0018-506x(02)00024-7
Meisner, J., & Albrechtsen, A. (2018). Inferring population structure and admixture proportions in low-depth NGS data. Genetics, *210*(2), 719-731.
Peterson, D. A., Hilborn, R., & Hauser, L. (2014). Local adaptation limits lifetime reproductive success of dispersers in a wild salmon metapopulation. Nat Commun, 5, 3696. https://doi.org/10.1038/ncomms4696
Quinlan, A. R. (2014). BEDTools: the Swiss-army tool for genome feature analysis. Current protocols in bioinformatics, 47(1), 11.12. 11-11.12. 34.
Ranola, J. M., Novembre, J., & Lange, K. (2014). Fast spatial ancestry via flexible allele frequency surfaces. Bioinformatics, 30(20), 2915-2922. https://doi.org/10.1093/bioinformatics/btu418
Rockwell, S. M., Wunderle, J. M., Jr., Sillett, T. S., Bocetti, C. I., Ewert, D. N., Currie, D.,…Marra, P. P. (2017). Seasonal survival estimation for a long-distance migratory bird and the influence of winter precipitation. Oecologia, 183(3), 715-726. https://doi.org/10.1007/s00442-016-3788-x
Rodriguez, M. D., Bay, R. A., & Ruegg, K. C. (2025). Telomere Length Differences Indicate Climate Change-Induced Stress and Population Decline in a Migratory Bird. Molecular Ecology, e17642.
Rollings, N., Uhrig, E. J., Krohmer, R. W., Waye, H. L., Mason, R. T., Olsson, M.,…Friesen, C. R. (2017). Age-related sex differences in body condition and telomere dynamics of red-sided garter snakes. Proceedings of the Royal Society B: Biological Sciences, 284(1852), 20162146.
Romero, L. M. (2004). Physiological stress in ecology: lessons from biomedical research. Trends in ecology & evolution, 19(5), 249-255.

Ruegg, K., Bay, R. A., Anderson, E. C., Saracco, J. F., Harrigan, R. J., Whitfield, M.,…Smith, T. B. (2018). Ecological genomics predicts climate vulnerability in an endangered southwestern songbird. Ecol Lett, 21(7), 1085-1096. https://doi.org/10.1111/ele.12977

Ruiz Minano, M., While, G. M., Yang, W., Burridge, C. P., Salvi, D., & Uller, T. (2022). Population genetic differentiation and genomic signatures of adaptation to climate in an abundant lizard. Heredity (Edinb), 128(4), 271-278. https://doi.org/10.1038/s41437-022-00518-0

Ryan Norris, D., & Marra, P. P. (2007). Seasonal Interactions, Habitat Quality, and Population Dynamics in Migratory Birds. The Condor, 109(3). https://doi.org/10.1093/condor/109.3.535

Sanford, E., & Worth, D. J. (2010). Local adaptation along a continuous coastline: prey recruitment drives differentiation in a predatory snail. Ecology, 91(3), 891-901. https://doi.org/10.1890/09-0536.1

Savolainen, O., Pyhäjärvi, T., & Knürr, T. (2007). Gene flow and local adaptation in trees. Annual Review of Ecology, Evolution, and Systematics, 38, 595-619.

Schweizer, T. M., & DeSaix, M. G. (2023). Cost-effective library preparation for whole genome sequencing with feather DNA. Conservation Genetics Resources, 15(1), 21-28.

Somveille, M., Bay, R. A., Smith, T. B., Marra, P. P., & Ruegg, K. C. (2021). A general theory of avian migratory connectivity. Ecol Lett, 24(9), 1848-1858. https://doi.org/10.1111/ele.13817

Somveille, M., Bossu, C. M., DeSaix, M. G., Alvarado, A. H., Gomez Villaverde, S., Rodriguez Otero, G.,…Ruegg, K. C. (2024). Broad-scale seasonal climate tracking is a consequence, not a driver, of avian migratory connectivity. Ecol Lett, 27(8), e14496. https://doi.org/10.1111/ele.14496

Sozou, P. D., & Kirkwood, T. B. (2001). A stochastic model of cell replicative senescence based on telomere shortening, oxidative stress, and somatic mutations in nuclear and mitochondrial DNA. J Theor Biol, 213(4), 573-586. https://doi.org/10.1006/jtbi.2001.2432

Taub, M. A., Conomos, M. P., Keener, R., Iyer, K. R., Weinstock, J. S., Yanek, L. R.,…Raffield, L. M. (2022). Genetic determinants of telomere length from 109,122 ancestrally diverse whole-genome sequences in TOPMed. Cell Genomics, 2(1).

Tigano, A., Shultz, A. J., Edwards, S. V., Robertson, G. J., & Friesen, V. L. (2017). Outlier analyses to test for local adaptation to breeding grounds in a migratory arctic seabird. Ecol Evol, 7(7), 2370-2381. https://doi.org/10.1002/ece3.2819

Van der Auwera, G. A., Carneiro, M. O., Hartl, C., Poplin, R., Del Angel, G., Levy-Moonshine, A.,…Thibault, J. (2013). From FastQ data to high-confidence variant calls: the genome analysis toolkit best practices pipeline. Current protocols in bioinformatics, 43(1), 11.10. 11-11.10. 33.

von Zglinicki, T. (2000). Role of oxidative stress in telomere length regulation and replicative senescence. Ann N Y Acad Sci, 908, 99-110. https://doi.org/10.1111/j.1749-6632.2000.tb06639.x

Von Zglinicki, T. (2002). Oxidative stress shortens telomeres. Trends in biochemical sciences, 27(7), 339-344.

Wauchope, H. S., Shaw, J. D., Varpe, Ø., Lappo, E. G., Boertmann, D., Lanctot, R. B., & Fuller, R. A. (2017). Rapid climate-driven loss of breeding habitat for Arctic migratory birds. Global Change Biology, 23(3), 1085-1094.

Webster, M. C., Marra, P. P., Susan, M. H., Bensch, S., & Holmes, R. T. (2002). Links between worlds: unraveling migratory connectivity. Trends in Ecology and Evolution, 17(2), 76-83.
Webster, M. S., & Marra, P. P. (2005). The importance of understanding migratory connectivity and seasonal interactions.
Xu, N. Y., Liu, Z. Y., Yang, Q. M., Bian, P. P., Li, M., & Zhao, X. (2022). Genomic Analyses for Selective Signatures and Genes Involved in Hot Adaptation Among Indigenous Chickens From Different Tropical Climate Regions. Front Genet, 13, 906447. https://doi.org/10.3389/fgene.2022.906447
Zurell, D., Gallien, L., Graham, C. H., & Zimmermann, N. E. (2018). Do long-distance migratory birds track their niche through seasons? Journal of Biogeography, 45(7), 1459-1468. https://doi.org/10.1111/jbi.13351

CHAPTER 4: RESEARCH SUMMARY

Chapter 1

My dissertation tests the hypothesis that integrating telomere dynamics with conservation genomics can enhance the identification and validation of fitness-related traits in studies of local adaptation. In my first chapter, I evaluate this hypothesis by testing the prediction that genetic variation associated with bill depth and telomere length is linked to precipitation, a key environmental factor previously identified as important for local adaptation in yellow warblers. Furthermore, I predict that mismatches between precipitation and bill morphology will correspond to shorter telomeres, suggesting that individuals experiencing such mismatches are maladapted to changes in precipitation. By examining these relationships, my research aims to establish telomere length as a meaningful biomarker of fitness and environmental maladaptation, reinforcing its value in the study of local adaptation.

My first chapter addressed a key goal of evolutionary biology; linking genotype and phenotype to environmental drivers of natural selection in a wild, non-model species. As climate change continues to drive fluctuations in temperature and precipitation, understanding the genetic basis of phenotypes critical to local adaptation, along with the environmental drivers of natural selection, is becoming increasingly important for predicting how species may respond to global change. Here we explore these connections on the breeding range of the yellow warbler. First, we conduct genome-wide association studies (GWAS) to identify loci related to bill shape and individual quality. In birds, bill shape is a good candidate phenotype for a GWAS because it often varies between populations, is highly heritable, and has established links to individual fitness across species (Lundregan et al. 2018, Bosse et al. 2017). Further, numerous studies have

connected bill morphology to climate, showing that larger bills are an adaptation to hot, dry conditions (Greenburg et al. 2012, Symonds and Tattersall 2010, Tattersall et a. 2017). After identifying genotype-phenotype links through a GWAS, a comprehensive understanding of the role of bill morphology in local adaptation necessitates examination of the environmental variables underlying natural selection. We therefore conduct a gene-environment association (GEA) analysis on resulting loci and find precipitation is underlying putative selection on bill shape. Although both GWAS and GEA are commonly employed in studies of local adaptation, using them independently can limit their scope. We combine these approaches and ultimately determine the link between precipitation and genetic variation at genes putatively affecting bill morphology.

In addition, I test whether contemporary individuals whose bill shape deviates from historical relationships with precipitation, exhibit increased stress—measured by telomere length—resulting from maladaptation. Our results indicate birds with shallow bills in regions becoming drier experience higher stress (*i.e.,* shorter telomeres) because of maladaptation.

Overall, my first chapter supports my predictions that genetic variation associated with bill depth and telomere length is linked to precipitation and that mismatches between precipitation and bill morphology will correspond to shorter telomeres. This study links genetic, phenotypic, and environmental data with telomere length to improve understanding of the process of local adaptation and effects of climate change on biodiversity.

Chapter 2

My second chapter again tests the hypothesis that integrating telomere dynamics with conservation genomics can enhance the identification and validation of fitness-related traits in studies of local adaptation. In this chapter, I evaluate this hypothesis by testing the prediction

that individuals inhabiting regions with high genomic offset are experiencing increased levels of telomere shortening because of climate change.

Maladaptation may become more pronounced as climate change continues and individuals are no longer optimally fit in their local environment (Wang, O'Neill et al. 2010). An increasingly popular approach to determining adaptive potential to climate change, which accounts for putative evolution and adaptation of populations to new environmental conditions, is genomic offset (Bay et al. 2018, Ruegg et al. 2018, Capblancq et al. 2020, Fitzpatrick and Keller 2015). This method uses genomic and environmental data to find a relationship between a climate factor and allele frequencies of a population, then finds the difference between current genotype-environmental relationships and those predicted under future climate change scenarios (Bay et al. 2018, Ruegg et al. 2018). In this way, genomic vulnerability can determine the degree of potential maladaptation of populations to future environmental conditions. However, evidence that genomic vulnerability reflects changes in physiological costs associated with environmental change is still needed. (Rellstab et al. 2021).

For many study systems, determining and measuring the physiological stress related to maladaptation is not feasible based on the biology of the organism or resources available for study. However, telomere length provides a mechanism that links organismal stress and survival, which makes for an ideal fitness proxy. Here we combine models of genomic offsets with measures of telomere shortening in a migratory bird, the yellow warbler (*Setophaga petechia*), and find a strong correlation between genomic offset, telomere length, and population decline. Our findings suggest that the yellow warblers in regions predicted to undergo significant climate change are situated in areas that have historically encountered substantial climate change. Furthermore, birds in these regions have experienced the most significant declines in abundance

and have the shortest telomeres, which may be a sign of increased stress. The work supports the idea that while genomic offset models predict how organisms will fare under future climate change, they can also be used to identify regions where populations may already be experiencing climate change-induced stress in cases where past and future climate changes are correlated.

Overall, my second chapter supports my prediction that individuals inhabiting regions with high genomic offset are experiencing increased levels of telomere shortening because of climate change. This study further supports my hypothesis and promotes the use of telomere length in studies of local adaptation.

Chapter 3

My third chapter again tests the hypothesis that integrating telomere dynamics with conservation genomics can enhance the identification and validation of fitness-related traits in studies of local adaptation. In this chapter, I evaluate this hypothesis by testing the prediction that if climate tracking is adaptive, we expect to see a positive association between level of climate tracking and telomere length.

To test this prediction, I first investigate whether yellow warblers exhibit local adaptation to climate conditions on their non-breeding grounds and how this compares to adaptation on the breeding grounds. Understanding local adaptation during the non-breeding season is critical, as conditions on wintering grounds strongly influence survival, migration timing, and fitness, collectively shaping population dynamics (Rockwell et al., 2017; Webster et al., 2002). Despite its importance, local adaptation on the non-breeding grounds of migratory birds remains largely unexplored due to the challenges of tracking individuals across vast distances and accurately quantifying their year-round climate exposure. Advances in genome-wide sequencing now enable investigation of genomic signals of local adaptation to both breeding and non-breeding

grounds. Using whole-genome sequencing data, we apply analytical approaches that estimate allele frequency surfaces on breeding grounds, allowing us to predict the geographic origins of individual birds captured on their wintering grounds (Ranola et al., 2014). This method enables us to determine the climatic variables experienced by individual birds on both breeding and non-breeding grounds, facilitating direct comparisons of the strength of local adaptation between these seasons. Our findings reveal that yellow warblers experience distinct selective pressures on their non-breeding grounds, albeit to a lesser extent than on their breeding grounds. Notably, adaptation on the non-breeding grounds is predominantly associated with temperature variables, contrasting with the precipitation-driven selection observed during the breeding season. We also tested whether climate tracking—a behavior aligning migration with consistent climatic conditions—reflects local adaptation across the annual cycle by assessing physiological stress through telomere length, a biomarker of stress. Contrary to expectations, we found no correlation between climate tracking and telomere length, suggesting that climate tracking is not driven by adaptation to similar climates across the annual cycle but may instead result from other ecological or energetic factors. These results challenge assumptions about the adaptiveness of climate tracking and highlight the need to consider alternative drivers of this behavior. They also underscore the complexity of selective pressures experienced by migratory species across their annual cycles and provide novel insights into the evolutionary ecology of migratory birds.

Overall, my third chapter supports the idea that climate tracking is not adaptive, as our results show no variation in telomere length across different levels of climate tracking. These results further support my hypothesis and provide an example of how telomere length can be used to answer longstanding evolutionary questions.

Conclusions and significance

Predicting species' responses to anthropogenic climate change is a critical concern in contemporary conservation efforts and requires the integration of data from multiple fields. My doctoral research combines genomic and telomere length analyses to characterize patterns of local adaptation and assess physiological effects in response to climate change in the migratory songbird, the yellow warbler. Overall, my dissertation tests the hypothesis that integrating telomere dynamics with conservation genomics can enhance the identification and validation of fitness-related traits in studies of local adaptation.

In my first study, I investigate the rarely documented links between genotype, phenotype, and the environmental drivers of local adaptation in wild populations, addressing a significant gap in our understanding of these dynamics. Examples of maladaptation, which can critically impact species fitness, are even rarer. Results from this study demonstrate the utility of combining genome-wide association studies (GWAS) and gene-environment association (GEA) analyses to identify genes underlying adaptive phenotypes and evaluate the role of environmental factors in shaping genetic variation within phenotype-linked genes. Additionally, I provide evidence of the negative effects of maladaptation to climate change by showing that individuals with bill morphologies mismatched to precipitation exhibit reduced telomere length (Chapter 1). These findings highlight the importance of understanding the genetic and environmental mechanisms driving adaptation and maladaptation to climate change, offering critical insights for predicting species resilience and informing conservation strategies.

My second study advances the use of genomic offset to predict maladaptation to current and future climate change by validating the assumption that individuals inhabiting regions with high genomic offset are expected to experience elevated physiological stress due to

maladaptation to changing environments. This study demonstrates that combining telomere length measurements with data on past population trends and changes in environmental variables critical for local adaptation provides a robust framework for assessing the impacts of climate change on wild populations (Chapter 2).

Finally, my last chapter is among the first to demonstrate local adaptation to the nonbreeding range of a migratory bird species, revealing the complexity of selective pressures experienced across the annual cycle. Furthermore, this study is the first to test the adaptiveness of climate tracking, challenging traditional assumptions about the drivers of migratory patterns and suggesting alternative ecological or energetic factors may play a larger role (Chapter 3). Together, this research highlights the power of integrating telomere length measurement with genomic data to bridge the gap between genetic variation, environmental pressures, and physiological stress, offering a more comprehensive approach to understanding local adaptation and predicting species' responses to climate change.

Additional research

In addition to the main studies covered in my dissertation, I have contributed to several other projects. I collaborated with researchers at Colorado State University, the Talon Ecological Research Group, and San Jose State University on a project demonstrating the value of genomic approaches for increasing genetic diversity in assisted breeding efforts in a highly inbred population of Western burrowing owls. My contribution involved determining telomere length in burrowing owl offspring to assess whether using genomic tools to optimize genetic diversity and reduce inbreeding between mating pairs was associated with reduced telomere shortening. We found that offspring from optimized breeding pairs had significantly longer telomeres,

suggesting that genomic approaches to pairing not only reduce the risk of inbreeding depression but also alleviate physiological stress over an individual's lifespan (Bossu et al. 2023).

I also collaborated on a methodological study with a researcher at CSU, using low-coverage whole-genome sequencing data to assign migratory birds caught on their wintering grounds to distinct genetic populations on their breeding grounds. I provided empirical examples of this method using yellow warbler data, demonstrating its utility for studying migratory connectivity in avian species (DeSaix et al. 2024).

I have also been collaborating on a project that aims to use telomere length to understand how the environment influences the distribution and abundance of hermit warblers (XX) on their breeding range. I trained a PhD student on measuring telomere length using laboratory methods and ran many of these assays myself. In addition, I helped run the telomere length analysis for this project. We hope to submit this study for publication by summer 2025.

Another project that I have been a part of outside of my dissertation is the validation of measuring telomere length using whole-genome sequencing data. For this project I am working with researchers from the Institute of Avian Research in Wilhelmshaven, Germany. I am contributing to this work by testing for an association between telomere length measurements using qPCR and whole-genome sequencing data in yellow warblers. With this analysis, I have found that whole-genome sequencing and qPCR measurements are highly correlated when accounting for sequencing library (conditional R^2=0.77). This work helps support the use of whole-genome sequencing data in avian telomere studies and has many implications for future telomere work in birds.

Finally, I worked with researchers from CSU to implement an experiential wildlife conservation immersion program for high school students identifying as girls and gender non-

conforming youth of color. This program aimed to attract minoritized youth to wildlife conservation studies by providing hands-on experiences and mentorship, fostering interest in and access to conservation careers (Murphy et al. 2024).

LITERATURE CITED

Bay, R. A., Harrigan, R. J., Underwood, V. H., Gibbs, H. L., Smith, T. B., & Ruegg, K. C. (2018). Genomic signals of selection predict climate-driven population declines in a migratory bird. Science, 359, 83-86.

Bosse, M., Spurgin, L. G., Laine, V. N., Cole, E. F., Firth, J. A., Gienapp, P., ... & Slate, J. (2017). Recent natural selection causes adaptive evolution of an avian polygenic trait. Science, 358(6361), 365-368.

Bossu, C. M., Rodriguez, M., Rayne, C., Chromczak, D. A., Higgins, P. G., Trulio, L. A., & Ruegg, K. C. (2023). Genomic approaches to mitigating genetic diversity loss in declining populations. Molecular Ecology, 32(19), 5228-5240.

Capblancq, T., Fitzpatrick, M. C., Bay, R. A., Exposito-Alonso, M., & Keller, S. R. (2020). Genomic prediction of (mal) adaptation across current and future climatic landscapes. Annu. Rev. Ecol. Evol. Syst., 51, 245-269.

DeSaix, M. G., Rodriguez, M. D., Ruegg, K. C., & Anderson, E. C. (2024). Population assignment from genotype likelihoods for low-coverage whole-genome sequencing data. Methods in Ecology and Evolution, 15(3), 493-510.

Greenberg, R., Cadena, V., Danner, R. M., & Tattersall, G. (2012). Heat loss may explain bill size differences between birds occupying different habitats. PloS one, 7(7), e40933.

Fitzpatrick, M. C., & Keller, S. R. (2015). Ecological genomics meets community-level modelling of biodiversity: Mapping the genomic landscape of current and future environmental adaptation. Ecology letters, 18(1), 1-16.

Lundregan, S. L., Hagen, I. J., Gohli, J., Niskanen, A. K., Kemppainen, P., Ringsby, T. H., ... & Jensen, H. (2018). Inferences of genetic architecture of bill morphology in house sparrow using a high-density SNP array point to a polygenic basis. Molecular ecology, 27(17), 3498-3514. Rellstab, C. (2021). Genomics helps to predict maladaptation to climate change. Nat. Clim. Change, 11, 85-86.

Murphy, M., Diaz-Clark, E., Rodriguez, M.D., Morado, M., Stafford, N., Frierson, R., Bombaci, S., Balgopal, M., Lavoie, A. (2025). Impact of a wildlife conservation immersion event on youth of color. Connected Science Learning.

Ranola, J. M., Novembre, J., & Lange, K. (2014). Fast spatial ancestry via flexible allele frequency surfaces. Bioinformatics, 30(20), 2915-2922. https://doi.org/10.1093/bioinformatics/btu418.

Rellstab, C. (2021). Genomics helps to predict maladaptation to climate change. Nat. Clim. Change, 11, 85-86.

Rockwell, S. M., Wunderle, J. M., Jr., Sillett, T. S., Bocetti, C. I., Ewert, D. N., Currie, D.,…Marra, P. P. (2017). Seasonal survival estimation for a long-distance migratory bird and the influence of winter precipitation. Oecologia, 183(3), 715-726. https://doi.org/10.1007/s00442-016-3788-x

Ruegg, K., Bay, R. A., Anderson, E. C., Saracco, J. F., Harrigan, R. J., Whitfield, M.,…Smith, T. B. (2018). Ecological genomics predicts climate vulnerability in an endangered southwestern songbird. Ecol Lett, 21(7), 1085-1096. https://doi.org/10.1111/ele.12977

Symonds, M. R., & Tattersall, G. J. (2010). Geographical variation in bill size across bird species provides evidence for Allen's rule. The American Naturalist, 176(2), 188-197.

Tattersall, G. J., Arnaout, B., & Symonds, M. R. (2017). The evolution of the avian bill as a thermoregulatory organ. Biological Reviews, 92(3), 1630-1656.
Wang, T., O'Neill, G. A., & Aitken, S. N. (2010). Integrating environmental and genetic effects to predict responses of tree populations to climate. Ecological applications, 20(1), 153-163.
Webster, M. C., Marra, P. P., Susan, M. H., Bensch, S., & Holmes, R. T. (2002). Links between worlds: unraveling migratory connectivity. Trends in Ecology and Evolution, 17(2), 76-83.

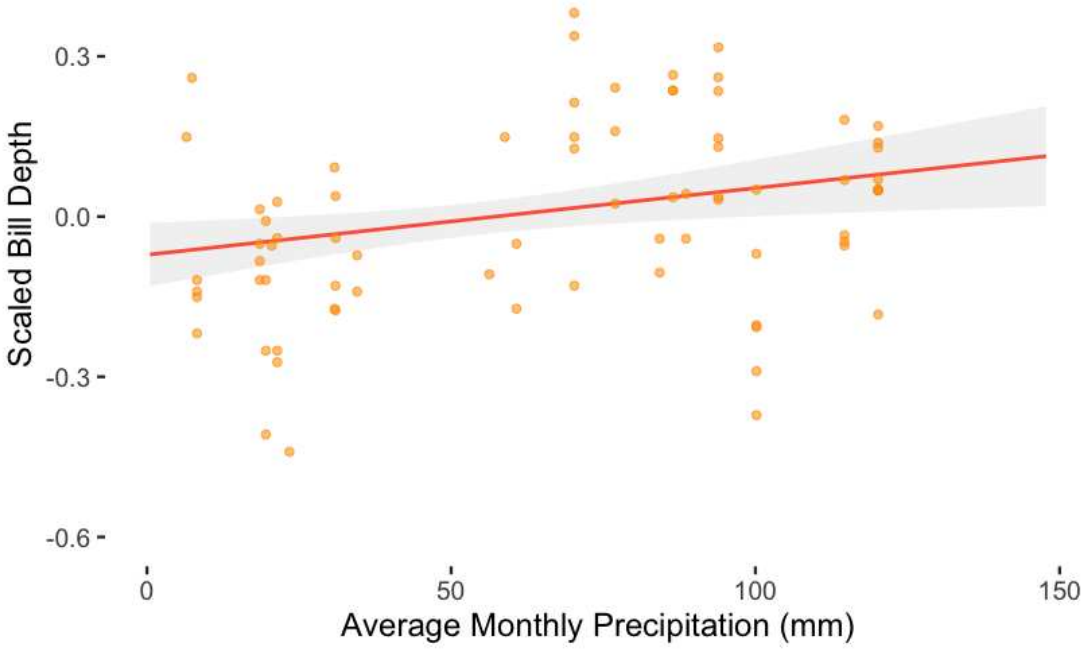

Figure S1.1. Residuals were calculated as the vertical distance between contemporary bill depth measurements and the line of best fit (red line) for historical associations in bill depth and average monthly precipitation for yellow warblers. These residuals were used as a measure of change between the historic and contemporary relationship between bill depth and precipitation; larger residuals indicate a larger mismatch between historic and contemporary relationships.

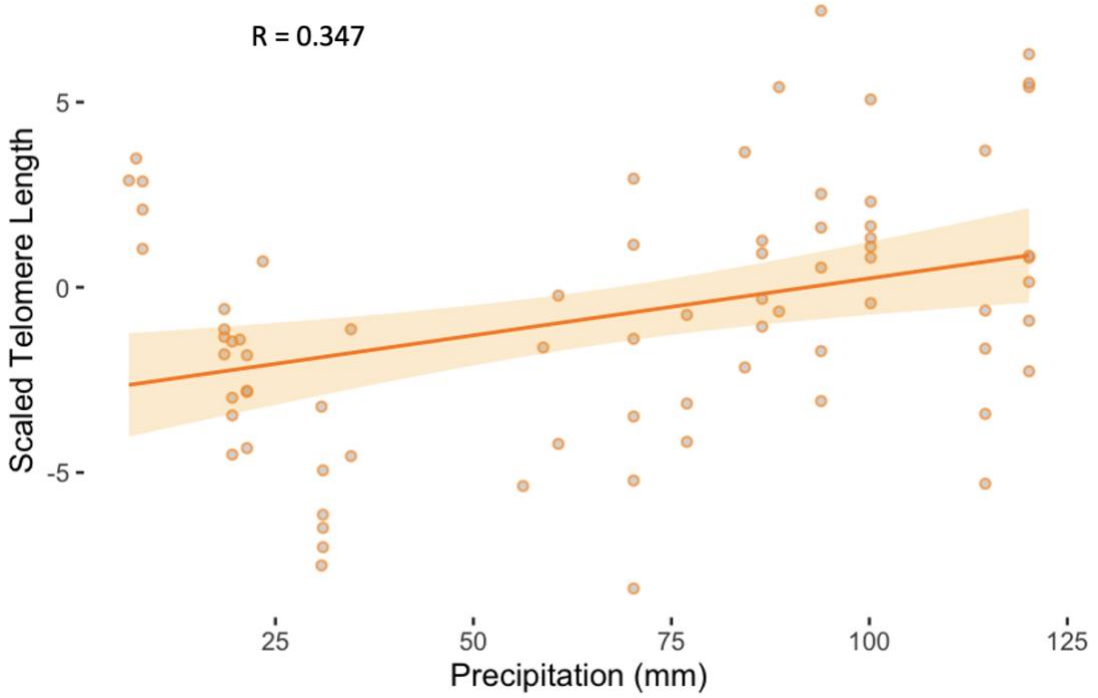

Figure S1.2. Telomere length increases with increasing precipitation across the breeding grounds of the yellow warbler.

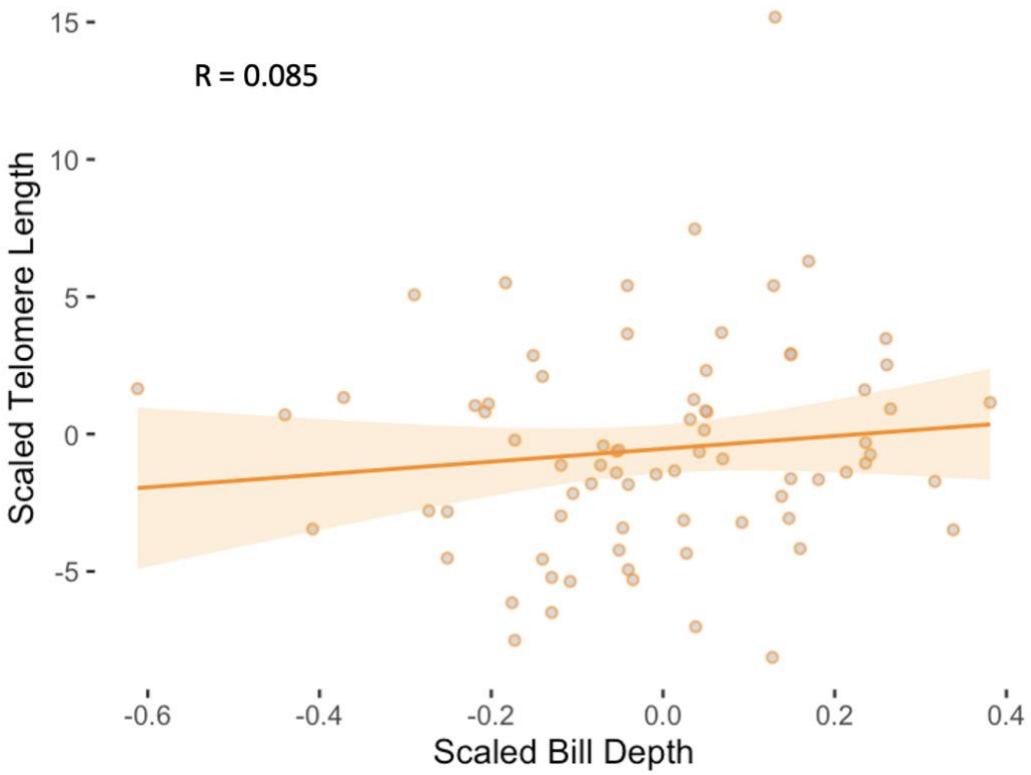

Figure S1.3. Telomere length slightly increases with increasing bill depth across the breeding grounds in the yellow warbler.

Table S1.1. Associations between allele frequency of the top-ranking SNPs and precipitation of the warmest quarter (BIO18) for yellow warblers across their breeding grounds. SNPs were identified through a genome-wide association study of bill depth and telomere length. Gray rows indicate a significant association when using a false discovery rate to correct for multiple testing.

SNP	*Gene*	*p-value*	R^2
SCAF_59.1151274	Unknown	0.0057	0.30
SCAF_6.33944704	MGAT5	0.0118	0.26
SCAF_25.4472163	Unknown	0.0189	0.23
SCAF_7.14703200	Unknown	0.0289	0.20
SCAF_1.27474479	Unknown	0.1265	0.10
SCAF_15.3601768	Unknown	0.1394	0.10
SCAF_1.9342730	PPP1CB	0.2792	0.05
SCAF_4.45165445	Unknown	0.3740	0.04
SCAF_162.713268	SKAP2	0.3920	0.03
SCAF_5.32737461	Unknown	0.4400	0.03
SCAF_2.54848922	RIMS2	0.5312	0.02
SCAF_8.12913741	Unknown	0.7183	0.00
SCAF_12.6242987	Unknown	0.7257	0.00
SCAF_8.22401258	Unknown	0.7326	0.01
SCAF_8.12913728	Unknown	0.7409	0.01
SCAF_3.65845632	Unknown	0.9178	0.00

Table S1.2. Associations between allele frequency of the top-ranking SNPs and precipitation of the wettest quarter (BIO16) for yellow warblers across their breeding grounds. SNPs were identified through a genome-wide association study of bill depth and telomere length. Gray rows indicate a significant association. False discovery rates were used to correct for multiple testing.

SNP	*Gene*	*p-value*	R^2
SCAF_8.12913728	Unknown	0.0171	0.23
SCAF_5.32737461	Unknown	0.0330	0.19
SCAF_8.12913741	Unknown	0.0439	0.17
SCAF_2.54848922	RIMS2	0.1506	0.09
SCAF_8.22401258	Unknown	0.2768	0.05
SCAF_3.65845632	Unknown	0.3816	0.04
SCAF_162.713268	SKAP2	0.6069	0.01
SCAF_12.6242987	Unknown	0.7331	0.01
SCAF_1.27474479	Unknown	0.7689	0.00
SCAF_6.33944704	MGAT5	0.7695	0.00
SCAF_7.14703200	Unknown	0.7757	0.00
SCAF_15.3601768	Unknown	0.8951	0.00
SCAF_4.45165445	Unknown	0.9256	0.00
SCAF_1.9342730	PPP1CB	0.9329	0.00
SCAF_59.1151274	Unknown	0.9620	0.00
SCAF_25.4472163	Unknown	0.9901	0.00

Table S1.3. Associations between allele frequency of the top-ranking SNPs and precipitation of the driest month (BIO14) for yellow warblers across their breeding grounds. SNPs were identified through a genome-wide association study of bill depth and telomere length. Gray rows indicate a significant association. False discovery rates were used to correct for multiple testing.

SNP	*Gene*	*p-value*	*R2*
SCAF_59.1151274	Unknown	0.0085	0.28
SCAF_25.4472163	Unknown	0.0343	0.19
SCAF_5.32737461	Unknown	0.0737	0.14
SCAF_2.54848922	RIMS2	0.1823	0.06
SCAF_12.6242987	Unknown	0.1877	0.08
SCAF_3.65845632	Unknown	0.3032	0.05
SCAF_7.14703200	Unknown	0.3951	0.03
SCAF_1.27474479	Unknown	0.5051	0.02
SCAF_8.12913741	Unknown	0.5460	0.02
SCAF_15.3601768	Unknown	0.5461	0.02
SCAF_8.12913728	Unknown	0.5847	0.01
SCAF_1.9342730	PPP1CB	0.7125	0.01
SCAF_8.22401258	Unknown	0.8431	0.00
SCAF_4.45165445	Unknown	0.8538	0.00
SCAF_162.713268	SKAP2	0.8780	0.00
SCAF_6.33944704	MGAT5	0.9555	0.00

Table S1.4. Associations between allele frequency of the top-ranking SNPs and isothermality (BIO3) for yellow warblers across their breeding grounds. SNPs were identified through a genome-wide association study of bill depth and telomere length. Gray rows indicate a significant association. False discovery rates were used to correct for multiple testing.

SNP	*Gene*	*p-value*	*R2*
SCAF_2.54848922	RIMS2	0.0026	0.34
SCAF_59.1151274	Unknown	0.0366	0.18
SCAF_25.4472163	Unknown	0.1131	0.11
SCAF_8.22401258	Unknown	0.1534	0.09
SCAF_7.14703200	Unknown	0.2246	0.07
SCAF_15.3601768	Unknown	0.2767	0.05
SCAF_1.9342730	PPP1CB	0.3440	0.04
SCAF_6.33944704	MGAT5	0.3903	0.03
SCAF_8.12913741	Unknown	0.4342	0.03
SCAF_12.6242987	Unknown	0.5127	0.02
SCAF_4.45165445	Unknown	0.5246	0.02
SCAF_162.713268	SKAP2	0.5369	0.02
SCAF_8.12913728	Unknown	0.6963	0.01
SCAF_3.65845632	Unknown	0.7857	0.00
SCAF_1.27474479	Unknown	0.8099	0.00
SCAF_5.32737461	Unknown	0.8485	0.00

Table S1.5. Telomere length of yellow warblers is influenced by an interaction between residuals (measure of change between historical and contemporary association between bill depth and precipitation), climate (average monthly precipitation of the summer months), and bill depth, as indicated by the model set and rankings. The number of parameters (K), -2 log-likelihood (-2LL), and model weights (w_i) are shown for each model and the models are ranked by their AICc differences relative to the best model in the set ($\Delta AICc_i$).

Model	*K*	$\Delta AICc_i$	-2LL	w_i
Residuals * Climate * Bill.Depth	8	0	-183.9	0.34
Climate	3	1.14	-190.41	0.19
Residuals * Climate	5	2.14	-188.64	0.12
Residuals + Climate	4	3.37	-190.41	0.06
Residuals + Bill.Depth	4	3.37	-190.41	0.06
Climate + Bill.Depth	4	3.37	-190.41	0.06
Residuals + Climate + Bill.Depth	4	3.37	-190.41	0.06
Residuals * Bill.Depth	5	4	-189.57	0.05
Climate * Bill.Depth	5	4.58	-189.86	0.03
Null	2	8.49	-195.17	0
Bill.Depth	3	10.12	-194.9	0
Residuals	3	10.51	-195.09	0

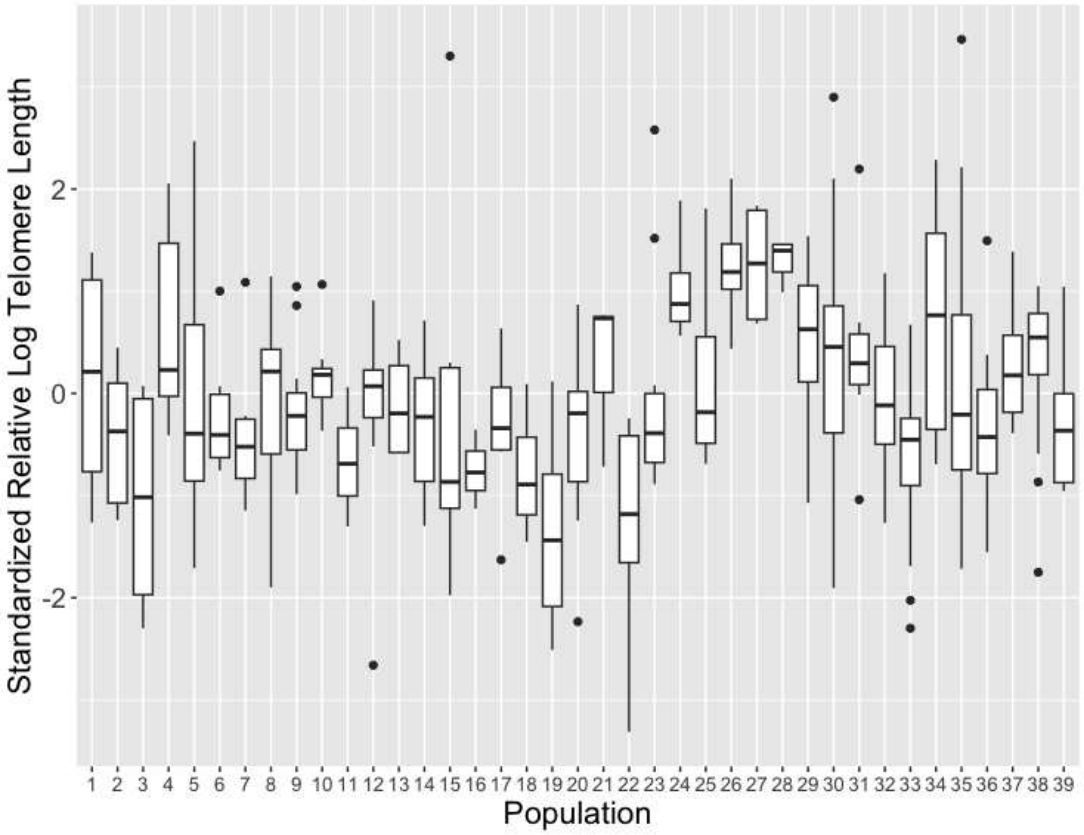

Figure S2.1. Mean standardized relative telomere length across 39 sampled populations of breeding yellow warblers (n=416).

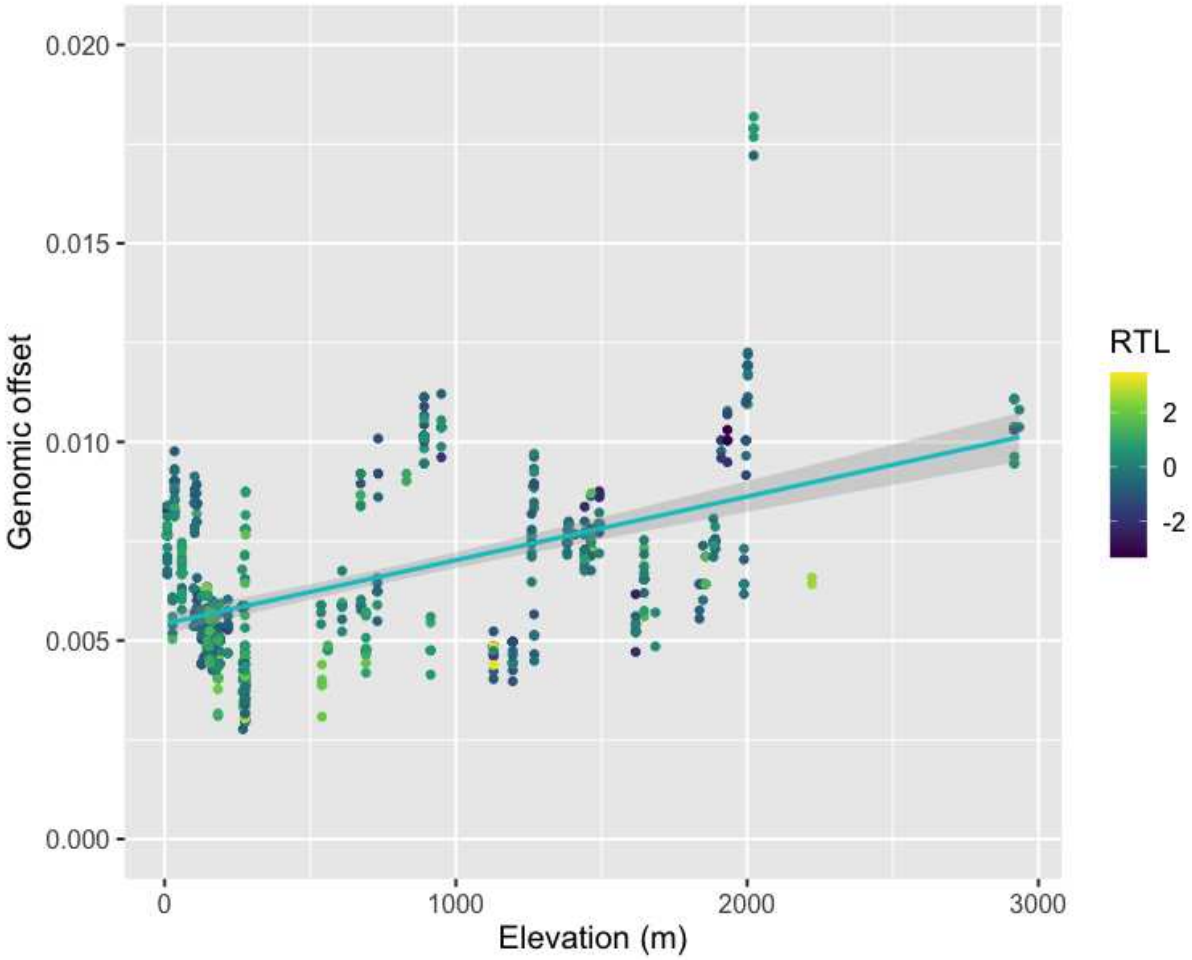

Figure S2.2. Genomic offset increases with elevation across sample sites (n=39) spanning the yellow warbler breeding range (R = 0.31). The color of each point represents individual standardized relative telomere length.

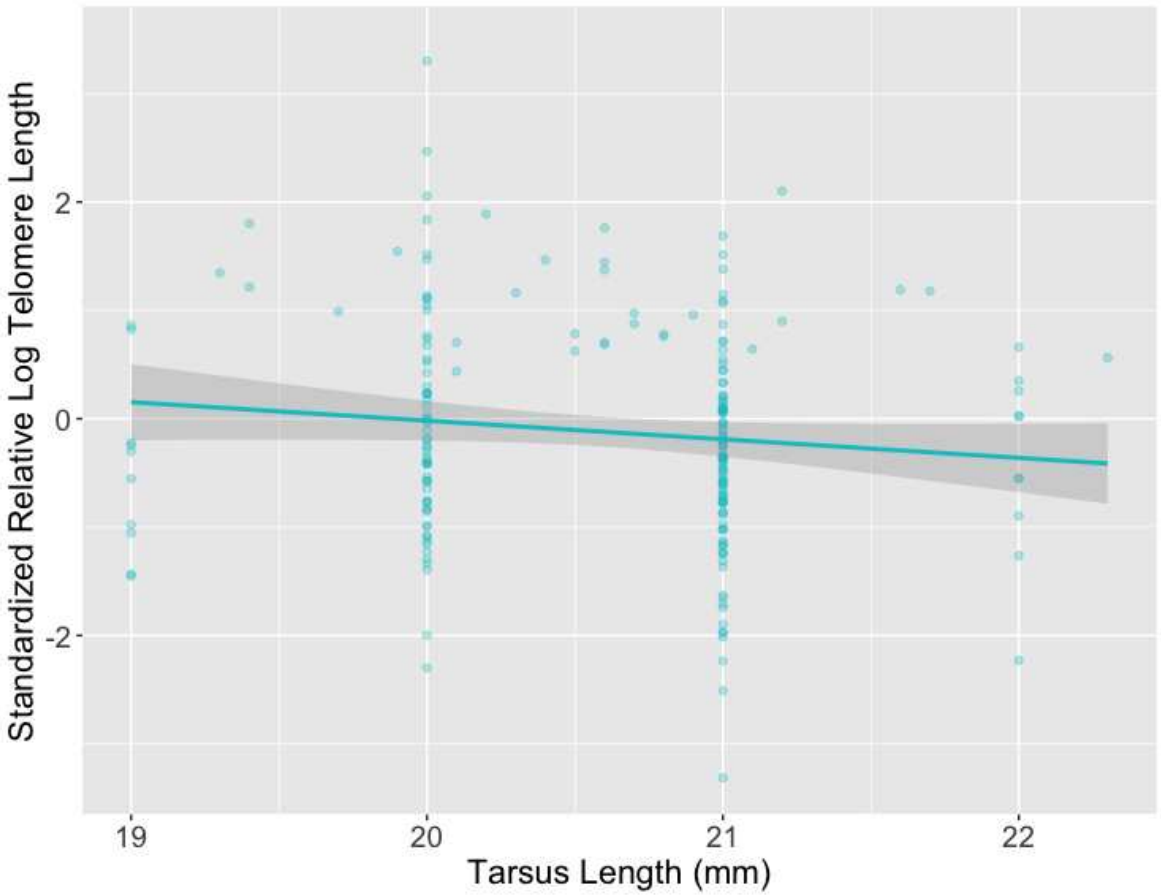

Figure S2.3. Standardized relative telomere length for breeding yellow warblers (n=416) across a gradient of tarsus length.

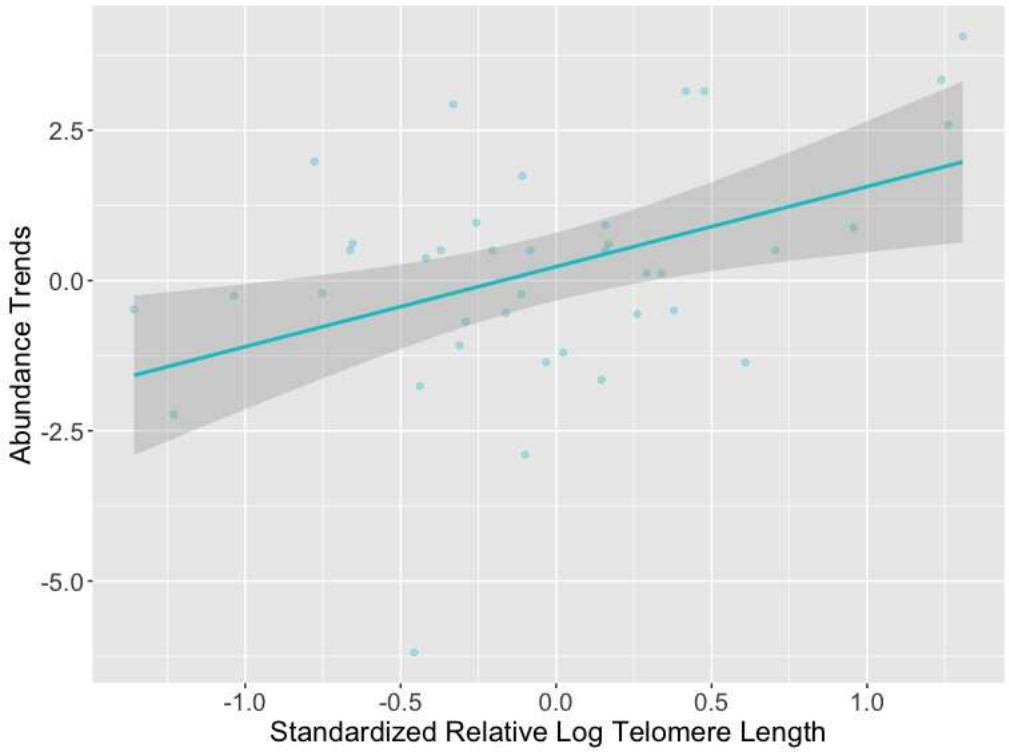

Figure S2.4. Correlation between average standardized relative log telomere length and abundance trends for breeding yellow warblers (n=39; R^2=0.19; P=0.005).

Table S2.1. Population-specific (mean±SD) efficiencies, and Cq-values for control gene (GAPDH) and telomere (TELO) assays. Three linear models were run (with GAPDH Cq, GAPDH efficiency, and TELO efficiency as dependent variables to test the differences among plates. Differences in GAPDH Cq-values were statistically significant ($p<0.001$), as were differences in both GAPDH ($p<0.001$) and TELO ($p<0.001$) efficiencies.

Population	**SCG Efficiency [mean±SD]**	**SCG Cq [mean±SD]**	**TELO Efficiency [mean±SD]**	**TELO Cq [mean±SD]**
1	1.99±0.02	23.53±1.52	1.98±0.02	13.37±1.72
2	2.01±0.00	24.28±1.52	2.00±0.01	13.42±1.02
3	2.01±0.01	25.77±0.72	2.01±0.01	15.29±0.57
4	1.98±0.02	22.48±1.65	1.98±0.02	12.04±1.83
5	1.99±0.01	25.30±3.85	2.00±0.04	13.61±3.09
6	1.99±0.02	26.47±3.71	2.03±0.05	16.55±4.03
7	2.01±0.01	26.50±1.15	2.01±0.02	16.18±2.32
8	1.99±0.01	23.27±1.84	1.98±0.02	13.04±1.68
9	2.01±0.01	25.72±0.54	2.01±0.01	14.70±0.65
10	2.00±0.02	26.04±1.69	2.01±0.03	15.40±2.76
11	1.98±0.00	25.64±1.67	2.00±0.00	14.01±0.55
12	1.98±0.00	24.86±0.32	2.00±0.00	14.38±1.05
13	2.00±0.01	26.51±3.57	1.99±0.03	15.82±4.65
14	2.00±0.01	26.48±2.62	2.02±0.03	15.99±3.69
15	1.99±0.01	26.60±1.97	2.01±0.03	16.37±2.00
16	1.99±0.01	28.65±1.61	2.03±0.05	19.19±2.64
17	2.00±0.01	25.44±2.40	2.00±0.01	15.17±2.12
18	2.00±0.01	24.25±0.80	1.99±0.00	13.60±1.05
19	1.99±0.01	25.47±3.33	2.03±0.04	17.47±2.76
20	1.99±0.01	26.71±2.34	2.00±0.04	16.96±3.55
21	1.99±0.00	23.84±0.60	2.00±0.00	15.05±0.35
22	1.98±0.01	25.15±4.16	2.02±0.04	17.01±3.56
23	1.99±0.01	24.47±1.90	1.99±0.01	14.65±1.86
24	1.97±0.00	30.42±1.02	1.95±0.00	20.35±1.10
25	2.00±0.00	29.43±2.17	1.99±0.00	19.43±2.45
26	1.97±0.00	30.38±0.73	1.95±0.00	20.14±0.68
27	1.96±0.00	30.00±0.59	1.96±0.00	19.54±0.72
28	1.96±0.00	30.42±0.38	1.96±0.00	19.96±0.31
29	2.00±0.00	27.15±2.06	2.00±0.01	15.17±1.31
30	1.99±0.01	27.82±2.49	1.98±0.02	16.38±3.46
31	2.01±0.01	23.81±0.76	1.99±0.01	12.90±0.64
32	2.01±0.04	27.37±2.32	1.99±0.02	15.30±2.52
33	2.01±0.00	23.77±1.67	2.01±0.01	14.42±1.02

34	2.01±0.03	24.44±2.72	2.00±0.01	15.05±2.71
35	2.00±0.01	25.08±4.49	2.00±0.01	15.99±3.82
36	2.00±0.01	25.06±2.37	2.00±0.01	14.34±2.87
37	2.00±0.00	29.86±0.72	1.99±0.00	19.54±0.46
38	2.03±0.05	25.19±1.04	2.00±0.01	14.14±1.04
39	2.06±0.05	25.38±0.80	2.00±0.01	14.77±0.47

Table S2.2. Plate-specific efficiencies, and Cq-values for control gene (GAPDH) and telomere (TELO) assays. Three linear models were run (with GAPDH Cq, GAPDH efficiency, and TELO efficiency as dependent variables to test the differences among plates. Differences in GAPDH Cq-values were statistically significant ($p<0.001$), as were differences in both GAPDH ($p<0.001$) and TELO ($p<0.001$) efficiencies.

Plate	SCG Efficiency [mean]	SCG Cq [mean±SD]	TELO Efficiency [mean]	TELO Cq [mean±SD]
1	1.99	24.85±0.63	1.99	14.54±0.43
2	1.97	21.81±1.59	1.96	12.00±0.43
3	2.01	25.48±0.59	2.01	14.47±0.62
4	2.00	25.73±1.80	2.00	14.65±0.70
5	1.99	23.01±1.31	2.00	15.00±0.74
6	1.98	25.04±0.84	2.00	14.29±0.74
7	2.00	23.82±0.95	2.00	13.28±0.77
8	2.00	30.12±0.70	1.99	19.85±0.78
9	2.01	22.27±0.79	2.01	13.99±0.83
10	2.10	24.91±0.39	1.99	14.63±0.84
11	2.00	28.08±1.08	2.01	12.85±0.86
12	2.00.	24.65±0.73	2.00	13.29±0.95
13	2.01	23.43±0.83	1.99	12.80±1.00
14	2.00	25.85±1.75	2.00	14.59±1.01
15	2.00	28.59±0.59	1.98	13.70±1.03
16	2.02	26.25±0.94	2.02	15.60±1.15
17	1.98	29.95±0.96	2.08	21.15±1.17
18	2.00	26.36±0.95	2.01	15.11±1.23
19	1.98	30.77±0.44	1.95	20.79±1.33
20	1.98	29.12±1.30	1.97	20.73±1.75
21	1.96	29.99±0.74	1.96	19.77±1.82
22	1.97	30.53±0.79	1.95	20.39±2.04

Table S2.3. Telomere length was influenced by genomic offset and elevation as indicated by the high model weights and rankings among the set of candidate models exploring the importance of genomic offset ('Offset'), 'Age', 'Sex', latitude ('Lat'), elevation ('Elev'), 'Tarsus', and 'Date' on telomere length in yellow warblers on the breeding range during the summers of 2020-2021. Sample location and qPCR plate were included as a random effects in each model. The number of parameters (K), -2 log-likelihood (-2LL), and model weights (wi) are shown for each model, and the models are ranked by their AICc differences relative to the best model in the set (ΔAICci).

Model	K	ΔAICc$_i$	-2LL	w_i
Offset * Elev + Tarsus	7	0	-267.26	0.88
Date + Tarsus	5	6.84	-272.81	0.03
Tarsus	4	8.27	-274.57	0.01
Offset + Date + Tarsus	6	8.78	-272.72	0.01
Date * Elev + Tarsus	7	9.06	-271.79	0.01
Offset + Tarsus	5	9.67	-274.22	0.01
Lat + Tarsus	5	10.04	-274.41	0.01
Sex + Tarsus	7	10.09	-272.31	0.01
Age + Tarsus	5	10.15	-274.47	0.01
Offset * Date + Tarsus	5	10.22	-274.5	0.01
Date * Sex * Tarsus	7	10.46	-272.49	0.00
Offset + Elev + Tarsus	6	10.48	-273.57	0.00
Offset + Lat + Tarsus	6	11.53	-274.1	0.00
Offset + Sex + Tarsus	6	11.58	-274.12	0.00
Offset + Age + Tarsus	6	11.65	-274.16	0.00
Elev * Tarsus + Offset	7	11.73	-273.12	0.00
Elev * Tarsus + Sex	7	11.74	-273.13	0.00
Elev * tarsus + Age	7	11.84	-273.18	0.00
Elev * Sex + Tarsus	7	12.5	-273.51	0.00
Ofsset * Sex + Tarsus	7	13.15	-273.83	0.00
Sex * Elev * Tarsus	10	17.39	-272.68	0.00
Offset * Elev + Sex	7	582.19	-558.49	0.00
Offset + Sex	5	582.72	-560.82	0.00
Offset * Date * Elev	10	582.88	-555.71	0.00
Offset + Secx + Elev	6	583.06	-559.96	0.00
Offset * Elev	6	583.27	-560.07	0.00
Sex + Elev	5	583.34	-561.13	0.00

Sex	4	583.57	-562.28	0.00
Offset	4	583.76	-562.37	0.00
Date * Elev + Sex	7	583.8	-559.3	0.00
Offset + Elev	5	583.98	-561.46	0.00
Elevation	4	584.14	-562.56	0.00
Offset + Sex + Lat	6	584.38	-560.62	0.00
Offset + Sex + Age	6	584.41	-560.64	0.00
Date * Elev + Offset	7	584.44	-559.62	0.00
Null Model	3	584.49	-563.76	0.00
Offset * Sex	6	584.57	-560.72	0.00
Offset + Sex + Date	6	584.6	-560.74	0.00
Offset * Sex + Elev	7	584.79	-559.8	0.00
Elev * Sex + Offset	7	585.03	-559.92	0.00
Offset * Elev + Age	7	585.04	-559.92	0.00
Sex + Age	5	585.24	-562.09	0.00
Sex * Elev	6	585.26	-561.06	0.00
Offset * Elev + Date	7	585.28	-560.04	0.00
Offffset + Lat	5	585.48	-562.2	0.00
Offset + Age	5	585.59	-562.26	0.00
Offset + Lat + Elev	6	585.61	-561.24	0.00
Offset + Date	5	585.72	-562.33	0.00
Date * Eelev + Age	7	585.76	-560.28	0.00
Offset + Age + Elev	6	585.78	-561.33	0.00
Age + Elev	5	585.92	-562.43	0.00
Offset + Date + Elev	6	586.03	-561.45	0.00
Lat + Elev	5	586.04	-562.48	0.00
Date + Elev	5	586.17	-562.55	0.00
Offset * Sex + Age	7	586.23	-560.52	0.00
Age	4	586.31	-563.64	0.00
Lat * Elev	6	586.39	-561.63	0.00
Date	4	586.43	-563.7	0.00
Lat	4	586.46	-563.72	0.00
Date * Sex + Offset	7	586.66	-560.73	0.00
Age * Elev	6	586.82	-561.84	0.00
Offset * Lat	6	586.84	-561.86	0.00
Sex * Age	6	586.85	-561.86	0.00
Elev * Sex + Age	7	586.89	-560.85	0.00
Offset * Age	6	587.13	-562	0.00
Offset + Age + Lat	6	587.31	-562.09	0.00
Offset + Lat + Date	6	587.54	-562.2	0.00

Offset + Age + Date	6	587.55	-562.21	0.00
Offset * Date + Elev	7	587.76	-561.28	0.00
Age * Date * Elev	10	587.81	-558.17	0.00
Offset * Sex * Elev	10	588.12	-558.33	0.00
Age + Date	5	588.24	-563.58	0.00
Offset * Lat * Elev	10	588.89	-558.71	0.00
Offset * Date + Agee	7	588.92	-561.86	0.00
Date * Sex + Age	7	589.14	-561.97	0.00
Sex * Elev * Date	10	589.95	-559.24	0.00
Age * Date	6	590.05	-563.46	0.00
Offset * Sex * Date	10	591.15	-559.84	0.00
Offset * Age * Date	10	594.35	-561.44	0.00

Table S2.4. Abundance trend was influenced by bio15 and latitude as indicated by the high model weights and rankings among the set of candidate models exploring the importance of precipitation amount of the wettest month ('Bio13), precipitation seasonality ('Bio15'), mean monthly precipitation amount of the warmest quarter ('Bio18'), latitude ('Lat'), and elevation ('Elev') on abndance trends in yellow warblers on the breeding range during the summers of 2020-2021. Location was included as a random effect in each model. The number of parameters (K), -2 log-likelihood (-2LL), and model weights (wi) are shown for each model, and the models are ranked by their AICc differences relative to the best model in the set (ΔAICci).

Model	K	ΔAICc$_i$	-2LL	w_i
Bio15 * Lat	5	0	-70.66	0.33
Bio15	3	1.59	-74.02	0.15
Bio15 + Lat	4	1.94	-72.95	0.12
14Bio15 + Elev	4	3.2	-73.58	0.07
Bio15 + Lat + Elev	5	3.4	-72.36	0.06
Bio15 + Bio18	4	3.97	-73.97	0.04
Bio15 + Bio18 + Lat	5	3.99	-72.66	0.04
Bio13 + Bio15	4	4.08	-74.02	0.04
Bio15 * Elev	5	4.63	-72.97	0.03
Bio15 * Elev + Lat	6	4.63	-71.57	0.03
Bio15 + Bio18 + Elev	5	5.3	-73.31	0.02
Bio13 + Bio15 + Elev	5	5.81	-73.56	0.02
Bio13 * Bio15	5	6.71	-74.02	0.01
Bio15 * Bio18 + Elev	6	7.99	-73.25	0.01
Bio13 * Bio15 + Elev	6	8.35	-73.43	0.01
Elev	3	9.01	-77.73	0.00
Lat * Elev	4	9.54	-76.75	0.00
Elev + Bio13	4	10.66	-77.31	0.00
Bio18 + Elev	4	11.39	-77.68	0.00
Null Model	2	11.4	-80.1	0.00
Lat + Elev + Bio13	5	11.4	-76.36	0.00
Bio18	3	11.96	-79.21	0.00
Bio18 + Lat + Elev	5	12.17	-76.75	0.00
Lat	3	12.49	-79.47	0.00
Bio13 + Bio18 + Elev	5	12.99	-77.15	0.00
Bio13 * Elev	5	13.28	-77.3	0.00
Bio13	3	13.36	-79.91	0.00
Bio18 + Bio13	4	13.41	-78.68	0.00
Bio13 * Bio18 + Elev	6	13.48	-76	0.00
Bio18 + Lat	4	13.69	-78.82	0.00
Bio18 * Elev	5	13.88	-77.6	0.00
Bio * Elev + Lat	6	14.14	-76.33	0.00

Bio13 * Elev + Lat	6	14.14	-76.33	0.00
Lat + Bio13	4	14.65	-79.3	0.00
Bio18 + Bio13 + Lat	5	15.44	-78.38	0.00
Bio18 * Bio13 * Bio15	9	15.56	-72.24	0.00
Bio13 * Lat	5	16.04	-78.68	0.00
Bio18 * Lat	5	16.33	-78.82	0.00

Table S2.5. Telomere length was influenced by bio15 as indicated by the high model weights and rankings among the set of candidate models exploring the importance of precipitation amount of the wettest month ('Bio13), precipitation seasonality ('Bio15'), mean monthly precipitation amount of the warmest quarter ('Bio18'), latitude ('Lat'), date, and elevation ('Elev') on telomere length in yellow warblers on the breeding range during the summers of 2020-2021. Location and qPCR plate ID was included as a random effect in each model. The number of parameters (K), -2 log-likelihood (-2LL), and model weights (wi) are shown for each model, and the models are ranked by their AICc differences relative to the best model in the set (ΔAICci).

Model	K	$\Delta AICc_i$	-2LL	w_i
Bio15 * Lat	7	0	-594.68	0.14
Lat	5	0.81	-597.14	0.10
Bio13 + Lat	6	1.08	-596.25	0.08
Bio18 + Lat	6	1.92	-596.67	0.05
Elev + Lat	6	2.31	-596.87	0.05
Bio15 + Lat	6	2.35	-596.89	0.04
Bio18 + Bio13 + Lat	7	2.71	-596.03	0.04
Bio13 + Elev + Lat	7	2.77	-596.07	0.04
Bio13 * Lat	7	2.83	-596.1	0.03
Lat + Date	6	2.85	-597.14	0.03
Bio18 + Bio13	7	3.09	-596.23	0.03
Bio18	5	3.41	-598.44	0.03
Null	4	3.45	-599.49	0.03
Bio13	5	3.66	-598.57	0.02
Bio18 * Lat	7	3.75	-596.55	0.02
Bio18 + Bio15 + Lat	7	3.86	-596.61	0.02
Bio18 + Elev + Lat	7	3.89	-596.62	0.02
Bio18 + Lat + Date	7	3.91	-596.64	0.02
Bio15 + Elev + Lat	7	4.1	-596.73	0.02
Elev + Lat + Date	7	4.33	-596.84	0.02
Bio18 + Bio13	6	4.4	-597.91	0.02
Date	5	4.84	-599.16	0.01
Bio15 + Bio13	6	4.91	-598.17	0.01
Bio13 + Date	6	5.05	-598.24	0.01
Bio18 + Date	6	5.21	-598.31	0.01
Bio15	5	5.26	-599.37	0.01
Bio18 + Elev	6	5.34	-598.38	0.01
Elev	5	5.41	-599.44	0.01
Bio18 + Bio15 t	6	5.46	-598.44	0.01
Bio18 * Bio15	7	5.65	-597.5	0.01
Bio13 + Elev	6	5.69	-598.56	0.01

Bio15 * Bio13	7	5.93	-597.64	0.01
Bio18 + Bio15 + Bio13	7	6.31	-597.83	0.01
Bio18 * Date	7	6.65	-598	0.01
Bio15 + Date	6	6.68	-599.05	0.01
Bio18 * Elev	7	6.81	-598.08	0.00
Elev + Date	6	6.83	-599.12	0.00
Bio13 * Date	7	7.08	-598.22	0.00
Bio15 + Elev	6	7.29	-599.35	0.00
Bio13 * Elev	7	7.74	-598.55	0.00
Bio15 + Bio13 + Elev + Date	8	8.38	-597.83	0.00
Bio15 * Date	7	8.66	-599.01	0.00
Bio15 * Elev	7	9.26	-599.31	0.00

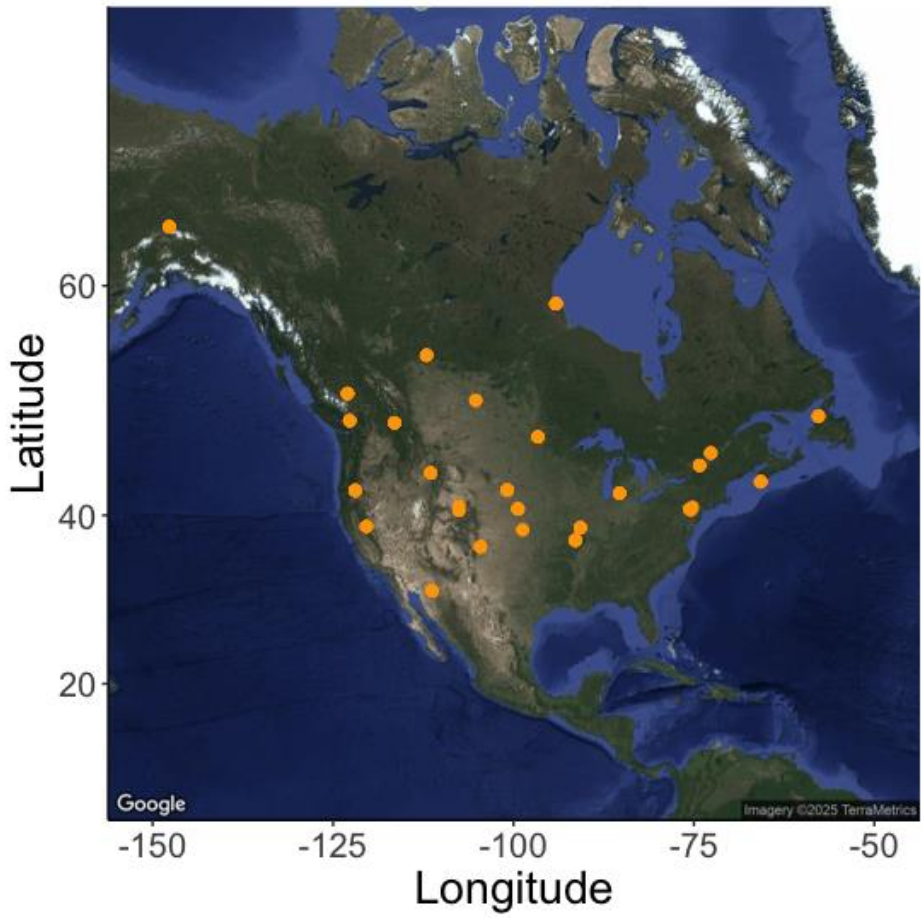

Figure S3.1. 159 yellow warbler samples from 18 populations across the breeding grounds were used to train the Origen model training and validation.

Figure S3.2. To determine which SNP subset most accurately assigned individuals to their breeding locations, we calculated the distance between the actual breeding sample location and the grid cell with the highest assignment probability for each validation sample.

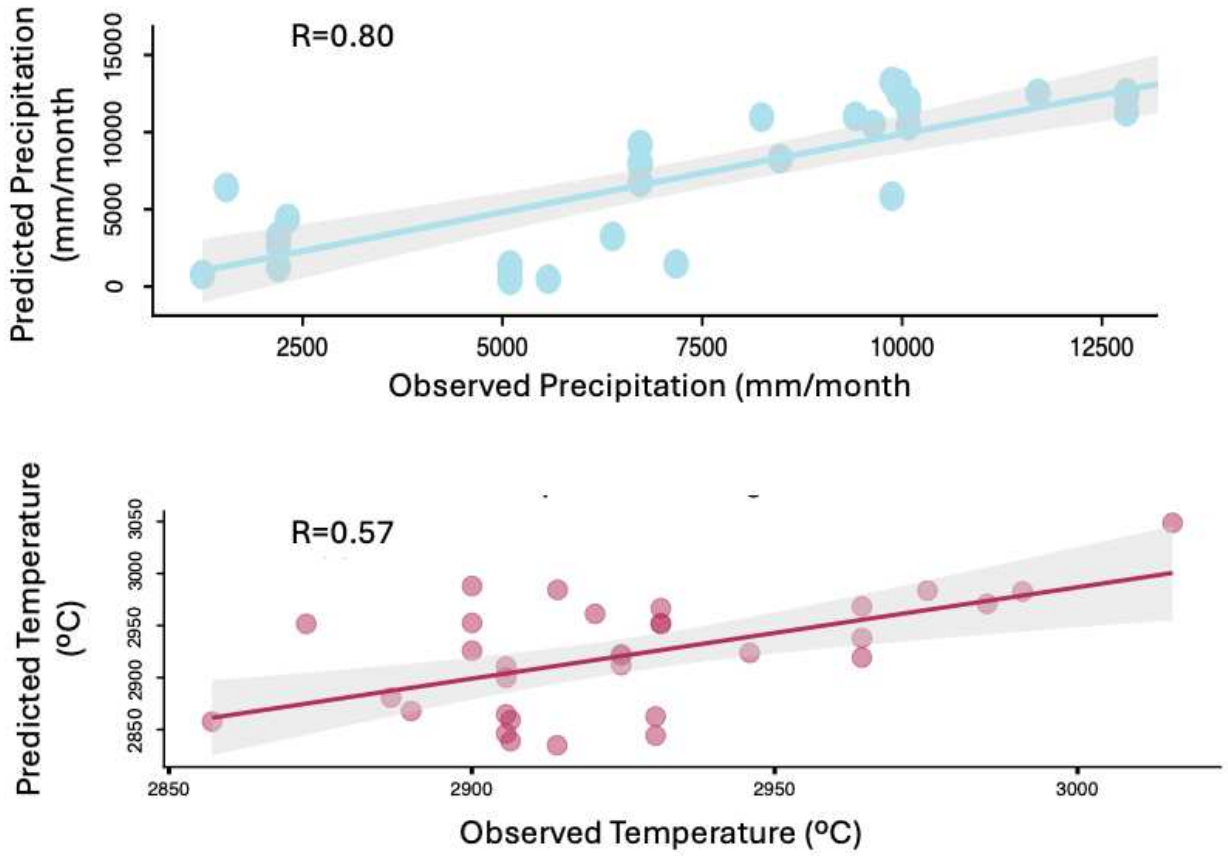

Figure S3.3. After using 410 SNPs to assign the 106 individuals caught on the wintering grounds to their predicted breeding location, we tested the accuracy of the climate predictions based on the Origen assignment by comparing the known and expected mean annual precipitation and mean annual temperature.

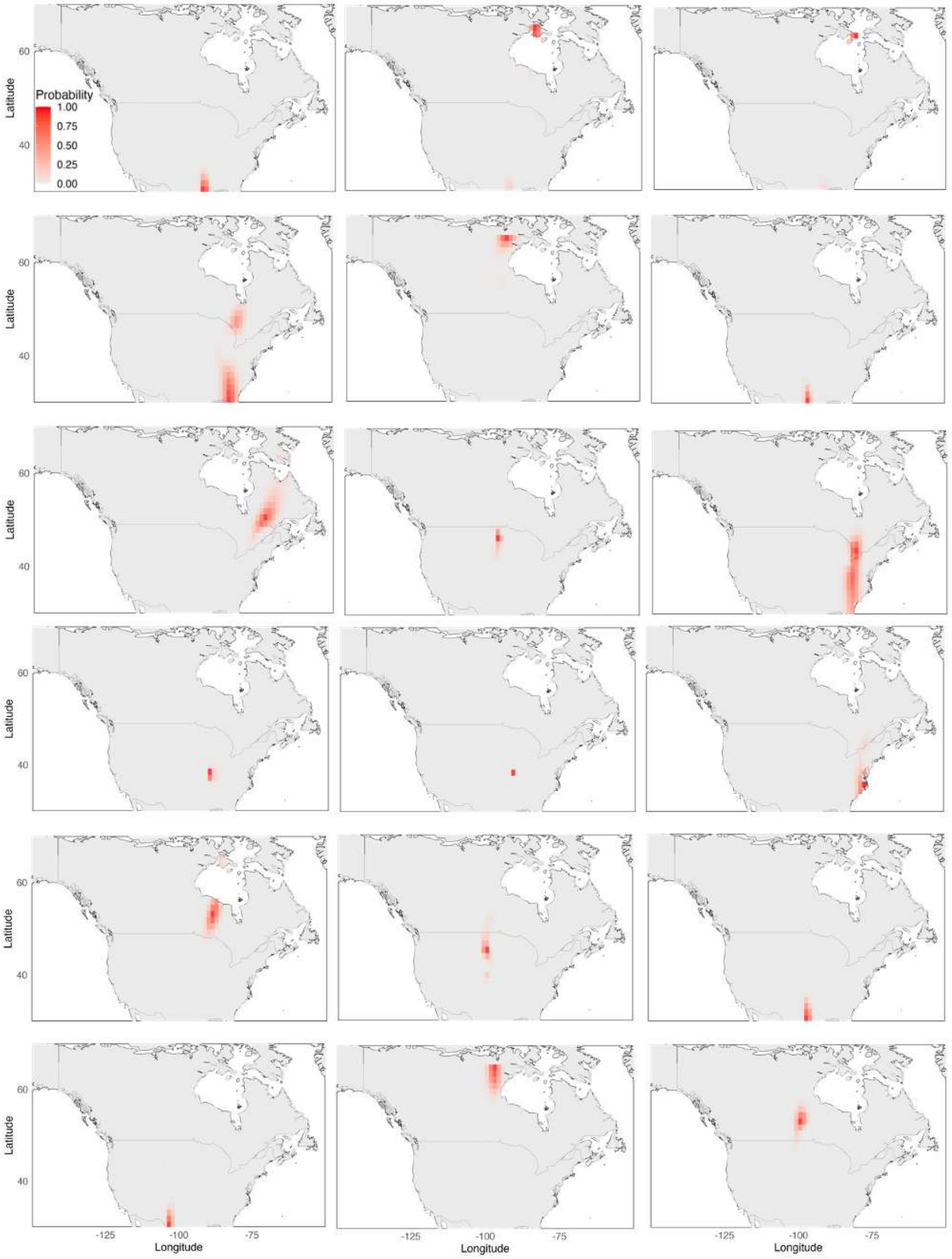
Probability
1.00
0.75
0.50
0.25
0.00
Latitude
60
40
-125
-100
-75
Longitude

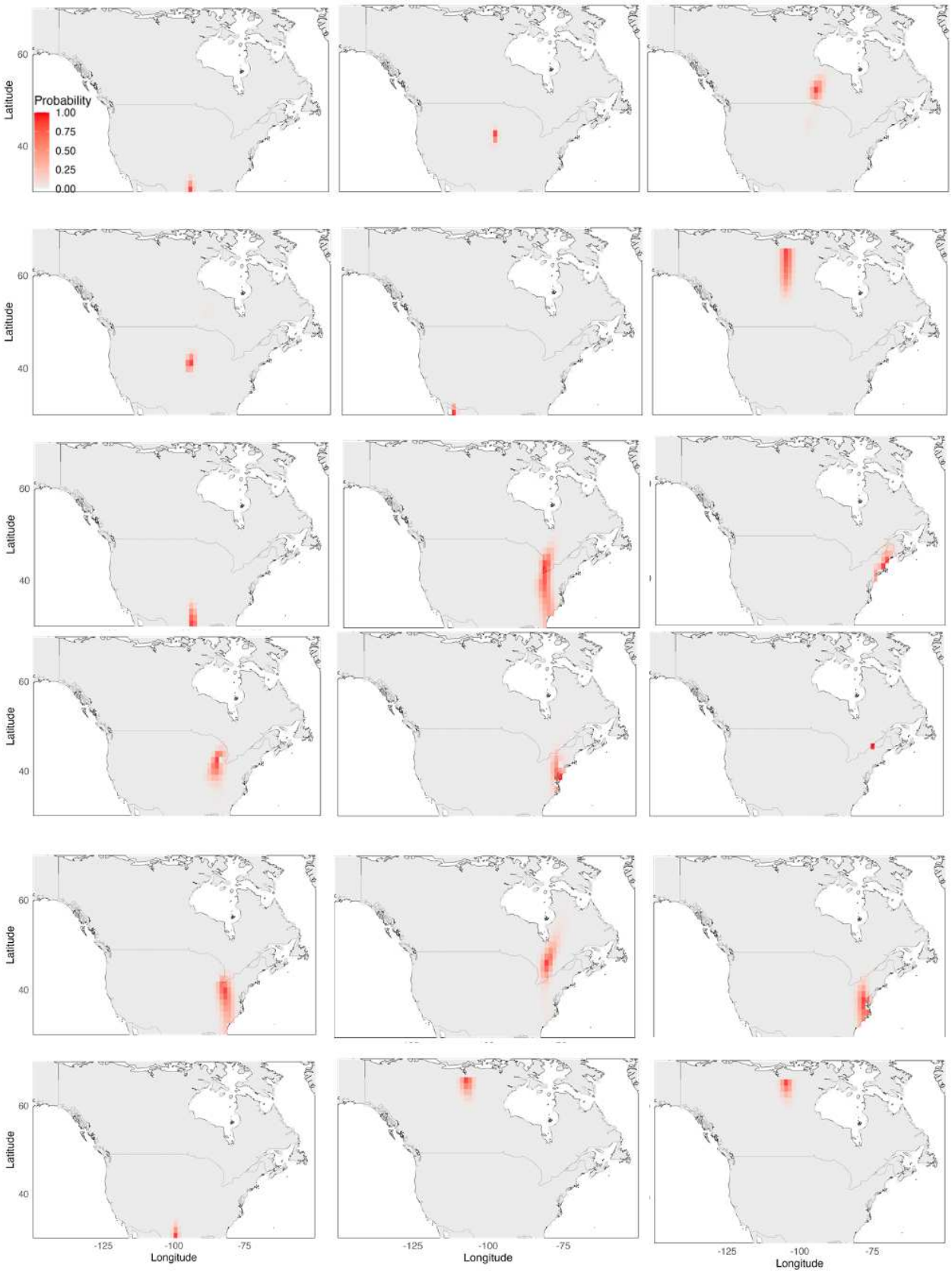
Probability
1.00
0.75
0.50
0.25
0.00
Latitude
60
40
-125
-100
-75
Longitude

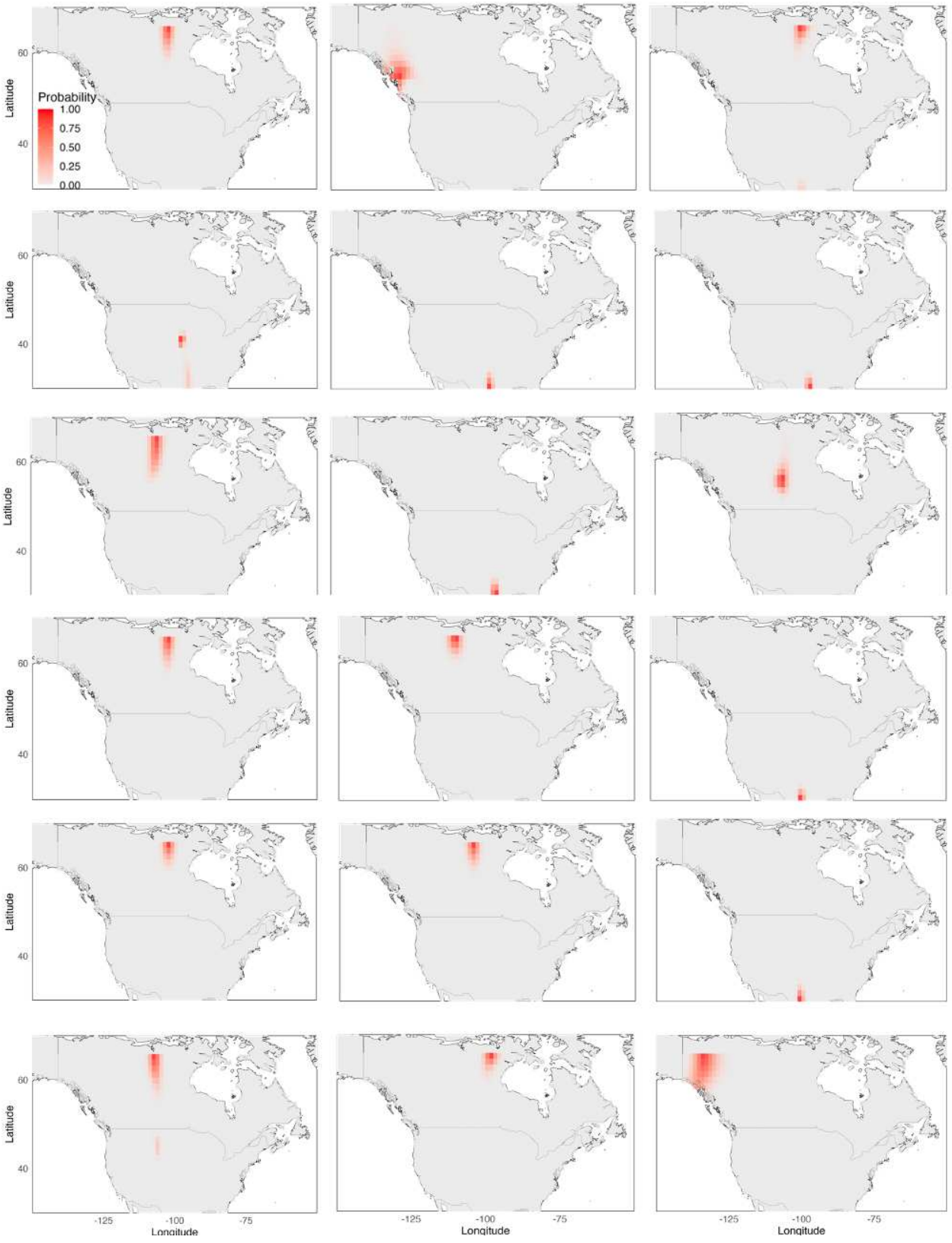
Probability
1.00
0.75
0.50
0.25
0.00
Latitude
60
40
-125
-100
-75
Longitude

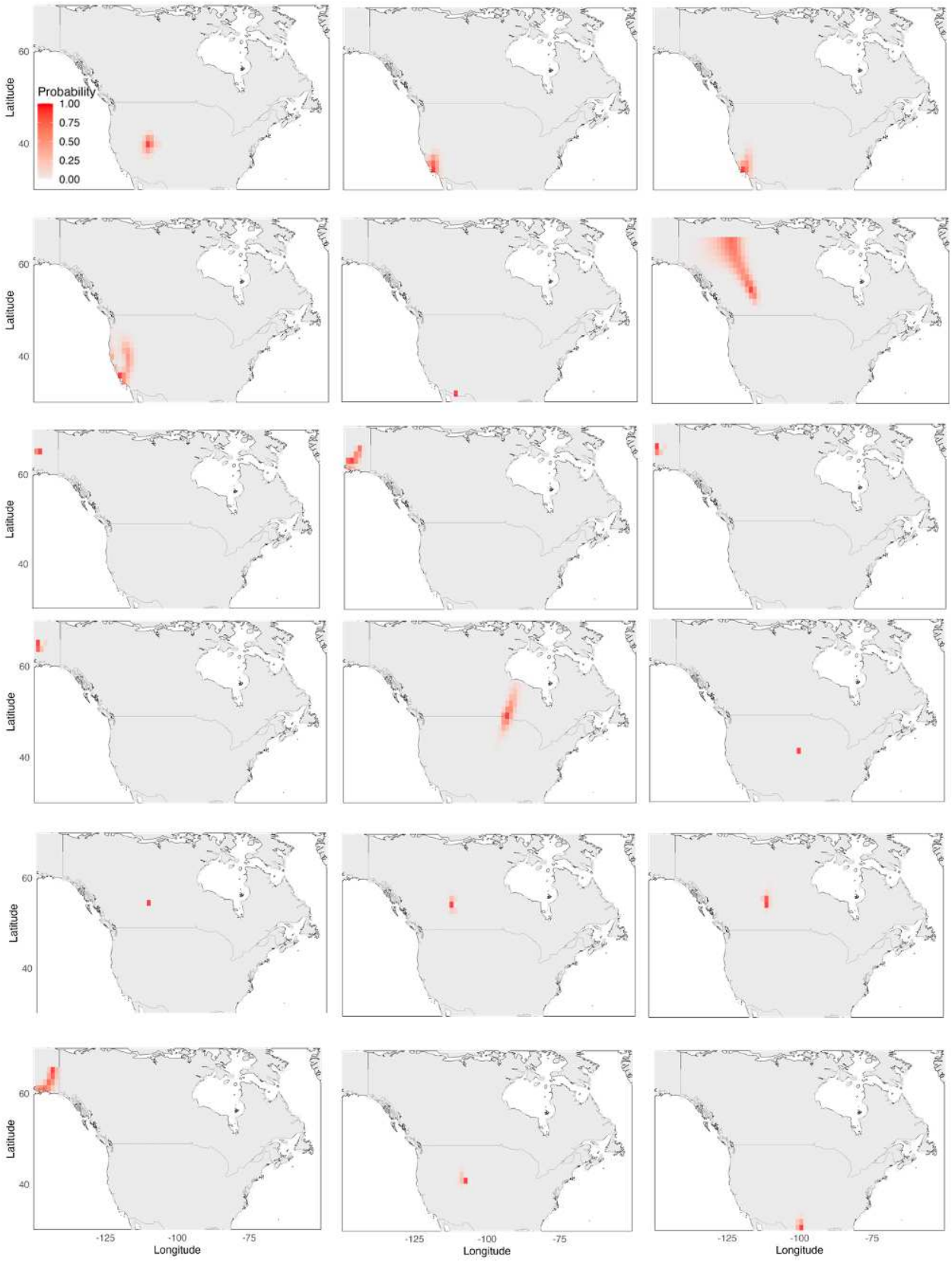
Probability
1.00
0.75
0.50
0.25
0.00
Latitude
60
40
-125
-100
-75
Longitude

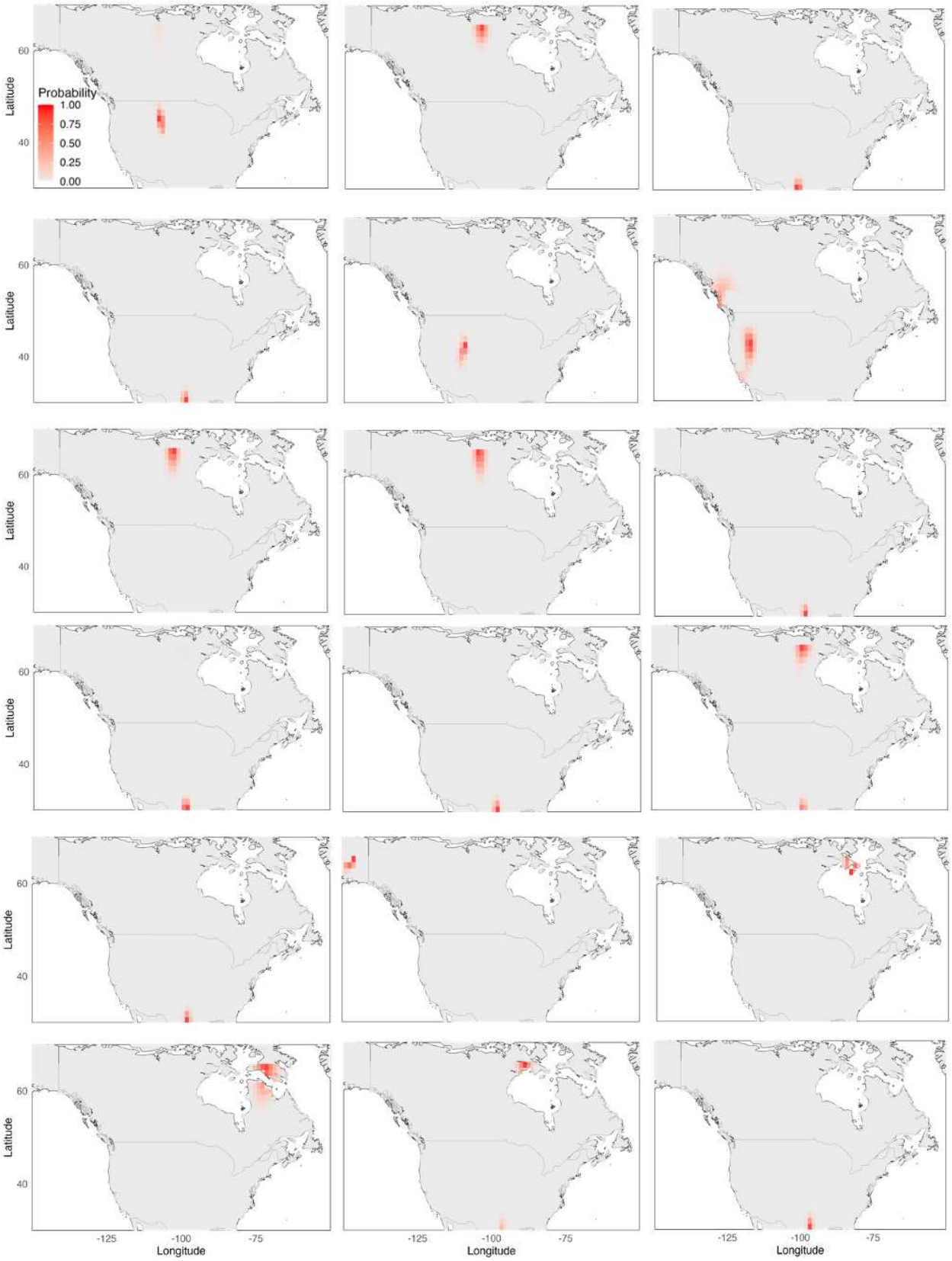
Probability
1.00
0.75
0.50
0.25
0.00
Latitude
60
40
-125
-100
-75
Longitude

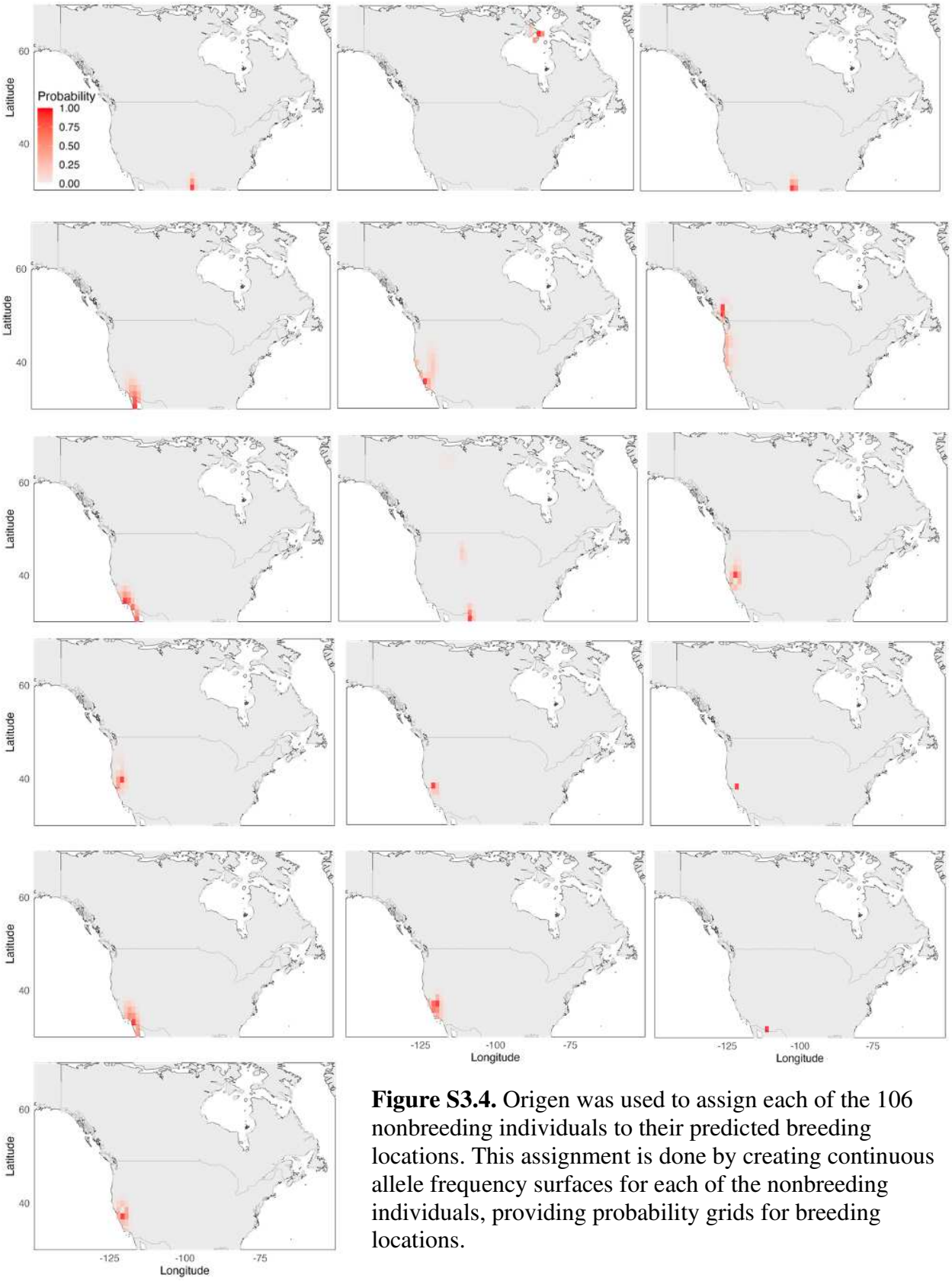

Figure S3.4. Origen was used to assign each of the 106 nonbreeding individuals to their predicted breeding locations. This assignment is done by creating continuous allele frequency surfaces for each of the nonbreeding individuals, providing probability grids for breeding locations.

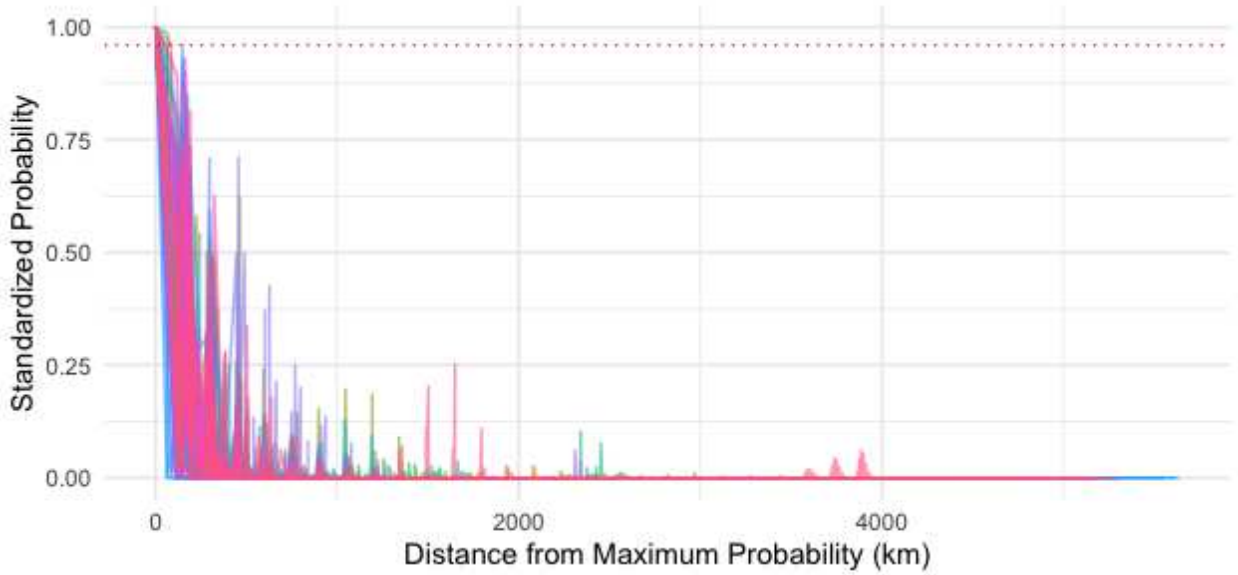

Figure S3.5. We accounted for spatial variability in breeding location assignment by defining a radius around the grid cell with the highest assignment probability of Origen assignment, which we used to extract climate variables. Assignment probabilities were scaled so that the highest probability within the grid was set to one by normalizing values across all grid cells for each individual. We then calculated the average radius encompassing a cumulative assignment probability of 0.99 (red dotted line) across all individuals, resulting in a radius of 114 km. This radius served as the extraction zone for climate data around the top-assigned breeding grid cell for each individual.

Table S3.1. To investigate the potential functional relevance of climate-linked SNPs, we compiled a list of candidate genes from the literature with gene ontology (GO) terms associated with thermal tolerance, bill morphology, and feather color. The GO list was derived using annotations from AmiGO (Carbon et al. 2009) and curated manually from literature.

Gene	Function	Reference
A0A8V1A1B4	Response to heat (GO term)	
ABCG2	Differentially expressed in heat-challenged Japanese quails; Associated with adaptation to hot climates in chickens	Carvalho et al. 2021; Xu et al. 2023
ABLIM2	Associated with adaptation to hot climates & differentially expressed under heat stress in chickens	Xu et al. 2023; Zhang et al. 2017
ACSF2	Associated with cold tolerance in chickens	Fedorova et al. 2022; Romanov et al. 2023
ADAMTS20	Involved in melanocyte differentiation (GO term)	
ADAMTS9	Involved in melanocyte differentiation (GO term)	
AKT1	Associated with cold tolerance in chickens; Involved in temperature homeostasis, response to heat, and oxidative stress (GO terms)	Romanov et al. 2023
Alx-4	Roof of mouth development (GO term)	
ANKRD27	Involved in the melanosome (GO term)	
ANO5	Associated with cold tolerance in chickens	Fedorova et al. 2022; Romanov et al. 2023
AP1M1	Involved in melanosome organization (GO term)	
AP3B1	Melanosome biogenesis, TYR recruitment in rosy finches, and melanosome organization (GO term)	Funk et al. 2023
APC	Associated with plumage color variation in yellow and red-shafted flickers.	Aguillon and Lovette, I. J. 2021
AQP3A	Involved in melanocyte differentiation (GO term)	
ARID5B	Roof of mouth development (GO term)	
ARNTL	Differentially expressed in heat-challenged Japanese quails; Involved in response to heat (GO term)	Carvalho et al. 2021
ARPP21	Cellular response to heat (GO term)	
ASIP	Associated with plumage color variation in passerines and with melanin biosynthetic processes (GO term)	Funk et al. 2019
ASPH	Roof of mouth development (GO term)	
ATF3	Differentially expressed under heat stress in quails and chickens	Carvalho et al. 2021; Zhang et al. 2017
ATRN	Involved in pigmentation (GO term)	
AUTS2	Associated with adaptation to hot climates & differentially expressed under heat stress in chickens	Xu et al. 2023; Zhang et al. 2017
B3GLCT	Roof of mouth development (GO term)	
BACE2	Involved in melanosome organization (GO term)	

BAG3	Cellular response to heat (GO term)	
BBS7	Roof of mouth development (GO term)	
BCL2	Involved in pigmentation (GO term)	
BCO2	Associated with plumage color variation in yellow-rumped warbler.	Toews et al. 2016
BCOR	Roof of mouth development (GO term)	
BDNF	Associated with cold tolerance in chickens; Involved in response to heat (GO term)	Fedorova et al. 2022; Romanov et al. 2023
BLNK	Differentially expressed in heat-challenged Japanese quails; Associated with body temperature under heat stress in chickens	Carvalho et al. 2021; Zhuang et al. 2019
BLOC1S5	Involved in melanosome transport (GO term)	
BLOC1S6	Involved in pigmentation (GO term)	
BMP4	Beak morphogenesis (GO term)	
BMPR1A	Roof of mouth development (GO term)	
BNC2	Roof of mouth development (GO term)	
BTBD9	Associated with cold tolerance in chickens; Involved in temperature homeostasis (GO term)	Romanov et al. 2023
C8ORF4	Cellular response to heat (GO term)	
CACNA1G	Associated with cold tolerance and adaptation to hot climates in chickens	Fedorova et al. 2022; Romanov et al. 2023; Xu et al. 2023
CAMK1D	Associated with adaptation to hot climates in chickens; Involved in respiratory system processes (GO term)	Xu et al. 2023
CAMTA1	Associated with adaptation to hot climates in chickens	Xu et al. 2023
CCDC109B	Associated with bill depth in yellow warblers	Rodriguez et al. 2024
CDK1	Cellular response to heat (GO term)	
CENPI	Associated with climate adaptation and differentially expressed under heat stress in chickens	Kumar et al. 2019; Zhang et al. 2017
ChALK5	Roof of mouth development (GO term)	
CHD7	Roof of mouth development (GO term)	
CHORDC1	Regulation of cellular response to heat (GO term)	
CITED1	Involved in melanocyte differentiation (GO term)	
CKAP2	Associated with climate adaptation and differentially expressed under heat stress in chickens	Kumar et al. 2019; Zhang et al. 2017
CKM	Response to heat (GO term)	
COL12A1	Associated with adaptation to hot climates & differentially expressed under heat stress in chickens	Xu et al. 2023; Zhang et al. 2017
COL141A	Associated with telomere length and bill morphology in yellow warblers	Rodriguez et al. 2024
CPLANE1	Roof of mouth development (GO term)	
CRAA	Response to heat (GO term)	

CSF1RA	Involved in melanocyte differentiation (GO term)	
CSRNP1	Roof of mouth development (GO term)	
CYP2J19	Associated with plumage color variation in red siskins and common canaries.	Lopes et al. 2016
DACH1	Associated with adaptation to hot climates in chickens; Involved in respiratory system processes (GO term)	Xu et al. 2023
DCT	Associated with the melanosome (GO term)	
DCTN2	Associated with melanosome ransport (GO term)	
DENND5A	Involved in melanocyte differentiation (GO term)	
DHRS3	Roof of mouth development (GO term)	
DHX36	Cellular response to heat (GO term)	
DIAPH3	Associated with adaptation to hot climates & differentially expressed under heat stress in chickens	Xu et al. 2023; Zhang et al. 2017
DICER1	Involved in melanocyte differentiation (GO term)	
DISC1	Associated with cold tolerance in chickens	Fedorova et al. 2022; Romanov et al. 2023
DLG1	Roof of mouth development (GO term)	
DLX5	Roof of mouth development (GO term)	
DLX6	Roof of mouth development (GO term)	
DNAJA1	Response to heat (GO term)	
DNAJA2	Response to heat (GO term)	
DNAJA3	Response to heat (GO term)	
DNAJA4	Response to heat (GO term)	
DNAJB1	Cellular response to heat (GO term)	
DNMT3A	Response to heat (GO term)	
ECE2B	Involved in melanocyte differentiation (GO term)	
EDA	Involved in pigmentation (GO term)	
EDAR	Involved in pigmentation (GO term)	
EDN3	Melanocyte production and Involved in melanocyte differentiation (GO term)	Funk et al. 2021
EDNRA	Involved in respiratory system processes and oxidative stress (GO terms)	
EDNRB2	Involved in melanocyte differentiation and neural crest cell migration (GO terms)	
EED	Associated with plumage color variation in yellow and red-shafted flickers.	Aguillon and Lovette 2021
EGFR	Associated with adaptation to hot climates in chickens; Involved in oxidative stress (GO term)	Romanov et al. 2023
EHF	Associated with cold tolerance in chickens	Romanov et al. 2023
EIF2B5	Response to heat (GO term)	
EN1	Involved in pigmentation (GO term)	

ENPP1	Involved in melanocyte differentiation (GO term)	
EPAS1	Involved in respiratory system processes and oxidative stress (GO terms)	
EPHB2	Roof of mouth development (GO term)	
EPHB3	Roof of mouth development (GO term)	
ERBB3B	Involved in melanocyte differentiation (GO term)	
ERN1	Associated with climate adaptation in chickens; Involved in response to heat (GO term)	Kumar et al. 2019
ESR1	Involved in response to heat (GO term)	
EXOC2	Differentially expressed in heat-challenged Japanese quails; Associated with body temperature under heat stress in chickens	Carvalho et al. 2021; Zhuang et al. 2019
FAM189A1	Associated with adaptation to hot climates and heat stress in chickens	Xu et al. 2023; Van Goor et al. 2016
FGFR2	Embryonic cranial skeleton morphogenesis (GO term)	
FIG4	Involved in pigmentation (GO term)	
FKBP4	Associated with cold tolerance and adaptation to hot climates in chickens; Involved in response to heat (GO term)	Romanov et al. 2023; Xu et al. 2023
FKBP8	Associated with plumage color variation in yellow and red-shafted flickers.	Aguillon and Lovette 2021
FOXD3	Involved in pigmentation cell differentiation (GO term)	
FOXE1	Roof of mouth development (GO term)	
FST	Associated with plumage color variation in passerines.	Funk and Taylor 2019
FTO	Involved in temperature homeostasis, respiratory system processes, and oxidative stress (GO terms)	
FZD1	Roof of mouth development (GO term)	
FZD2	Roof of mouth development (GO term)	
GABRB2	Associated with bill depth in yellow warblers	Rodriguez et al. In prep
GAS2	Associated with cold tolerance in chickens	Fedorova et al. 2022; Romanov et al. 2023
GCLC	Associated with adaptation to hot climates in chickens; Involved in response to heat, oxidative stress, and temperature homeostasis (GO terms)	Xu et al. 2023
GDF11	Roof of mouth development (GO term)	
GFPT1	Involved in melanocyte differentiation (GO term)	
GHOX-7	Roof of mouth development (GO term)	
GJA5B	Involved in pigmentation (GO term)	
GK5	Associated with climate adaptation in chickens	Kumar et al. 2019; Xu et al. 2023
GLI3	Associated with adaptation to hot climates in chickens; Linked to bill morphology in great tits; Involved in respiratory system processes and melanocyte differentiation (GO term)	Xu et al. 2023; Bosse et al. 2017

GNA11	Involved in the regulation of melanocyte differentiation (GO term)	
GPR143	Assiciated with melanosome organization (GO term)	
HAND2	Associated with plumage color variation in dark-eyed junco.	Abolins-Abols et al. 2018
HDAC1	Involved in melanocyte differentiation (GO term)	
HIF1A	Involved in oxidative stress and response to heat (GO terms)	
HIKESHI	Cellular response to heat (GO term)	
HMOX1	Cellular response to heat (GO term)	
HPS	Involved in pigmentation (GO term)	
HPS1	Involved in melanosome assembly (GO term)	
HPS3	Involved in pigmentation (GO term)	
HPS4	Assiciated with melanosome assembly (GO term)	
HPS5	Involved in melanocyte differentiation (GO term)	
HPS9	Involved in melanosome assembly (GO term)	
HPS90AA1	Response to heat (GO term)	
HSBP1	Cellular heat acclimation (GO term)	
HSF1	Response to heat (GO term)	
HSF3	Response to heat (GO term)	
HSPB2	Response to heat (GO term)	
HSPB3	Response to heat (GO term)	
HSPH1	Associated with cold tolerance and differentially expressed under heat stress in chickens	Romanov et al. 2023; Wang et al. 2020
HTRA2	Cellular response to heat (GO term)	
IER5	Cellular response to heat (GO term)	
IFT172	Roof of mouth development (GO term)	
IGF1	Response to heat (GO term)	
IGFBP1	Associated with climate adaptation and cold tolerance in chickens	Kumar et al. 2019; Fedorova et al. 2022
IL1RAPL1	Associated with cold tolerance, adaptation to hot climates, and local adaptation in chickens	Romanov et al. 2023; Xu et al. 2023; Xie et al. 2024
IMMP2L	Associated with cold tolerance in chickens; Involved in respiratory system processes (GO term)	Romanov et al. 2023
INHBA	Roof of mouth development (GO term)	
INSIG1	Roof of mouth development (GO term)	
INSIG2	Roof of mouth development (GO term)	
INTU	Roof of mouth development (GO term)	
IRF6	Roof of mouth development (GO term)	
IRX5	Embryonic cranial skeleton morphogenesis (GO term)	
ITGB6	Roof of mouth development (GO term)	
ITGB8	Roof of mouth development (GO term)	

JAG2	Associated with cold tolerance in chickens; Involved respiratory system processes (GO term)	Romanov et al. 2023
KCNJ13	Associated with plumage color variation in dark-eyed junco and in pigmentation (GO term)	Abolins-Abols et al. 2018
KDF1	Keratinocyte development (GO term)	
KIT	Differentially expressed under heat stress in chickens; Involved in bone morphogenesis and in melanocyte differentiation (GO term)	Zhang et al. 2017
KITLG	Associated with plumage color variation in Lonchura munias.	Stryjewsk and Sorenson 2017
KLF2	Associated with cold tolerance and heat stress in chickens	Romanov et al. 2023; Van Goor et al. 2016
LEF1	Associated with cold tolerance in chickens; Involved in bone morphogenesis and respiratory system processes (GO term)	Romanov et al. 2023
LEO1	Involved in melanocyte differentiation (GO term)	
LOC101156879	Involved in the melanosome and melanocyte differentiation (GO terms)	
LOC101161292	Involved in the melanosome and melanocyte differentiation (GO terms)	
LOC101165733	Involved in melanocyte differentiation (GO term)	
LOC107050773	Response to heat (GO term)	
LOC121106916	Cellular response to heat (GO term)	
LOC419080	Involved in melanocyte differentiation (GO term)	
LOC420362	Cellular response to heat (GO term)	
LOC425431	Response to heat (GO term)	
LOC427025	Embryonic viscerocranium morphogenesis (GO term)	
LOC427439	Embryonic viscerocranium morphogenesis (GO term)	
LRMDA	Involved in melanocyte differentiation (GO term)	
LRP11	Response to heat (GO term)	
LRP2	Associated with cold tolerance and adaptation to hot climates in chickens	Romanov et al. 2023; Xu et al. 2023
LTK	Involved in pigmentation (GO term)	
LYST	Involved in pigmentation (GO term)	
MAPK13	Associated with adaptation to hot climates in chickens; Involved in oxidative stress (GO term)	Xu et al. 2023
MC1R	Associated with plumage color variation in snow geese and arctic skuas and in melanocyte differentiation (GO term)	Mundy et al. 2004
MEF2C	Involved in melanocyte differentiation (GO term)	
MEOX2	Roof of mouth development (GO term)	
METTL21C	Heat shock protein binding (GO term)	
MFSD12	Associated with plumage color variation in yellow and red-shafted flickers and in pigmentation (GO term).	Aguillon and Lovette, I. J. 2021

MGAT5	Associated with climate adaptation, telomere length, and bill morphology in yellow warblers	Rodriguez et al. 2024
MIB1	Involved in melanocyte differentiation (GO term)	
MIB2	Involved in melanocyte differentiation (GO term)	
MITF	Regulates transcription of many key melanogenesis genes and involved in melanocyte differentiation (GO term)	Funk et al. 2023
MLANA	Associated with plumage color variation in dark-eyed junco.	Abolins-Abols et al. 2018
MLPH	Involved in melanocyte differentiation (GO term)	
MMP16	Embryonic cranial skeleton morphogenesis (GO term)	
MREG	Involved in pigmentation and melanocyte differentiation (GO terms)	
MTHFD1L	Embryonic viscerocranium morphogenesis (GO term)	
MTOR	Response to heat (GO term)	
MYO1B	Differentially expressed under heat stress in chickens	Zhang et al. 2017
MYO5A	Involved in the melanosome (GO term)	
MYO7A	Associated with plumage color variation in dark-eyed junco and with the melanosome (GO term)	Abolins-Abols et al. 2018
MYO9B	Associated with plumage color variation in yellow and red-shafted flickers.	Aguillon et al. 2021
NBEAL1	Associated with cold tolerance in chickens	Fedorova et al. 2022; Romanov et al. 2023
NELL1	Associated with cold tolerance and muscle development and growth in chickens; Linked to bill morphology in great tits	Fedorova et al. 2022; Romanov et al. 2023; Bosse et al. 2017; Yin et al. 2019
NOS1	Response to heat (GO term)	
NPAS2	Differentially expressed in heat-challenged Japanese quails; Involved in response to heat (GO term)	Carvalho et al. 2021
NPRL3	Roof of mouth development (GO term)	
NR3C1	Response to heat (GO term)	
NRXN3	Associated with adaptation to hot climates and body temperature under heat stress in chickens	Xu et al. 2023; Zhuang et al. 2019
NUF2	Associated with climate adaptation and differentially expressed under heat stress in chickens	Kumar et al. 2019; Zhang et al. 2017
OCA2	Associated with plumage color variation in dark-eyed junco and involved in melanocyte differentiation (GO term)	Abolins-Abols et al. 2018
OR51E2	Involved in melanocyte differentiation (GO term)	
OSR1	Roof of mouth development (GO term)	
OSR2	Roof of mouth development (GO term)	
OTUD7A	Associated with adaptation to hot climates and heat stress in chickens	Xu et al. 2023; Van Goor et al. 2016
P08106	Response to heat (GO term)	

PAM	Associated with plumage color variation in yellow and red-shafted flickers.	Aguillon and Lovette 2021
PARK2	Involved in response to heat and oxidative stress (GO terms)	
PDCD6	Cellular response to heat (GO term)	
PDGFRA	Roof of mouth development (GO term)	
PIKFYVE	Associated with cold tolerance in chickens and with melanosome organization (GO term)	Fedorova et al. 2022; Romanov et al. 2023
PKDCCA	Roof of mouth development (GO term)	
PLCB1	Associated with plumage color variation in yellow and red-shafted flickers.	Aguillon and Lovette 2021
PLCB4	Associated with plumage color variation in yellow and red-shafted flickers.	Aguillon and Lovette 2021
PLEKHA1	Roof of mouth development (GO term)	
PMEL	Associated with plumage color variation in dark-eyed junco and melanocyte differentiation (GO term).	Abolins-Abols et al. 2018
PMELA	Involved in melanocyte differentiation (GO term)	
PPARGC1A	Associated with cold tolerance, heat stress, and environmental adaptation in chickens; Involved in respiratory system processes and oxidative stress (GO terms)	Romanov et al. 2023; Wang et al. 2020; Gheyas et al. 2021
PPP1CB	Associated with telomere length and bill morphology in yellow warblers	Rodriguez et al. 2024
PPP1R1C	Associated with cold tolerance in chickens	Fedorova et al. 2022; Romanov et al. 2023
PRCP	Associated with cold tolerance and differentially expressed under heat stress in chickens	Romanov et al. 2023; Zhang et al. 2017
PRRX1	Roof of mouth development (GO term)	
PSIP1	Response to heat (GO term)	
PTPRG	Associated with adaptation to hot climates in chickens	Xu et al. 2023
PTPRS	Associated with cold tolerance and heat stress in chickens	Romanov et al. 2023; Van Goor et al. 2016
PYGO2	Roof of mouth development (GO term)	
RAB11A	Involved in melanosome transport (GO term)	
RAB17	Involved in melanosome transport (GO term)	
RAB1B	Involved in melanosome transport (GO term)	
RAB27A	Involved in melanocyte differentiation (GO term)	
RAB32	Associated with the melanosome (GO term)	
RAB38	Associated with plumage color variation in dark-eyed junco and with melanosome assembly (GO term)	Abolins-Abols et al. 2018
RAB7L1	Involved in the melanosome (GO term)	
RAB8A	Associated with plumage color variation in yellow and red-shafted flickers.	Aguillon and Lovette 2021
RAR4	Beak morphogenesis (GO term)	

RDH10	Neural crest cell development (GO term)	
RGP1	Associated with plumage color variation in yellow and red-shafted flickers.	Aguillon and Lovette 2021
RGS6	Associated with adaptation to hot climates in chickens	Xu et al. 2023
RIMS2	Associated with climate adaptation, telomere length, and bill morphology in yellow warblers	
RNF41	Involved in melanocyte differentiation (GO term)	Rodriguez et al. 2024
RSU1	Associated with climate adaptation in chickens	Kumar et al. 2019; Xu et al. 2023
RYR2	Associated with cold tolerance and altitudinal adaptation in chickens	Fedorova et al. 2022; Wang et al. 2015; Li et al. 2013
SATB2	Linked to bill morphology in great tits; Associated with adaptation to hot climates in chickens	Bosse et al. 2017; Xu et al. 2023
SKAP2	Associated with telomere length and bill morphology in yellow warblers	Rodriguez et al. 2024
SCARF2	Associated with plumage color variation in yellow-rumped warbler	Brelsford et al. 2017.
SDK1	Associated with adaptation to hot climates & differentially expressed under heat stress in chickens	Xu et al. 2023; Zhang et al. 2017
SEMA3B	Associated with plumage color variation in yellow and red-shafted flickers.	Aguillon and Lovette 2021
SESN1	Associated with adaptation to hot climates in chickens; Involved in oxidative stress (GO term)	Xu et al. 2023
SF3B1	Involved in melanocyte differentiation (GO term)	
SGPL1	Roof of mouth development (GO term)	
SHH	Roof of mouth development (GO term)	
SLC24A5	Associated with plumage color variation in dark-eyed junco.	Abolins-Abols et al. 2018
SLC39A3	Embryonic cranial skeleton morphogenesis (GO term)	
SLC45A2	Associated with plumage color variation in dark-eyed junco and melanocyte differentiation (GO term).	Abolins-Abols et al. 2018
SLU7	Cellular response to heat (GO term)	
SMPD3	Differentially expressed under heat stress in chickens; Involved in oxidative stress (GO term)	Zhang et al. 2017
SNAI1	Roof of mouth development (GO term)	
SNCA	Involved in response to heat, respiratory system processes, and oxidative stress (GO terms)	
SOD1	Response to heat (GO term)	
SOS1	Roof of mouth development (GO term)	
SOX10	Involved in melanocyte differentiation (GO term)	
SOX11	Roof of mouth development (GO term)	
SPAG16	Associated with adaptation to hot climates in chickens; Involved in respiratory system processes (GO term)	Xu et al. 2023

SPAG9	Associated with cold tolerance in chickens	Fedorova et al. 2022; Romanov et al. 2023
STAB2	Associated with cold tolerance and differentially expressed under heat stress in chickens	Romanov et al. 2023; Zhang et al. 2017
STAC	Cellular response to heat (GO term)	
STK25	Associated with cold tolerance in chickens; Involved in oxidative stress (GO term)	Fedorova et al. 2022
SUMO1	Cellular response to heat (GO term)	
SZT2	Involved in pigmentation (GO term)	
TBC1D32	Roof of mouth development (GO term)	
TBX15	Embryonic cranial skeleton morphogenesis (GO term)	
TBX2	Involved in roof of mouth development (GO term)	
TBX3	Roof of mouth development (GO term)	
TCF21	Roof of mouth development (GO term)	
TENM2	Associated with climate variation in chickens, sheep, and Anolis lizards	Fleming et al. 2016; Vallejo-Trujillo 2021; Zhang et al. 2022; Wogan et al. 2020; Prates et al. 2018
TFEC	Cellular response to heat (GO term)	
TGFBR2	Associated with cold tolerance in chickens; Involved in respiratory system processes (GO term)	Romanov et al. 2023
THSD4	Differentially expressed under heat stress in chickens; Potentially involved in metabolism of protein-rich food in chickens	Zhang et al. 2017; Van Goor et al. 2016; Gheyas et al. 2021
THSD7A	Associated with adaptation to hot climates and body temperature under heat stress in chickens	Xu et al. 2023; Zhuang et al. 2019
TIPARP	Roof of mouth development (GO term)	
TMEM38A	Associated with cold tolerance and heat stress in chickens	Romanov et al. 2023; Van Goor et al. 2016
TP53!NP1	Response to heat (GO term)	
TPCN2	Involved with the melanosome membrane (GO term)	
TPO	Associated with cold tolerance in chickens; Involved in oxidative stress (GO term)	Romanov et al. 2023
TRIP12	Associated with adaptation to hot climates and body temperature under heat stress in chickens	Xu et al. 2023; Zhuang et al. 2019
TRPC7	Associated with cold tolerance and body temperature under heat stress in chickens	Romanov et al. 2023; Zhuang et al. 2019
TRPM1	Associated with cold tolerance and heat stress in chickens	Romanov et al. 2023; Van Goor et al. 2016
TRPM2	Temperature homeostasis (GO term)	
TRPV1	Cellular response to heat (GO term)	
TRPV4	Cellular response to heat (GO term)	

TTC7A	Differentially expressed under heat stress in chickens	Wang et al. 2020
TTLL5	Associated with adaptation to hot climates and body temperature under heat stress in chickens	Xu et al. 2023; Zhuang et al. 2019
TYR	Associated with plumage color variation in dark-eyed junco and involved in pigmentation (GO term)	Abolins-Abols et al. 2018
TYRP1	Associated with the melanosome (GO term)	
TYRP1A	Associated with plumage color variation in dark-eyed junco and involved in pigmentation and melanocyte differentiation (GO terms)	Abolins-Abols et al. 2018
USP13	Involved in melanocyte differentiation (GO term)	
UVRAG	Involved in melanocyte differentiation (GO term)	
VANGL1	Involved in pigmentation (GO term)	
VAV3	Differentially expressed under heat stress in chickens; Associated with angiogenesis and altitudinal adaptation in birds	Zhang et al. 2017; Lai et al. 2019; Yuan et al. 2022
VAX1	Roof of mouth development (GO term)	
VPS11	Involved in melanocyte differentiation (GO term)	
VPS13B	Linked to bill morphology in Darwin's finches and great tits	Lamichhaney et al. 2015; Bosse et al. 2017
VPS33A	Regulation of developmental pigmentation (GO term)	
VPS33B	Involved in melanosome localization (GO term(	
W5MBB4	Involved in melanocyte differentiation (GO term)	
W5MNX6	Involved in melanocyte differentiation (GO term)	
W5MZ12	Involved in melanocyte differentiation (GO term)	
W5N6U1	Involved in the melanosome and melanocyte differentiation (GO terms)	
WDPCP	Roof of mouth development (GO term)	
WDR19	Embryonic cranial skeleton morphogenesis (GO term)	
WFIKKN1	Roof of mouth development (GO term)	
WFIKKN2	Roof of mouth development (GO term)	
WNT11	Roof of mouth development (GO term)	
WNT5A	Roof of mouth development (GO term)	
WNT7A	Roof of mouth development (GO term)	
WNT9B	Roof of mouth development (GO term)	
XRN1	Associated with adaptation to hot climates and body temperature under heat stress in chickens	Xu et al. 2023; Zhuang et al. 2019
YWHAE	Cellular response to heat (GO term)	
ZBTB16	Associated with climate adaptation and differentially expressed under heat stress in chickens	Kumar et al. 2019; Wang et al. 2020
ZFPM2	Associated with cold tolerance in chickens; Involved in response system processes (GO term)	Romanov et al. 2023
MGAT4C	Bill morphology in Darwins finches.	Lawson and Petren 2017